letnik/volume **53** - št./no. **6/07** - str./pp. **353-422**
Ljubljana, jun./June 2007, zvezek/issue **506**

STROJNIŠKI VESTNIK

JOURNAL OF MECHANICAL ENGINEERING

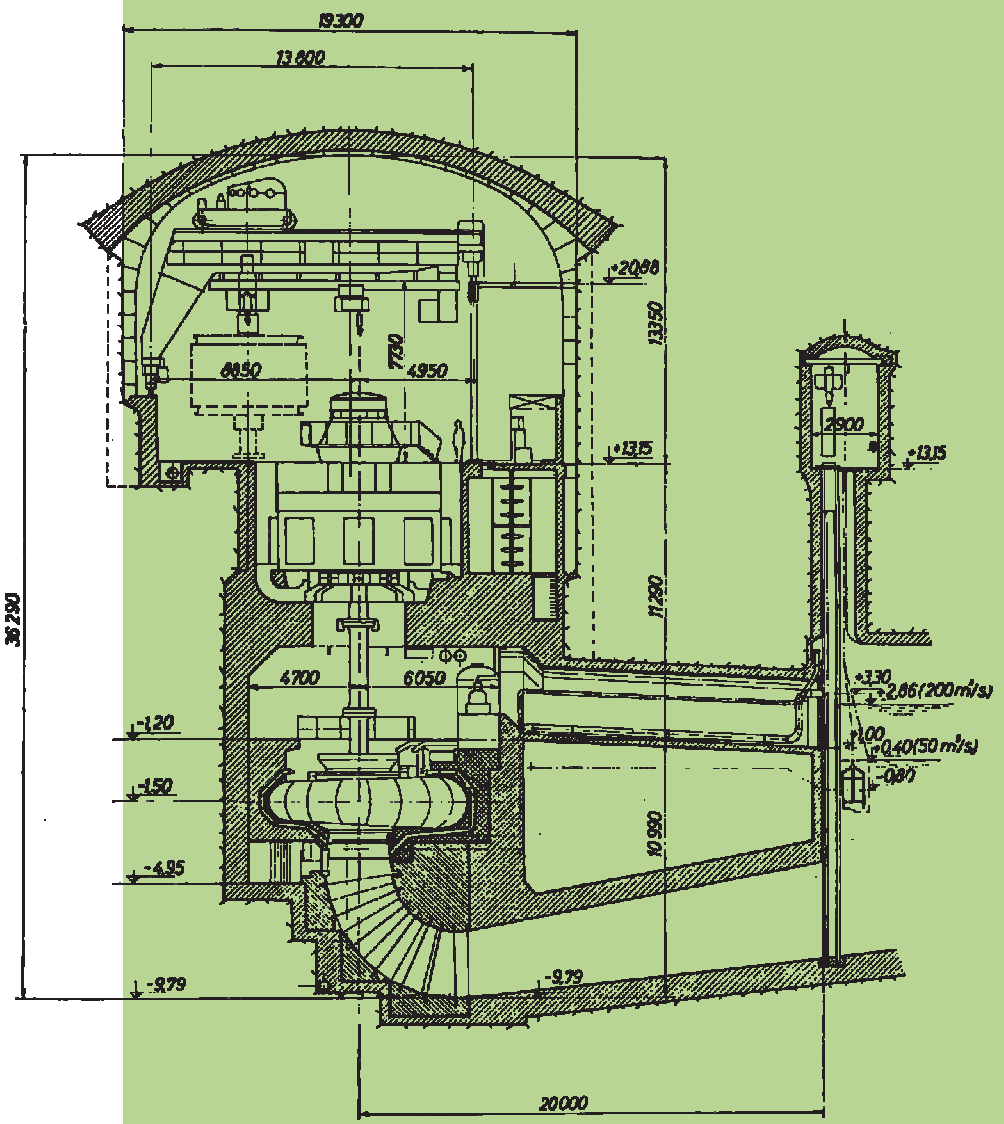

cena 3,34 EUR

ISSN 0039-2480

Vsebina - Contents

Strojniški vestnik - Journal of Mechanical Engineering
letnik - volume 53, (2007), številka - number 6
Ljubljana, junij - June 2007
ISSN 0039-2480

Izhaja mesečno - Published monthly

Strojniški vestnik - Journal of Mechanical Engineering 53(2007)6, 354-368
UDK - UDC 621.914:004.89
Izvirni znanstveni članek - Original scientific paper (1.01)

Optimiranje značilnih parametrov frezanja z uporabo razvojne tehnike optimizacije jate delcev

Optimization of the Characteristic Parameters in Milling Using the PSO Evolution Technique

Uroš Župerl[1] - Franci Čuš[1] - Valentina Gecevska[2]
([1]Fakulteta za strojništvo, Maribor; Fakulteta za strojništvo v Skopju, Makedonija)

Izbira rezalnih parametrov je najpomembnejši korak pri postopku načrtovanja proizvodnje, zato izdelamo novo tehniko razvojnega računanja za optimiranje procesa odrezovanja. V prispevku je uporabljena tehnika, ki oponaša dinamiko delcev v velikih skupinah (optimizacija jate delcev - OJD), za učinkovito in simultano optimiranje postopkov frezanja. V omenjenih postopkih smo soočeni s problemom več ciljnih dejavnikov. Najprej uporabimo umetno nevronsko mrežo (UNM) za napovedovanje rezalnih sil, nato z algoritmom OJD pridobimo optimalno rezalno hitrost in podajanja. Cilj optimizacije je, ob upoštevanju omejitev, določiti ekstrem ciljne funkcije (napovedna površina največjih sil). Med optimizacijo se delci inteligentno "gibljejo" v prostoru rešitev in "iščejo" optimalne rezalne pogoje po strategiji algoritma OJD. Rezultati pokažejo, da je integriran sistem nevronskih mrež in spoznavanja jate učinkovita metoda pri reševanju večciljnih optimizacijskih problemov. Njena velika učinkovitost na širokem območju rezalnih parametrov potrjuje, da sistem lahko praktično uporabimo v proizvodnji. Rezultati simulacij nakazujejo, da predlagan algoritem v primerjavi z rodovnimi algoritmi (GA) in simuliranim (SA) žarjenjem (popuščanjem) lahko poveča natančnost rešitve in konvergenco postopka. Nova tehnika razvojnega računanja ima nekoliko prednosti ter koristi in je primerna za uporabo v kombinaciji z modeli na osnovi umetnih nevronskih vezij, pri katerih niso na voljo izrecne relacije med vstopnimi in izstopnimi veličinami. Raziskava odpira vrata na področju obdelave z odrezovanjem za nov razred optimizacijskih tehnik, ki slonijo na razvojnem računanju.

(Ključne besede: odrezovanje, končno frezanje, rezalni parametri, nevronske mreže)

The selection of machining parameters is an important step in process planning; therefore, a new evolutionary computation technique has been developed to optimize the machining process. In this paper, Particle Swarm Optimization (PSO) is used to efficiently optimize the machining parameters simultaneously in milling processes where multiple conflicting objectives are present. First, an artificial neural network (ANN) predictive model is used to predict the cutting forces during machining and then the PSO algorithm is used to obtain the optimum cutting speeds and feed rates. The goal of the optimization is to determine the objective function maximum (the predicted cutting-force surface) by considering the cutting constraints. During optimization the particles 'fly' intelligently in the solution space and search for optimal cutting conditions according to the strategies of the PSO algorithm.The results showed that an integrated system of neural networks and swarm intelligence is an effective method for solving multi-objective optimization problems. The high accuracy of the results within a wide range of machining parameters indicates that the system can be practically applied in industry. The simulation results show that compared with genetic algorithms (GAs) and simulated annealing (SA) the proposed algorithm can improve the quality of the solution while speeding up the convergence process. The new computational technique has several advantages and benefits and is suitable for use when combined with ANN-based models where no explicit relation between the inputs and the outputs is available. This research opens the door for a new class of optimization techniques that are based on evolution computation in the area of machining.

(Keywords: cutting, end-milling, cutting parameters, neural networks)

0 UVOD

Povečevanje storilnosti, zmanjševanje stroškov in sočasno ohranjanje kakovosti izdelka so glavni izzivi, s katerimi se srečujejo proizvajalci. Pravilna izbira rezalnih parametrov je pomemben korak k zadoščanju teh ciljev in ohranjanju konkurenčne prednosti na trgu [1]. Mnogo raziskovalcev se je ukvarjalo s proučevanjem učinkov optimalne izbire rezalnih razmer pri frezanju [2]. Problem optimiranja frezanja se lahko oblikuje in reši kot večciljni optimizacijski problem [3]. V praksi učinkovita izbira frezalnih parametrov zahteva sočasno upoštevanje več ciljnih dejavnikov, to so: največja obstojnost orodja, zahtevana hrapavost obdelane površine, ciljna storilnost opravil, stopnja odvzemanja materiala itn. [4]. V nekaterih primerih nastavitve parametrov, ki so optimalne za eno definirano ciljno funkcijo, morda ne bodo posebej primerne za drugo ciljno funkcijo. Reševanje večciljnih problemov z običajnimi optimizacijskimi metodami je težko. Edini način rešitve je zmanjšati niz ciljnih dejavnikov v en nadomestni ciljni dejavnik in ga potemtakem obdelati. Zatorej so razvojni algoritmi, kakršni so genetski algoritmi (GA) in ORD, bolj primerni in pogosteje uporabljeni pri reševanju večciljnih optimizacijskih problemov. Te metode so podane v delu [5]. ORD je učinkovita alternativa drugim naključnim in na populacijah temelječim iskalnim algoritmom, še posebej ko imamo opravka z večciljnimi optimizacijskimi problemi. Njena izvedba je razmeroma preprosta, potrebno je manj nastavljanja parametrov v primerjavi z genetskimi algoritmi.

V naši raziskavi so nevronske mreže uporabljene za modeliranje zapletenih razmerij v procesu. Integriran sistem nevronskih mrež in optimizatorja roja delcev je nato uporabljen pri reševanju večciljnega problema pri opravilih frezanja (sl. 1).

1 OPTIMIZACIJA PSO

Optimizacija, ki temelji na dinamiki jate delcev (OJD), je razmeroma nova tehnika za optimiranje nelinearnih funkcij [6]. Prvič je bila predstavljena leta 1995 [7]. Jim Kennedy jo je odkril med simuliranjem poenostavljenega socialnega modela, ki oponaša skladno in nepredvidljivo gibanje jate ptic [8]. Reynolds z izdelanim modelom jate s preprostimi pravili vzbuja njeno zapleteno gibanje [9]. Takšne raziskave poimenujemo "spoznavanje jate".

0 INTRODUCTION

Increasing productivity, decreasing costs, and maintaining high product quality at the same time are the main challenges faced by manufacturers today. The proper selection of machining parameters is an important step towards meeting these goals and thus gaining a competitive advantage in the market [1]. Many researchers have studied the effects of the optimal selection of machining parameters on end milling [2]. This problem can be formulated and solved as a multiple objective optimization problem [3]. In practice, the efficient selection of milling parameters requires the simultaneous consideration of multiple objectives, including maximum tool-life, desired roughness of the machined surface, target operation productivity, metal removal rate, etc [4]. In some instances, parameter settings that are optimal for one defined objective function may not be particularly suited to another objective function. Solving multi-objective problems with traditional optimization methods is difficult and the only way is to reduce the set of objectives into a single objective and handle it accordingly. Therefore evolutionary algorithms such as genetic algorithms (GAs) and particle swarm optimization (PSO) are more convenient and usually utilized in multi-objective optimization problems. These methods are summarized in [5]. The PSO is an efficient alternative over other stochastic and population-based search algorithms, especially when dealing with multi-objective optimization problems. It is relatively easy to implement and has fewer parameters to adjust compared to genetic algorithms.

In our research neural networks are used to model complex relationships in the process, and an integrated system of neural networks and a particle swarm optimizer are utilized in solving multi-objective problems observed in milling operations (Fig. 1).

1 PSO OPTIMIZATION

Particle swarm optimization (PSO) is a relatively new technique for the optimization of continuous non-linear functions [6]. It was first presented in 1995 [7]. Jim Kennedy discovered the method through the simulation of a simplified model, i.e., the graceful but unpredictable movement of a bird swarm [8]. Reynolds developed a swarm model with simple rules and generated complicated swarm behavior [9]. These researches are called "Swarm Intelligence"

OJD je zelo preprosta zasnova, vzorce gibanja ponazorimo le z nekaj vrsticami računalniškega zapisa. Metoda uporablja le osnovne matematične operatorje, zato je računsko nezahtevna glede na hitrost in zasedenost spomina. OJD je bila prepoznana kot tehnika razvojnega računanja [10]. Ima lastnosti tako genetskih algoritmov (GA) kakor tudi razvojnih strategij (RS). Preostale tehnike razvojnega računanja (RR), npr.: genetski algoritmi prav tako uporabljajo več iskalnih točk v prostoru rešitev. Z GA ima to podobnost, da se sistem pri obeh začne s populacijo naključnih rešitev.

Medtem ko z GA lahko rešujemo združevalne optimizacijske probleme, lahko s OJD rešujemo neprekinjene optimizacijske probleme. Vendar se v nasprotju z GA vsakemu osebku v populaciji priredi naključna hitrost, s katero leti skozi evklidski prostor rešitev. OJD so nadgradili tudi za reševanje združevalnih optimizacijskih problemov. Očitno je, da je mogoče sočasno iskanje optimuma v več razsežnostih. OJD lahko izvedemo z majhnim programom v nasprotju z drugimi tehnikami RR. Živa bitja se včasih združujejo in gibajo v rojih, jatah. Eden izmed glavnih ciljev raziskovalcev umetnega življenja je ugotoviti, kako se živa bitja obnašajo v rojih in kako modelirati njihovo obnašanje na računalniku.

OJD ima dve preprosti zasnovi. Z nekaj preprostimi pravili lahko modeliramo obnašanje jate delcev. Čeprav so pravila obnašanja posameznega delca v jati preprosta, je lahko dinamika celotne jate zelo zapletena. Gibanje delca v jati ponazorimo s preprostimi vektorji. Ta značilnost je prva osnova OJD.

Po Boydovi raziskavi [11] ljudje pri odločanju upoštevajo dva pomembna tipa informacij: lastne izkušnje in izkušnje drugih ljudi. Prvi tip so lastne izkušnje, iz katerih vedo, katere odločitve so bile v preteklosti uspešne. Vsaka oseba se torej odloča na podlagi lastnih izkušenj in izkušenj drugih ljudi. Ta značilnost je druga osnova tehnike OJD.

Uporabe OJD najdemo v: učnih algoritmih nevronskih mrež [12], izdelavi pravil v mehkih nevronskih mrežah [13], optimiranju računalniško vodenega frezanja [14], nadzoru električne moči in napetosti [15]. Uporab OJD na drugih področjih je malo, vendar pričakujemo njihov porast. Večina člankov obravnava samo metodo, njene spremembe in primerja njene zmogljivosti s preostalimi metodami RR ([14] in [15]).

PSO is a very simple concept, and paradigms are implemented in a few lines of computer code. It requires only primitive mathematical operators, so is computationally inexpensive in terms of both memory requirements and speed. PSO has been recognized as an evolutionary computation technique [10] and has features of both genetic algorithms (GAs) and evolution strategies (ESs). Other evolutionary computation (EC) techniques such as genetic algorithms also utilize some searching points in the solution space. It is similar to a GA in that the system is initialized with a population of random solutions.

While GAs can handle combinatorial optimization problems, PSO can handle continuous optimization problems. However, unlike a GA each population individual is also assigned a randomized velocity, in effect, flying them through the solution hyperspace. PSO has been expanded to also handle combinatorial optimization problems. As is obvious, it is possible to simultaneously search for an optimum solution in multiple dimensions. Unlike other EC techniques, PSO can be realized with only a small program. Natural creatures sometimes behave as a swarm. One of the main goals of artificial life researches is to examine how natural creatures behave as a swarm and reconfigure the swarm models inside a computer.

PSO has two simple concepts. The swarm behaviour can be modelled with a few simple rules. Even if the behaviour rules of each individual (particle) are simple, the behaviour of the swarm can be very complex. The behaviour of each agent inside the swarm can be modelled with simple vectors. This characteristic is the basic concept of PSO.

According to Boyd's examination [11], people utilize two important kinds of information in the decision process. The first one is their own experience; they have tried the choices and know which state has been better so far, and they know how good it was. Therefore, each person makes his or her decision using his or her own experiences and other peoples' experiences. This characteristic is another basic concept of PSO.

The applications of PSO are as follows: neural network learning algorithms [12], rule extraction in fuzzy neural networks [13], computer-controlled milling optimization [14], as well as power and voltage control [15]. The application of PSO in other fields is at the early stage, and more applications can be expected. Most papers are related to the method itself, and its modification and comparison with other EC methods ([14] and [15]).

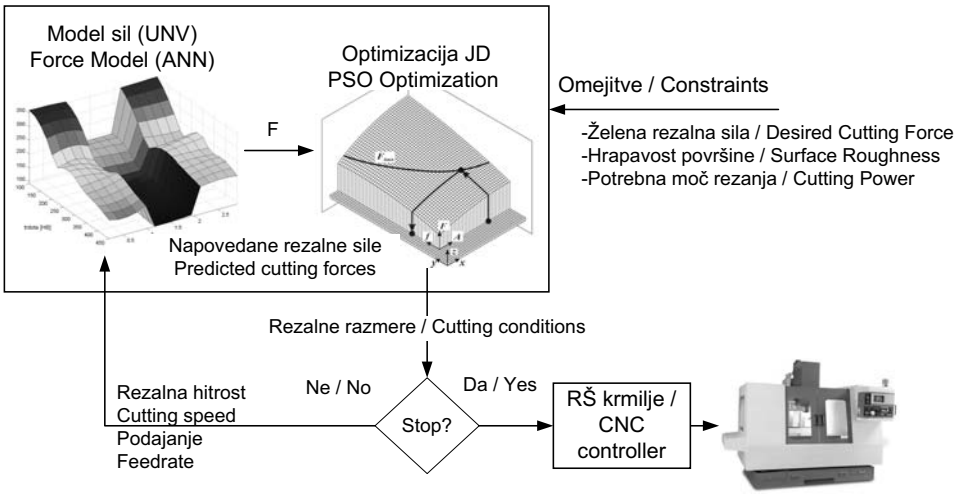

Sl. 1. *Optimizacijska shema, ki temelji na metodi OJD in nevronski mreži*
Fig. 1. PSO-based neural network optimization scheme

2 OSNOVE OPTIMIZACIJE JD

OJD je izdelana na osnovi simulacij gibanja jate ptic v dvorazsežnem prostoru. Lega vsakega delca je določena s koordinato *XY*. Hitrost delca je izražena z *vx* (hitrost v smeri osi *X*) in *vy* (hitrost v smeri osi *Y*). Spremembe lege delca je izvedena na podlagi informacije o legi in hitrosti. Jata ptic optimira določeno ciljno funkcijo. Vsak delec pozna svojo najboljšo vrednost do zdaj (*pbest*) in svojo *XY* lego. V analogiji predstavlja ta informacija osebne izkušnje posameznega delca.

Nadalje, vsak delec pozna najboljšo vrednost v skupini (*gbest* med *pbest*). Ta informacija pomeni uspešnost preostalih delcev. Vsak delec skuša spremeniti svojo lego na temelju naslednjih informacij: trenutne lege (*x, y*), trenutne hitrosti (*vx, vy*), razdalje med trenutno lego in mestom *pbest*, razdalje med trenutno lego in mestom *gbest*. To modifikacijo lahko ponazorimo z zasnovo hitrosti.

Hitrost delca se lahko spreminja po naslednji enačbi:

2 BASICS OF PSO OPTIMIZATION

PSO is developed through the simulation of bird flocking in two-dimensional space. The position of each agent is represented by the *XY* axis position and the velocity is expressed by *vx* (the velocity in the *X* axis) and *vy* (the velocity in the *Y* axis). The modification of the agent position is realized using the position and velocity information. Bird flocking optimizes a certain objective function. Each agent knows its best value so far (*pbest*) and its *XY* position. This information is an analogy with the personal experiences of each agent.

Furthermore, each agent knows the best value so far in the group (*gbest*) among the best values (*pbests*). This information is an analogy of the knowledge of how the other agents around them have performed. Each agent tries to modify its position using the following information: the current positions (*x, y*), the current velocities (*vx, vy*), the distance between the current position and (*pbest*), and the distance between the current position and (*gbest*). This modification can be represented by the concept of velocity.

The velocity of each agent can be modified by the following equation:

$$v_i^{k+1} = w \cdot v_i^k + c_1 \cdot rand_1 \cdot (pbest_i - s_i^k) + c_2 rand_2 \cdot (gbest - s_i^k) \quad (1),$$

kjer so:
- v_i^k - hitrost delca *i* v iteraciji *k,*
- w - utežna funkcija,
- c_j - utežni faktor,
- $rand$ - naključno število med 0 in 1,
- s_i^k - trenutna lega delca *i* v iteraciji *k*,

where:
- v_i^k - velocity of agent *i* at iteration *k*,
- w - weighting function,
- c_j - weighting factor,
- $rand$ - random number between 0 and 1,
- s_i^k - current position of agent *i* at iteration *k*,

- $pbest_i$ - najboljša lega delca *i*,
- *gbest* - v celoti najboljša lega delca v jati.

Po navadi uporabimo naslednjo utežno funkcijo (1):

- $pbest_i$ - pbest of agent *i*,
- *gbest* - gbest of the group.

The following weighting function is usually utilized (1):

$$w = w_{\max} - \frac{w_{\max} - w_{\min}}{iter_{\max}} \times iter \tag{2},$$

kjer so:
- w_{max} - začetna utež,
- w_{min} - končna utež,
- $iter_{max}$ - največje število iteracij,
- *iter* - trenutno število iteracij.

Z uporabo zgornje enačbe se lahko izračuna hitrost, ki se postopno približuje k *pbest* in *gbest*. Trenutna lega (iskalna točka v prostoru rešitev) se lahko popravi po naslednji enačbi:

where:
- w_{max} - initial weight,
- w_{min} - final weight,
- $iter_{max}$ - maximum iteration number,
- *iter* - current iteration number.

Using the above equation, a velocity, which gradually gets close to *pbest* and *gbest*, can be calculated. The current position (searching for the point in the solution space) can be modified by the following equation:

$$s_i^{k+1} = s_i^k + v_i^{k+1} \tag{3}.$$

Na sliki 2 je prikazana zasnova spreminjanja iskalne točke z algoritmom OJD. Na sliki 3 je prikazana zasnova iskanja z delci v prostoru rešitev. Vsak delec spreminja svojo trenutno lego po postopku seštevanja vektorjev, ki so podani na sliki 2.

Splošen diagram poteka metode OJD je podan z naslednjimi koraki:

Korak 1: Ustvarjanje začetnih pogojev vsakega posameznega delca. Začetne iskalne točke (s_i^0) in hitrosti (v_i^0) vsakega posameznega delca se določijo naključno znotraj dovoljenih mej. Trenutna iskalna točka vsakega delca se shrani v *pbest*. Najboljša vrednost *pbest* se shrani v *gbest*. Številka delca z najboljšo vrednostjo se prav tako shrani.

Figure 2 shows the concept of modifying a searching point using the PSO algorithm. Figure 3 shows a searching concept with agents in a solution space. Each agent changes its current position using the integration of vectors, as shown in Figure 2.

The general flow chart of the PSO method can be described as follows:

Step 1: Generation of the initial condition of each agent. The initial searching points (s_i^0) and velocities (v_i^0) of each agent are generated randomly within the allowable range. The current searching point is set to *pbest* for each agent. The best-evaluated value of *pbest* is set to *gbest* and the agent number with the best value is stored.

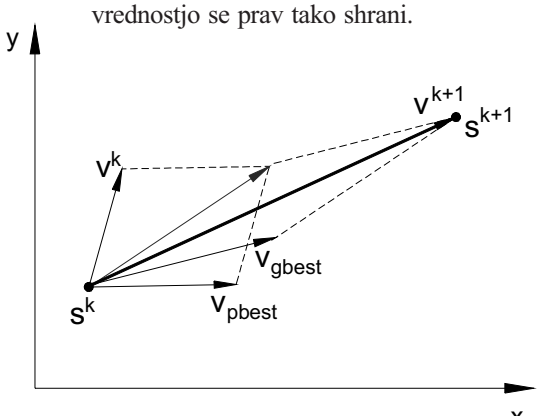

Sl. 2. *Zasnova spreminjanja iskalne točke po algoritmu OJD*

Fig. 2. *Concept of modifying a searching point according to a PSO algorithm*

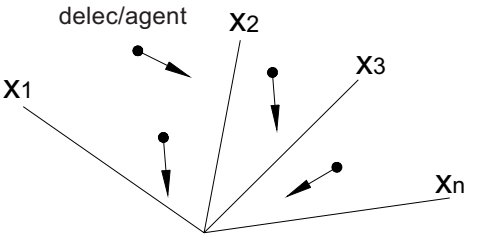

Sl. 3. *Z delci ponazorjeno načelo iskanja v prostoru rešitev*

Fig. 3. *Concept of searching with agents in a solution space*

Korak 2: Ocenjevanje uspešnosti iskanja vsakega posameznega delca. Izračun ciljne vrednosti za vsak delec. Če je vrednost boljša od trenutne vrednosti *pbest* delca, se *pbest* nadomesti z novo vrednostjo. Če je najboljša vrednost *pbest* boljša kakor trenutna *gbest*, potem se *gbest* nadomesti z najboljšo vrednostjo. Številka delca se skupaj z najboljšo vrednostjo shrani.

Korak 3: Sprememba vsake posamezne iskalne točke. Trenutna iskalna točka se spreminja z uporabo enačb (1), (2) in (3).

Korak 4: Preverjanje ustavitvenega pravila. Ko je doseženo vnaprej določeno največje število iteracij, se algoritem ustavi. V nasprotnem primeru se preide na korak 2.

Na sliki 4 je prikazan splošen algoritem strategije OJD.

Lastnosti postopka OJD lahko povzamemo v naslednjih točkah:

1. Iz enačb (1), (2) in (3) je razvidno, da lahko z OJD rešujemo zvezne optimizacijske probleme.
2. PSO uporablja več iskalnih točk, tako kakor genetski algoritem (GA). Iskalne točke se z

Step 2: Evaluation of the searching point of each agent. The objective function value is calculated for each agent. If the value is better than the current *pbest* of the agent, the *pbest* value is replaced by the current value. If the best value of *pbest* is better than the current *gbest*, *gbest* is replaced by the best value and the agent number with the best value is stored.

Step 3: Modification of each searching point. The current searching point of each agent is changed using (1), (2) and (3).

Step 4: Checking the exit condition. The current iteration number reaches the predetermined maximum iteration number, then exits. Otherwise, go to step 2.

Fig. 4 shows the general flow chart of the PSO strategy.

The features of the PSO procedure can be summarized as follows:

1. As shown in (1), (2) and (3), the PSO can handle continuous optimization problems.
2. The PSO utilizes several searching points, like a genetic algorithm (GA), and the searching points

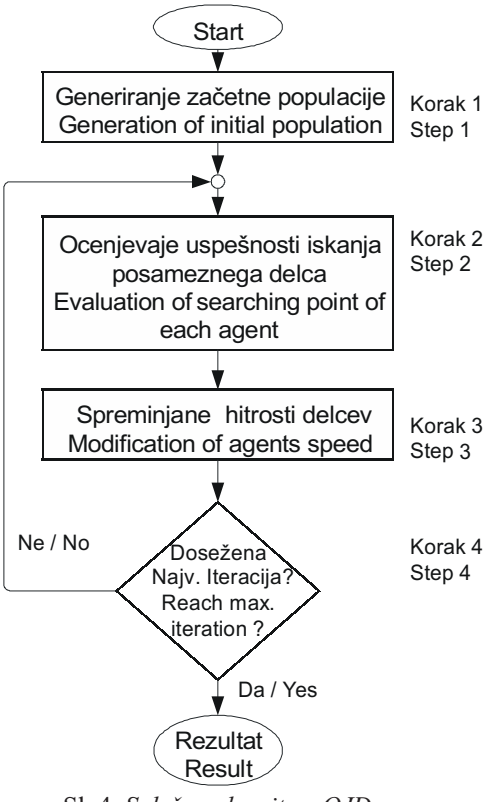

Sl. 4. *Splošen algoritem OJD*
Fig. 4. *A general PSO algorithm*

uporabo *pbest* in *gbest* počasi približujejo optimalni točki.

3. Zgornja zasnova je razložena le na oseh *XY* (dvorazsežni prostor). Vendar lahko metodo z lahkoto uporabimo na *n*-razsežnem prostoru.

Z namenom izboljšati stopnjo konvergence algoritma OJD so raziskovalci ([8] in [9]) predlagali spremembe sedanje OJD. Te spremembe se nanašajo na uporabo najboljše lege, največjega skoka hitrosti, vztrajnosti, izletavanja, izbranega delca in izbrane hitrosti.

Največja hitrost

Na osnovi numeričnih preizkusov izberemo začetno vrednost v^0_{max} =100, nato to vrednost zmanjšamo za delež ψ. Numerični preizkusi dajejo slutiti, da ta postopek izboljša stopnjo konvergence algoritma:

$$v^{k+1}_{\max} = \psi \cdot v^{k}_{\max}; \quad 0 \le \psi \le 1 \tag{4}.$$

Najboljša lega

Pomeni, da do zdaj najboljša lega v jati nadomesti najboljšo lego jate. S postopkom se poveča pritisk na delec, da konvergira k celotnemu optimumu, brez preračunavanj funkcij. Numerični preizkusi dajejo slutiti, da ta postopek izboljša stopnjo konvergence algoritma.

Izletavanje

Ta dejavnik oponaša naključno (začasno) izletavanje ptic iz jate, ki povečuje smerno razpršitev v jati in ima nekaj podobnosti z opravilom sprememb v genetskem algoritmu. Ptice tako preiskujejo do zdaj neznano področje, kar na splošno poveča verjetnost, da se najde optimum.

Izbrani delec

Ta zasnova je izposojena pri GA, kjer gen z najboljšo prilagoditvijo nikoli ne izgine. Skladni delec nadomesti najslabšega v jati. Numerični rezultati kažejo, da skladni delec izboljša stopnjo konvergence.

3 PRILAGODITEV TEHNIKE OJD OPTIMIZACIJSKEMU PROBLEMU FREZANJA

Z namenom iskanja optimalnih rezalnih parametrov integriramo nevronski model rezalnih

gradually get close to the optimal point using their pbests and the gbest.

3. The above concept is explained using only the XY-axes (two-dimensional space). However, the method can be easily applied to an n-dimensional problem.

With the objective to improve the rate of convergence of the PSO algorithm, researchers ([8] and [9]) proposed some modifications to the existing PSO. These modifications relate to the use of the best ever position, the maximum velocity, the inertia, the craziness, the elite particle and the elite velocity.

Maximum velocity

Based on a numerical experimentation, we select a starting value v^0_{max} =100 and then decrease this value by the fraction ψ. The numerical experimentation suggests that this approach improves the convergence rate of the algorithm:

Best ever position

This means that the best ever position in the swarm replaces the best position of the swarm. This procedure increases the pressure exerted on the agent to converge towards the global optimum without additional function evaluations. Numerical experimentation suggests that this approach improves the convergence rate of the algorithm.

Craziness

The craziness operator mimics the random (temporary) departure of birds from the flock. Craziness has some similarity to the mutation operator in a genetic algorithm, since it increases the directional diversity in the flock. "Crazy" birds explore previously uncovered ground, which in general increases the probability of finding the optimum.

Elite agent

The concept is borrowed from the GA where the gene with the best fitness never vanishes. The elite particle replaces the worst positioned particle in the swarm. Numerical results indicate that the elite particle improves convergence rates.

3 ADAPTING THE PSO TECHNIQUE TO A MILLING OPTIMIZATION PROBLEM

In order to search for optimal process parameters, the neural network model of cutting force

sil z optimizatorjem OJD. Zgradba sistema je prikazana na sliki 1. Skupek nevronskih modelov je razvrščen v splošni nevronski model, njegovi izhodi so posredovani večciljnemu optimizatorju jate delcev, kjer so definirane ciljne funkcije in omejitve. Algoritem OJD je začet z naključno ustvarjenimi delci, ki so kandidati za optimalno rešitev. Model nevronske mreže napove rezalne sile za vsak delec. Napovedane sile se uporabijo pri izračunu ciljne funkcije, ki jo želi OJD najbolj zvečati.

Postopek optimiranja poteka v dveh fazah. V prvi fazi nevronski model rezalnih sil ustvari v odvisnosti od priporočenih rezalnih pogojev 3-D površino rezalne sile, ki predstavlja prostor mogočih rešitev za algoritem OJD. Ta površina je omejena z ravninami, ki ponazarjajo omejitve postopka odrezavanja. Med postopkom optimiranja frezanja upoštevamo 7 omejitev, ki izvirajo iz tehnoloških določil. Podane so v preglednici 1. Soočimo se z nelinearno ciljno funkcijo skupaj z nizom omejitvenih neenačb, ki so prav tako lahko močno nelinearne. Prisotnost nelinearnosti povzroča dodatne težave pri iskanju optimuma.

Največji problem pri uvajanju tehnike OJD je izpeljava ciljne funkcije, ki ponazarja naravo optimizacijskega problema. Ciljna funkcija se uporabi kot edina povezava med optimizacijskim problemom in algoritmom OJD. Za ciljno funkcijo je

was integrated with a particle swarm optimizer. The architecture of the system is shown in Figure 1. Multiple neural network models are grouped together under the general neural network model, and its output is fed into the multi-objective particle swarm optimizer, where the objective functions and constraints are defined. The PSO algorithm is initiated with randomly generated particles that are optimum solution candidates. The neural network model predicts the cutting forces for each of the particles. The predicted forces are used in the calculation of an objective function in which the PSO tries to maximize.

The optimization process executes in two phases. In first phase, the neural prediction model, on the basis of the recommended cutting conditions, generates the 3D surface of the cutting forces, which represent the feasible solution space for the PSO algorithm. The cutting force surface is limited with planes that represent the constraints of the cutting process. Seven constraints, which arise from technological specifications, are considered during the optimization process. Those constraints are listed in Table 1. Here we are faced with a non-linear objective function along with a set of inequality constraints that may also be highly non-linear. The presence of non-linearities creates additional problems for finding the minimum.

The biggest problem in the implementation of the PSO technique is the construction of a fitness (objective) function that adequately epitomizes the nature of the problem. The objective function serves as the only link between the optimization problem

Preglednica 1. *Uporabljene omejitve z neenačbami*
Table 1. *Used constraints and their expressions*

Constraints	Izraz / Expression	Spremenljivke / Variables
podajanje feedrate	$f_{\min} \le \frac{1000 \cdot z}{\pi \cdot D} v_c \cdot f_z \le f_{\max}$	z – število zob / number of teeth, f_z – podajanje na zob / feeding per tooth, D – premer frezala / diameter of cutter
vrtilna frekvenca spindle speed	$n_{\min} \le \frac{1000}{\pi \cdot D} v_c \le n_{\max}$	v_c – rezalna hitrost / cutting speed
prečna globina rezanja radial depth of cut	$R_D \le ae_{\max}$	ae_{max} – najv. radialna globina reza / max. radial depth of cutting
vzdolžna globina rezanja axial depth of cut	$A_D \le ap_{\max}$	ap_{max} – najv. aksialna globina rezanja / max. axial depth of cutting
moč rezanja power of cutting	$\frac{MRR \cdot Kc}{60} \le P_{dov}$	MRR – stopnja odrezavanja materiala / metal removal rate, Kc – specifična rezalna sila / specific cutting force
rezalna sila cutting force	$F(f,n) \le F_{ref}$	F_{ref} – želena rezalna sila / desired cutting force
hrapavost površine surface roughness	$R_a \le R_{a\,ref}$	$R_{a\,ref}$ - želena hrapavost površine / desired surface roughness

izbrana z UNV ustvarjena površina največje rezalne sile.

V drugi fazi algoritem OJD ustvari jato delcev na površini rezalne sile. Jata delcev potuje po površini in išče skrajnost rezalne sile. Koordinate tistega delca, ki je našel največjo rezalno silo, predstavljajo optimalne rezalne pogoje (v, n). Naloga algoritma OJD je s prilagajanjem podajanja in vrtljajev ohranjati največjo rezalno silo na ravni referenčne vrednosti. Na sliki 5 je prikazan diagram postopka OJD za optimiranje postopka frezanja.

Potek optimizacije je podan z naslednjimi koraki:

1. Ustvarjanje in začenjanje matrike 50 delcev z naključnimi legami in hitrostmi. Vektor hitrosti ima dve razsežnosti. Prva je podajanje, druga je vrtilna frekvenca. Tako je zastavljena generacija 0.
2. Ovrednotenje optimizacijske funkcije (površina rezalnih sil) za vsak delec.
3. Izračun vrednosti sil za novo lego vsakega delca. Če delec doseže ugodnejšo lego, njegova trenutna vrednost nadomesti vrednost *pbest*.

and the PSO algorithm. For the objective function a surface of maximum cutting forces is selected, generated by the ANN.

The PSO algorithm generates a swarm of particles on the cutting-force surface during the second phase. The swarm of particles flies over the cutting-force surface and searches for the maximal cutting force. The coordinates of a particle that has found the maximal (but still allowable) cutting force represent the optimal cutting conditions. Figure 5 shows the PSO flowchart for the optimization of the milling process.

The optimization process is described by the following steps:

1. Generation and initialization of an array of 50 particles with random positions and velocities. The velocity vector has two dimensions: feed rate and spindle speed. This constitutes Generation 0.
2. The evaluation of the objective (cutting-force surface) function for each particle.
3. The cutting-force values are calculated for new positions of each particle. If a better position is achieved by particle, the *pbest* value is replaced by the current value.

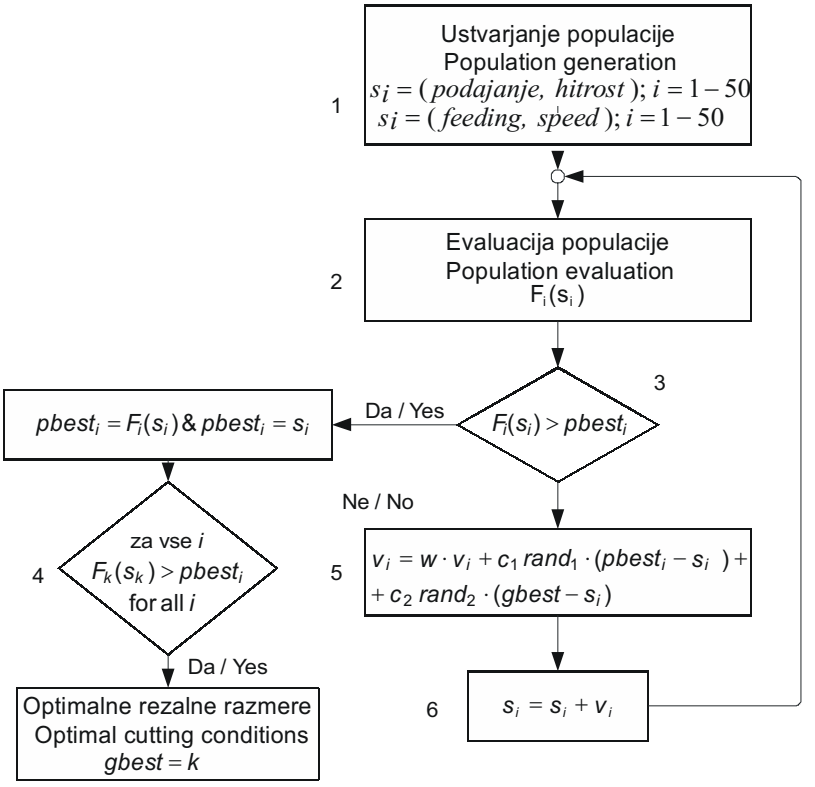

Sl. 5. *Algoritem OJD za optimiranje rezalnih razmer*
Fig. 5. *PSO algorithm for optimizing the cutting conditions*

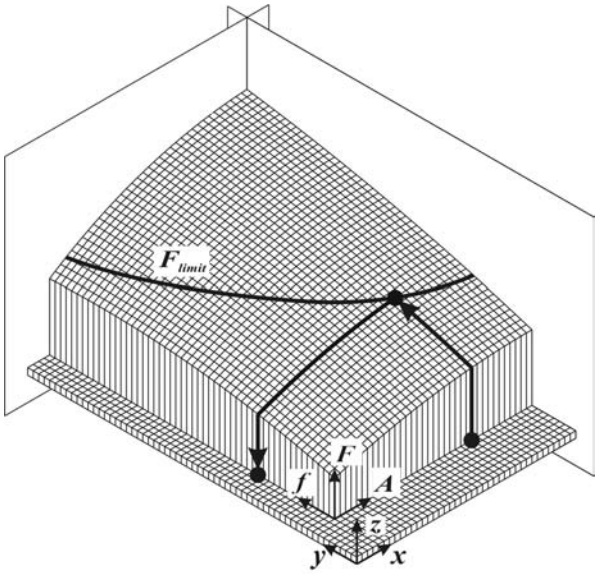

Sl. 6. *Postopek iskanja optimalnega podajanja*
Fig. 6. *Optimal feeding searching procedure*

4. Preverjanje, ali je delec našel največjo rezalno silo v populaciji. Če je nova *gbest* vrednost boljša od prejšnje se shrani v spremenljivko *gbest*. Rezultat optimizacije je vektor *gbest* (podajanje, vrtilna hitrost)
5. Izračun nove hitrosti delca.
6. Popravek lege delca s pomikom k največji rezalni sili.
7. Ponavljanje korakov 1 in 2, dokler ne dosežemo vnaprej določene iteracije.

Na sliki 6 je prikazano poenostavljeno načelo optimiranja rezalnih razmer pri frezanju z uporabo metode OJD. V tem primeru jata delcev potuje po površini sile in išče optimalno podajanje pri nespremenljivem prerezu odrezka A. Optimalno podajanje je v presečišču naslednjih treh ploskev: površine rezalne sile, ploskve z nespremenljivim prerezom odrezka (navpična ravnina) in ravnine primerjalne sile. Koordinata delca v jati, ki se najbolj približa presečišču ravnin, pomeni optimalno vrednost podajanja.

4 RAČUNALNIŠKI PROGRAM ZA OPTIMZACIJO OJD

Programsko opremo OJD sestavlja zbirka Matlabovih m- datotek. Programska oprema se lahko uporabi za optimizacijo poljubnega nelinearnega sistema. Zahtevane vrednosti se lahko vnesejo v programskem oknu, ki je prikazano na sliki 7. V levem

4. The determination if the particle has found the maximal force in the population. If the new gbest value is better than previous gbest value, the gbest value is replaced by the current *gbest* value and stored. The result of the optimization is the vector *gbest* (feedrate, spindle speed).
5. Computation of the particles' new velocity
6. Update particle's position by moving towards the maximal cutting force.
7. Steps 1 and 2 are repeated until the iteration number reaches a predetermined iteration

Figure 6 shows the simplified principle of the optimization of the cutting conditions using the PSO. In this case the swarm flies over the force surface and searches for optimal feeding at a constant cheap cross-section A. The optimal feed rate is located at the cross-section of the following three planes: the cutting force surface, the plane with the constant cheap cross-section (vertical plane) and the desired cutting force plane. The coordinate of the particle that is the nearest to the mentioned cross-section represents the optimal feed rate.

4 COMPUTER SOFTWARE FOR PSO OPTIMIZATION

A collection of Matlab's m-files forms the PSO software for the optimization. This software can be used for the optimization of an arbitrary non-linear system. The required input values can be inserted into the software window shown in Figure 7. On the

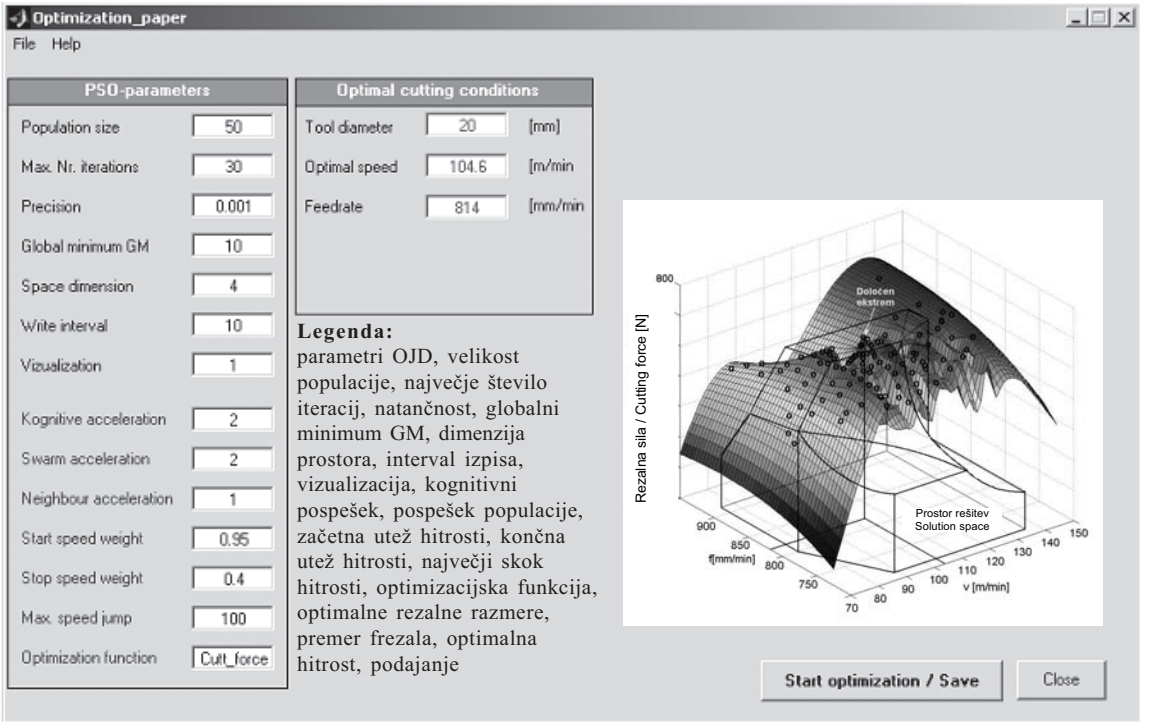

Sl. 7. *Programsko okno optimizacije OJD*
Fig. 7. *Software window for PSO optimization*

delu okna se nastavijo parametri, ki so potrebni za delovanje algoritma OJD. Rezultat optimizacije (optimalni rezalni parametri) se prikažejo na sredini okna. Postopek optimizacije grafično spremljamo na grafu.

5 TESTNI PRIMER OPTIMIZACIJE PSO REZALNIH POGOJEV

Na naslednjem testnem primeru je prikazana ponovljivost in robustnost algoritma OJD. Da preverimo stabilnost in robustnost predlagane optimizacijske strategije, sistem najprej analiziramo s simulacijami, nato sistem preverimo na RK frezalnem stroju (tip HELLER BEA1) za Ck 45 in 16MnCrSi5 XM jeklene obdelovance [16]. Za preizkuse uporabimo krogelno končno frezalo (R220-20B20-040) premera 20 mm z dvema rezalnima robovoma in kotom vijačnice 10°. Uporabljeni so naslednji rezalni parametri in omejitve: Širina rezanja R_D=3 mm, globina rezanja A_D=5 mm, rezalna hitrost v_c=80 m/min, $n \leq 2000$ min^{-1}, $10 \leq f \leq 900$ mm/min, $F(f, n) \leq Fref$ = 600 N. Ciljna funkcija je določena z nevronskim modelom rezalnih sil (simulator rezalnih sil). Cilj primera je do skrajnosti zvečati ciljno funkcijo ob upoštevanju danih omejitev [17]. Ta problem je

left-hand side of the window, the parameters required for executing the PSO algorithm can be set. The result of the optimization (the optimal cutting parameters) is shown in the middle of the window. The process of optimization is monitored on a graph.

5 PSO OPTIMIZATION OF TEST-CASE CUTTING CONDITIONS

The repeatability and robustness of the PSO algorithm is demonstrated with the following test case. To examine the stability and robustness of the proposed optimization strategy, the system is first analyzed by simulations; then the system is verified by experiments on a CNC milling machine (type HELLER BEA1) for Ck 45 and 16MnCrSi5 XM steel workpieces [16]. The ball-end milling cutter (R220-20B20-040) with two cutting edges, of 20 mm diameter and 10° helix angle, was selected for the experiments. The following cutting parameters and constraints are used: milling width R_D=3 mm, milling depth A_D=5 mm, cutting speed v_c=80 m/min, $n \leq 2000$ min^{-1}, $10 \leq f \leq 900$ mm/min, and $F(f, n) \leq Fref$ = 600 N. The objective function is determined by the neural cutting-force model (the cutting-force simulator). The goal of this case is to maximize the objective function

Preglednica 2. *Ponovljivost rezultatov*
Table 2. *Repeatability of results*

Test/Run	n min^{-1}	f mm/min	F N	Št. iteracij Nr. of iterations
1	1998	808,2	598	22
2	1995	810,1	600	25
3	1997	811,2	600	28
4	1997	819,7	598	32
5	2000	819,1	598	22
6	1999	819,2	598	31
7	1999	808,0	597	26
8	1998	808,8	598	21
9	1998	808,9	598	32
10	2000	808,1	597	30

rešen z uporabo algoritma OJD. V algoritmu OJD uporabimo 50 delcev. Postopek iskanja se izvaja, dokler napaka gradienta ni manjša od izbrane vrednosti. Matlab® simulira naučeno nevronsko mrežo pri napovedovanju rezalnih sil za dane rezalne razmere, te vrednosti se nato uporabijo pri izračunu ciljne funkcije, ki jo algoritem OJD skuša najbolj povečati. Rezultati so prikazani v preglednici 2. Številka testa ustreza vsakemu poskusu programa, da poišče optimalne rezalne parametre. V preglednici 2 so prikazane optimalne rezalne razmere skupaj s številom iteracij, ki so potrebne za dosego omenjenega optimuma.

Ta optimizacijska metoda ima večjo konvergenco v nasprotju od običajnih metod in je

under given constraints [17]. This problem is solved using the PSO algorithm. In the PSO, 50 particles were used and the search continues until the error gradient is smaller than a specified value. Matlab simulates the trained neural network to predict the cutting forces under given cutting conditions and these values are used to calculate the objective function, which the PSO algorithm attempts to maximize. The results are presented in Table 2. Each run corresponds to each time the program is run to find the optimum machining parameters. Table 2 shows the optimal cutting conditions along with the number of generations it took to reach that optimum.

This optimization method has better convergence, unlike traditional methods, and it is always

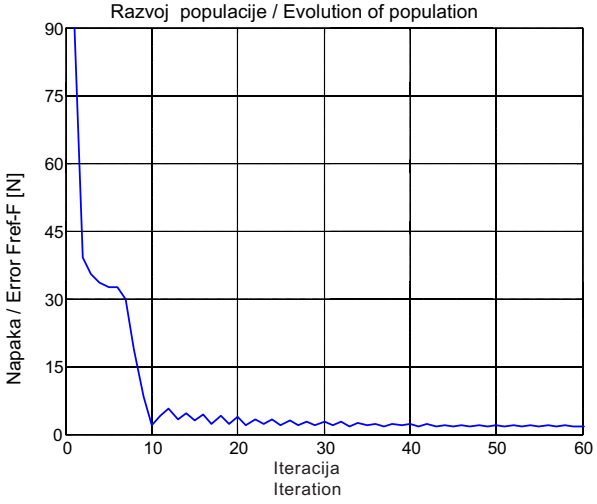

Sl. 8. *Zmanjševanje napake optimacije med razvojem jate*
Fig. 8. *Decrease of optimization error during swarm evolution*

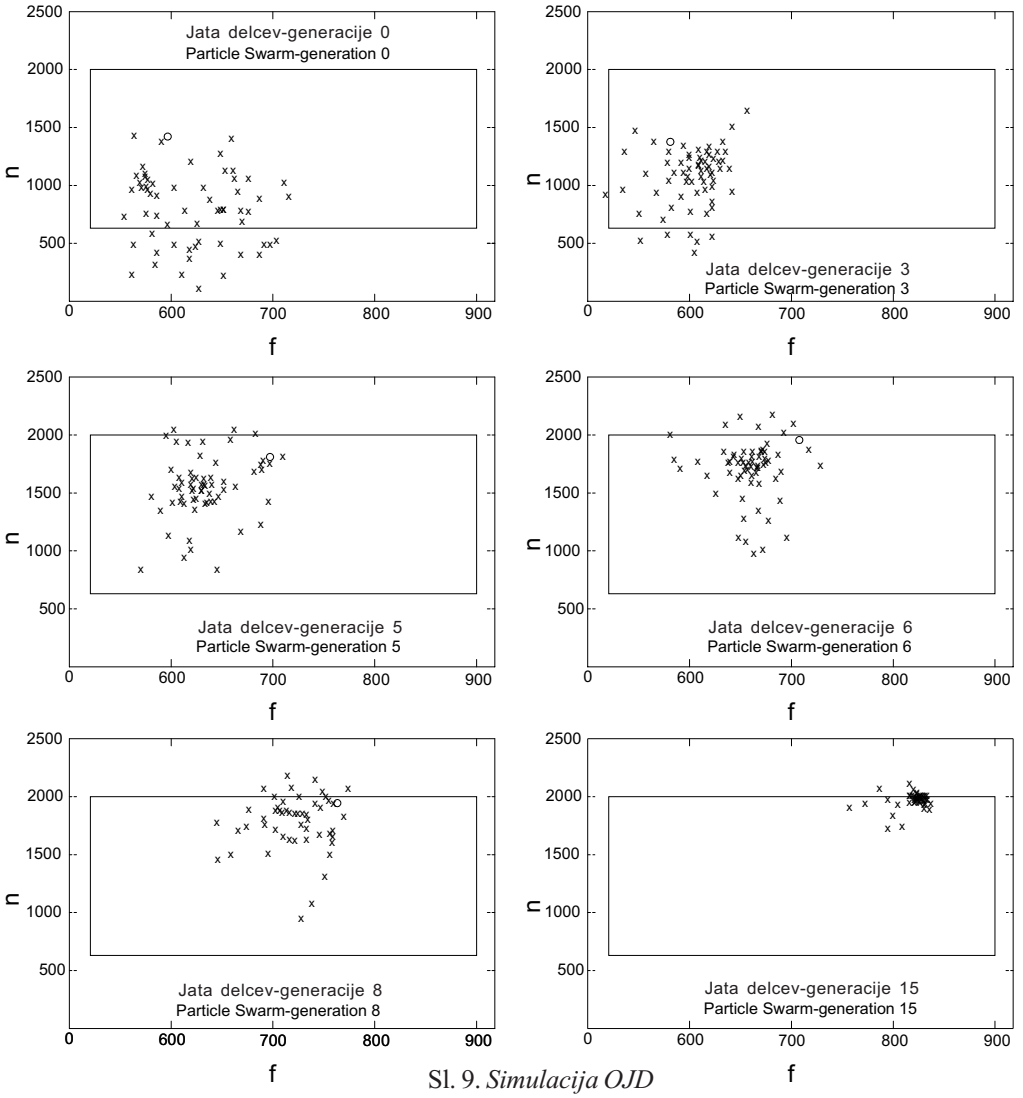

Sl. 9. *Simulacija OJD*
Fig. 9. *PSO simulation*

vedno uspešna pri iskanju celotnega optimuma. Rezultat optimiranja podajanja in hitrosti je 35-odstotno zmanjšanje obdelovalnega časa. Na sliki 8 je prikazan primer razvoja jate delcev.

Slika 9 prikazuje tipičen vzorec gibanja jate delcev proti optimalni rešitvi. Generacija 0 pomeni naključno začenjanje koordinat delca v prostoru rešitev. V nadaljnjih generacijah sledimo jati z oznako "x". Najboljši član populacije je označen z "O". S pravokotnikom je grafično ponazorjen prostor rešitev. Sprejemljivo rešitev mora biti poiskana znotraj tega dvorazsežnega prostora. Tretjo omejitev - silo tudi upoštevamo, čeprav ni prikazana na slikah. S simulacijami prikažemo robustnost in učinkovitost algoritma.

successful in finding the global optimum. The machining time is reduced by 35% as a result of optimizing the feed and the speed. A sample of the evolution of the particle swarm is presented in Fig. 8.

Figure 9 shows a typical particle swarm movement pattern toward the optimum solution. Generation 0 represents the random initialization of the particle's coordinates in the solution space. In subsequent generations, the swarm is tracked with "x". The best member in the population is represented by "O". The solution space is graphed by the rectangle. An acceptable solution has to be found within this two-dimensional space. A third constraint, acting on the force is also active, and as such is not part of these illustrations. Using simulations the robustness and the efficiency of the algorithm are demonstrated.

6 POVZETEK IN NADALJNJE RAZISKAVE

V raziskavi je prikazan postopek večciljnega optimiranja postopka frezanja z uporabo nevronskega modeliranja in optimizacije, ki temelji na zakonitostih gibanja majhnih delcev v velikih jatah. Za napovedovanje rezalnih sil je uporabljen model rezalnih sil, za določitev optimalne rezalne hitrosti in podajanja uporabimo algoritem OJD. Med optimizacijo smo uporabili zbirko sedmih omejitev. Nato z nevronskim modelom rezalnih sil napovemo ciljno funkcijo. Nadalje je uporabljen algoritem OJD, s katerim optimiramo tako podajanje in rezalno hitrost za značilen primer iz industrije. Eksperimentalni rezultati pokažejo, da se MRR izboljša za 28%. Opažena je tudi 20-odstotno zmanjšanje časa obdelave. Prispevek pripravlja teren za nov razred RR optimizacijskih tehnik na področju obdelave z odrezovanjem. V prispevku so prav tako predstavljene osnove optimizacije OJD. Medtem ko je bilo veliko tehnik razvojnega računanja izdelanih za reševanje sestavnih optimizacijskih problemov, je bila OJD izdelana za reševanje neprekinjenih problemov. Metoda OJD je lahko učinkovito orodje za reševanje nelinearnih neprekinjenih, sestavnih in kombiniranih - integriranih optimizacijskih problemov.

6 CONCLUSION AND FUTURE RESEARCH

This study has presented the multi-objective optimization of the milling process by using neural network modelling and particle swarm optimization. A neural network model was used to predict the cutting forces during the machining and the PSO algorithm was used to obtain the optimum cutting speed and feed rate. A set of seven constraints were used during the optimization. Next, the neural force model was used to predict the objective function. Next, the PSO algorithm was used to optimize both the feed and the speed for a typical case found in industry. The experimental results show that the MRR is improved by 28%. Machining time reductions of up to 20% were also observed. This paper opens the door for a new class of EC-based optimization techniques in the area of machining. This paper also presents the fundamentals of PSO optimization techniques. While a lot of evolutionary computation techniques have been developed for combinatorial optimization problems, the PSO has been basically developed for continuous optimization problems. The PSO can be an efficient optimization tool for solving nonlinear continuous optimization problems, combinatorial optimization problems, and mixed-integer nonlinear optimization problem.

7 LITERATURA
7 REFERENCES

[1] Župerl, U., F. Čuš (2004) Določevanje značilnih tehnoloških in gospodarskih parametrov med postopkom odrezovanja = A determination of the characteristic technological and economic parameters during metal cutting. *Stroj. vestn*., 5(2004), pp. 252-266.

[2] Čuš, F., J. Balič (2003) Optimization of cutting process by GA approach. *Robot. Comput. Integr. Manuf.* 19(2003), pp. 113-121.

[3] Župerl, U., F. Čuš (2003), Optimization of cutting conditions during cutting by using neural networks, *Robot. Comput. Integr. Manuf*., 19(2003),pp. 189-199.

[4] Balič, J. (2000) A new NC machine tool controller for step-by-step milling, *Int. J. Adv. Manuf. Technol.* 8(2000) pp. 399-403.

[5] Ozcan, E., C. Mohan (1998), Analysis of a simple Particle Swarm Optimization system, *Intelligent Engineering Systems Through Artificial Neural Networks*, 8(1998), pp. 253-258.

[6] Shi Y., R. Eberhart (1998), Parameter selection in Particle Swarm Optimization, *In Evolutionary Programming VII: Proc. EP98*, New York: Springer-Verlag (1998), pp. 591-600.

[7] Angeline, P.J. Evolutionary optimization versus Particle Swarm Optimization: philosophy and performance differences, *in: Proceedings of the 7th ICEC*, (1998), pp. 601-610.

[8] Kennedy, J., R.C. Eberhart (1995) Particle Swarm Optimization, *Proceedings of IEEE Int. Conference on Neural Networks*, 4(1995), pp. 1942-1948.

[9] Reynolds, C. (1990) Flocks, herds, and schools: a distributed behavioural model, *Computer Graphics*, 21(1990), pp. 25-34.

[10] R.C., Eberhart, Y. Shi (2003), Comparison between genetic algorithm and Particle Swarm Optimization, *Proceedings of the 7th ICEC*, (1998), pp. 611-616.
[11] Boyd, J. (2003), Thinking is Social: Experiments with the adaptive culture model, *Journal of Conflict Resolution*, 42(1998), pp. 56-76.
[12] Balic J. (2003), Optimization of cutting process by GA approach, *Robot. Comput. Integr. Manuf*. 19(2003) 113-121.
[13] He, Z., C. Wei, L. Yang, X. Gao, S. Yao, R. Eberhart, Y.: Shi, (1998), Extracting rules from fuzzy neural network by Particle Swarm Optimization, *Proc. of IEEE International Conference on Evolutionary Computation (ICEC'98),* (1998), pp. 66-71.
[14] Cus, F., U. Zuperl, E. Kiker, M. Milfelner (2006), Adaptive controller design for feedrate maximization of machining process, *Journal of Achievements in Materials and Manufacturing Engineering* 17(2006),pp. 237-240.
[15] Abido M.A. (2002), Optimal power flow using Particle Swarm Optimization, *International Journal of Electrical Power & Energy Systems,* 24(2002), pp. 563-571.
[16] Kopač, J. (2002) Rezalne sile in njihov vpliv na gospodarnost obdelave = Cutting forces and their influence on the economics of machining. *Stroj. vestn*. 3(2002), pp. 121-132.
[17] Župerl, U., F. Čuš (2004) Tool cutting force modeling in ball-end milling using multilevel perceptron, *J. Mater. Process. Technol.*, (2004), pp. 67-72.

Naslova avtorjev: dr. Uroš Župerl
Prof. Dr. Franci Čuš
Univerza v Mariboru
Fakulteta za strojništvo
Smetanova 17
2000 Maribor
uros.zuperl@uni-mb.si

prof. dr. Valentina Gecevska
Univerza v Skopju
Fakulteta za strojništvo
P.P. 464
1000 Skopje, Makedonija

Authors' addresses: Dr. Uroš Župerl
Prof. Dr. Franci Čuš
University of Maribor
Faculty of Mechanical Eng.
Smetanova 17
SI-2000 Maribor, Slovenia
uros.zuperl@uni-mb.si

Prof. Dr. Valentina Gecevska
University in Skopje
Faculty of Mechanical Eng.
PO Box 464
1000 Skopje, Macedonia

Prejeto: 26.2.2007
Received:
Sprejeto: 25.4.2007
Accepted:
Odprto za diskusijo: 1 leto
Open for discussion: 1 year

Strojniški vestnik - Journal of Mechanical Engineering 53(2007)6, 369-378
UDK - UDC 005.6
Pregledni znanstveni članek - Preview scientific paper (1.02)

Izboljšanje kakovosti - krog PDCA v primerjavi z DMAIC in DFSS

Quality Improvement - PDCA Cycle vs. DMAIC and DFSS

Mirko Soković[1] - Duško Pavletić[2]
([1]Fakulteta za strojništvo, Ljubljana; [2]Tehnična fakulteta na Rijeki, Hrvaška)

Za doseganje stalnih izboljšav kakovosti vsaka organizacija potrebuje ustrezno izbiro orodij in tehnik. Osnovne zahteve za uspeh v teh prizadevanjih so popolno razumevanje tako orodij in tehnik kakor tudi postopka, v katerem naj bi bili uporabljeni. Prispevek prinaša pregled in področja uporabe kroga PDCA, Šest Sigma in tehnik DFSS za stalno izboljšanje kakovosti izdelkov, postopkov in storitev. Krog PDCA je enostaven za razumevanje zasnove stalnih izboljšav kakovosti, Šest Sigma metodologija DMAIC je sistematičen pristop k vodenju projekta na osnovi dejstev, metoda DFSS pa je sistematični pristop k načrtovanju izdelka ali postopka, ki vključuje vse funkcije organizacije.

(Ključne besede: kakvost izdelkov, izboljšanje kakovosti, krog PDCA , DMAIC metoda, Šest Sigma, DFSS)

To achieve continuous quality improvements every organization needs to use an appropriate selection of tools and techniques. The fundamental requirements for success are a clear understanding, both of the tools and techniques as well as the process by which they should be applied. In this paper we provide an overview and the fields of application of the PDCA, Six Sigma and DFSS techniques for the continuous quality improvement of products, processes and services. The PDCA cycle is a simple-to-understand concept of continuous quality improvement; the Six Sigma DMAIC methodology is a systematic and fact-based project-management approach; while DFSS methodology is a systematic approach to product or process design that includes all organization functions.

(Keywords: product quality, quality improvement, PDCA cycle, DMAIC, Six Sigma, DFSS)

0 UVOD

Metodologija uvajanja upravljanja kakovosti in programa stalnega izboljšanja kakovosti je lahko različna. Program bo imel verjetno različno ime ali oznako, npr. TQM (Celovito obvladovanje kakovosti), Šest Sigma, BPR (Re-inženiring poslovnega postopka) ali proizvodna odličnost. Ne glede na metodologijo ali ime programa stalnih izboljšav bo vsaka organizacija verjetno potrebovala izbiro orodij in tehnik v svojem postopku izvajanja. Večina izmed teh orodij in tehnik je preprosta za razumevanje in bo lahko uporabna za večino ljudi v podjetju (npr. PDCA- ali Demingov krog). Vendar pa je nekaj tehnik na tem področju bolj zapletenih (Šest Sigma, Vitka Sigma ali načrtovanje za Šest Sigma - DFSS). Specialisti za reševanje specifičnih problemov uporabljajo prav te napredne tehnike. Zelo

0 INTRODUCTION

The methodology for implementing quality management and programmes for continuous quality improvement can be varied. The programme is likely to have a different name or label, such as TQM (Total Quality Management), Six Sigma, BPR (Business Process Reengineering) or Operational Excellence. Regardless of the methodology or the name of the continuous improvement programmes, each organization will certainly need to use a selection of tools and techniques in its implementation process. Most of these tools and techniques are simple to understand and can be used by a large number of people in the company, e.g., the PDCA cycle or Deming's circle. However, some techniques in this area are more complex, e.g., Six Sigma, Lean Sigma, and Design for Six Sigma. Specialists for specific problem-solving applications use these advanced techniques. It is very important that tools and techniques should be

pomembno je, da so orodja in tehnike izbrani od ustrezne skupine ter pravilno uporabljeni v ustreznem postopku. Osnovni pogoji za uspeh pri tej nalogi so popolno razumevanje samih orodij in tehnik ter postopka, v katerem bi lahko bili ti uporabljeni.

Namen tega prispevka je seznaniti bralca z značilnostmi orodja PDCA in tehnik Šest Sigma in DFSS, ki jih je mogoče uporabiti za izboljšanje kakovosti izdelkov, postopkov in storitev.

1 KROG PDCA

1.1 Definicija

V osrednjem postopku se rezultati dejavnosti primerjajo s ciljem ali nastavitveno točko. Razlika med obema vrednostma se potem vzame za popravne ukrepe, če ta razlika postaja prevelika. Ponavljajoča se in nepretrgana narava stalnih izboljšav sledi tej običajni definiciji upravljanja in je predstavljena s PDCA-krogom (načrtuj-naredi-preveri-ukrepaj) [1].

Pogosto se tudi omenja kot Demingov krog, imenovan po W.E. Demingu. Naslednja mogoča inačica PDCA je PDSA (načrtuj-naredi-študiraj-ukrepaj) [2].

1.2 Uporaba

Uporaba Kroga PDCA se je pokazala bolj učinkovita kot uporaba postopka *"naredi prav prvič"*. Uporaba Kroga PDCA pomeni nenehno iskanje učinkovitejših metod izboljšanja. PDCA je učinkovit na obeh področjih: pri *opravljanju dela* in *vodenju programa*. Omogoča dva tipa popravnih ukrepov – začasne in trajne.

Začasni ukrep se doseže kot rezultat praktične obravnave in poprave napake. Po drugi strani pa *trajni popravni ukrep* sestoji iz raziskave in odprave glavnega vzroka - cilj je vzdrževanje tako izboljšanega postopka.

Vidiki kroga PDCA, ki so uporabljeni za njegove notranje postopke zagotavljanja kakovosti:

- *Kaj bomo poskusili izpolniti?*
- *Kako bomo vedeli, da je sprememba izboljšanje?*
- *Katere spremembe lahko naredimo za izboljšanje?*

Slika 1 podrobno prikazuje krog PDCA ([3] in [4]).

selected for the appropriate team and applied correctly to the appropriate process. The fundamental requirements for success in this task are a clear understanding, both of the tools and techniques themselves and the process by which they can be applied.

The purpose of this paper is to introduce the reader to the characteristics of the PDCA tool and Six Sigma and DFSS techniques, which are possible to use for the quality improvement of products, processes and services.

1 THE PDCA CYCLE

1.1 Definition

In a central process, the actual results of an action are compared with a target or a set point. The difference between the two is then mentioned and corrective measures are adopted if the disparity becomes large. The repeated and continuous nature of continuous improvement follows this usual definition of control and is represented by the PDCA (Plan-Do-Check-Act) cycle [1].

This is also referred to as the Deming circle, named after W. E. Deming. Another variation of PDCA is PDSA (Plan, Do, Study, Act) [2].

1.2 Application

The application of the PDCA cycle has been found more effective than adopting *"the right first time"* approach. Using the PDCA cycle means continuously looking for better methods of improvement. The PDCA cycle is effective in both *doing a job* and *managing a programme.* The PDCA cycle enables two types of corrective action – temporary and permanent.

The *temporary action* is aimed at results by practically tackling and fixing the problem. The *permanent corrective action,* on the other hand, consists of investigation and eliminating the root causes and thus targets the sustainability of the improved process.

The aspects of the PDCA cycle were applied to internal quality-assurance procedures:

- *What are we trying to accomplish?*
- *How will we know that a change is an improvement?*
- *What changes can we make to improve?*

Figure 1 shows the PDCA cycle in detail ([3] and [4]).

Ukrepaj / Act

- Upravljanje neskladnosti / Managing Nonconformity
- Izboljševanje / Improvement
- Certifikat ISO 9001 / ISO 9001 Certification
- Kulturni in organizacijski vidiki / Cultural and Organizational Aspects
- Celovito obvladovanje kakvosti / Total Quality Management
- Sistem upravljanja z okoljem / Environmental Management Systems
- Povezovanje sistema upravljanja / Management System Integration

Načrtuj / Plan

- Zamisel kakovosti in cilji / The Quality Concept and Objectives
- Upoštevaj predpise / Statutory Considerations
- Funkcija in varnost izdelka / Product Liability and Product Safety
- Usposabljanje za kakovost / Training for Quality
- Nadzor načrtovanja / The Control of Design

Preveri / Check

- Uvod v statistiko / An Introduction to Statistics
- Kontrolne karte / Control Charts
- Pregled, kontrola / Inspection
- Funkcionalno preizkušanje / Functional Testing
- Oprema za kontrolo in merjenje / Inspection and Measurement Equipment
- Meroslovje / Metrology
- Presoja kakovosti in pregledi / Quality Audits and Reviews
- Stroški povezani s kakovostjo in varnostjo / Quality- and Safety-related Costs
- Primerjanje z najboljšimi / Benchmarking

Naredi / Do

- Nabava / Procurement
- Dobava ravno ob pravem času / Just-in-Time Supplies
- Zmogljivost procesa / Process Capability
- Zanesljivost izdelka / Product Reliability
- Strega materiala / Materials Handling
- Servisiranje / Servicing
- Kakovost storitev / Service Quality
- Dokumentacija in zapisi / Documentations and Records
- Nadziranje sprememb / Controlling Changes
- Standardi, standardizacija, skladnost, harmonizacija / Standards, Standardization, Conformity and Compatibility

Sl. 1. *Krog PDCA*
Fig. 1. *PDCA cycle*

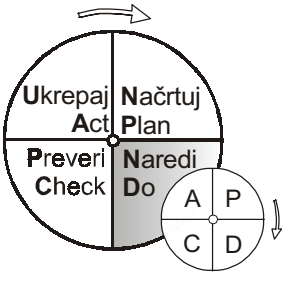

Sl. 2. *Napredni krog PDCA [5]*
Fig. 2. *Advanced PDCA cycle [5]*

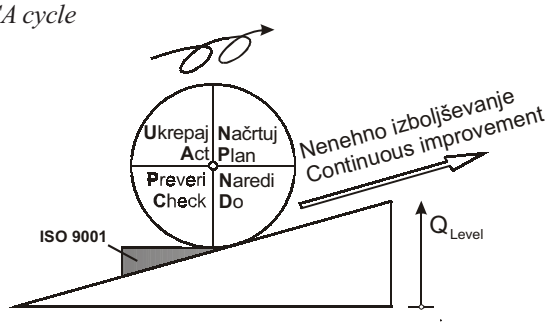

Sl. 3. *Krog PDCA v procesu stalnih izboljšav*
Fig. 3. *PDCA cycle in continuous improvement process*

V fazi *naredi* je mogoče vključiti *manjši* Krog PDCA (slika 2), dokler se problemi pri izvajanju ne razrešijo [5].

PDCA je več kakor samo orodje; je zasnova stalnega izboljšanja postopkov (sl. 3), ki je vgrajena v kulturo organizacije (podjetja). Najpomembnejši vidik PDCA leži v fazi *ukrepaj* po izpolnitvi projekta, ko celotni krog ponovno zaženemo za naslednje izboljšanje.

Krog PDCA prav tako lahko uporabimo znotraj zasnove Kaizen (sl. 4). V tem primeru govorimo o SDCA (standardiziraj, naredi, preveri, ukrepaj) in krogih PDCA [6].

In the *Do* stage or implementation stage it is possible to involve a *mini-PDCA cycle* (Fig. 2) until the issues of implementation are resolved [5].

The PDCA cycle is more than just a tool; it is a concept of continuous improvement processes (Fig. 3) embedded in the organization's culture. The most important aspect of PDCA lies in the *"act"* stage after the completion of a project when the cycle starts again for the further improvement.

The PDCA cycle is also possible to use within the Kaizen concept, Figure 4. In this case we are talking about the SDCA–PDCA cycle [6].

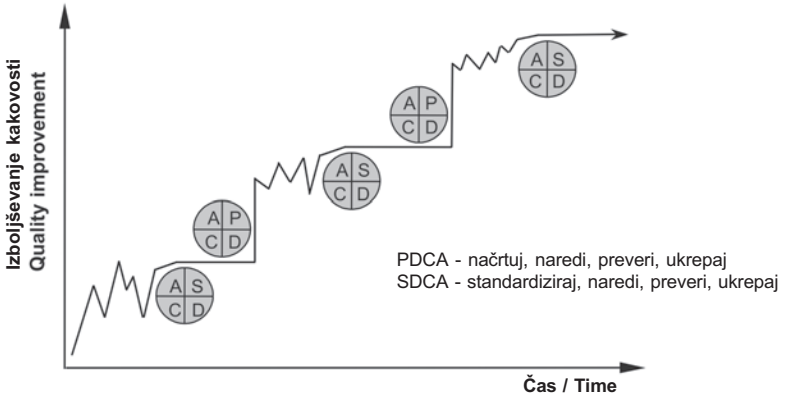

Sl. 4. *Krogi SDCA – PDCA za izboljševanje kakovosti v zasnovi Kaizen*
Fig. 4. *SDCA–PDCA cycles for quality improvement in the Kaizen concept*

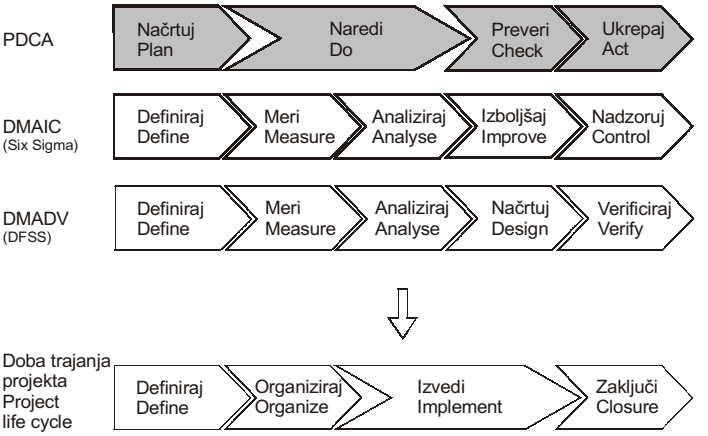

Sl. 5. *Krog PDCA nasproti DMAIC (Šest Sigma), DMADV (DFSS) in Dobi trajanja projekta (PLC)*
Fig. 5. *The PDCA cycle vs. DMAIC (Six Sigma), DMADV (DFSS) and the Product Life-Cycle (PLC)*

Medtem ko se Demingov Krog PDCA na veliko uporablja v razvoju in pri razširjanju politike kakovosti, sta DMAIC (Šest Sigma) in DMADV (DFSS) dodali natančnost dobi trajanja projekta (PLC) pri uvajanju in sklenitvi Šest Sigma projektov. Slika 5 kaže zvezo med PDCA-krogom, DMAIC, DMADV in tipično dobo trajanja projekta (PLC) ([1] in [2]).

2 DMAIC

2.1 Definicija

DMAIC izkorišča zasnovo s podatki upravljane dobe trajanja Šest Sigma projektov za izboljšanje postopka in je bistven del programa Šest Sigma v podjetju. DMAIC je kratica za pet medsebojno povezanih faz: definiraj, meri, analiziraj, izboljšaj in krmili (nadziraj). Preproste definicije posameznih faz so [1]:

While Deming's PDCA cycle has been extensively used in the development and deployment of quality policies, DMAIC (Six Sigma) and DMADV (DFSS) have added the rigour of a project life-cycle (PLC) to the implementation and close-out of Six Sigma projects. Figure 5 shows the relationship between the PDCA cycle, DMAIC, DMADV and a typical project life-cycle ([1] and [2]).

2 DMAIC

2.1 Definition

DMAIC (Define, Measure, Analyse, Improve, and Control) refers to a data-driven life-cycle approach to Six Sigma projects for improving processes; it is an essential part of a company's Six Sigma programme. DMAIC is an acronym for five interconnected phases: define, measure, analyse, improve and control. The simplified definitions of each phase are [1]:

- o *Definiraj* pravi projekt z razpoznavo, prednostjo in izbiro.
- o *Meri* ključne značilke postopka, pomembnost parametrov in njihovo izvajanje.
- o *Analiziraj* postopek z določevanjem ključnih vzrokov in določb postopka.
- o *Izboljšaj* postopek z njegovim spreminjanjem in optimiranjem izvajanja.
- o *Krmili* postopek pri trajnostnih ciljih.

2.2 Uporaba

Orodji Šest Sigma in Proizvodna odličnost se uporabljata najbolj pogosto znotraj okvira DMAIC, ki pa je integralni del pobude Šest Sigma.

DMAIC se tudi uporablja za oblikovanje *"zaprtih postopkov"* za nadzor projekta. Merila za posamezne faze so definirana, in če so ti pri posamezni fazi projekta doseženi, se lahko začne izvajanje naslednje faze, kakor to prikazuje slika 6 ([1] in [7]).

- o *Define* by identifying, prioritizing and selecting the right project,
- o *Measure* key process characteristic, the scope of parameters and their performances,
- o *Analyse* by identifying key causes and process determinants,
- o *Improve* by changing the process and optimizing performance,
- o *Control* by sustaining the gain.

2.2 Application

The tools of Six Sigma and operational excellence are most often applied within the framework of DMAIC. As such, DMAIC is an integral part of a Six Sigma initiative.

DMAIC also used to create a *"gated process"* for project control. The criteria for a particular phase are defined and the project is reviewed, and if the criteria are met then the next phase starts, Figure 6, according to ([1] and [7]).

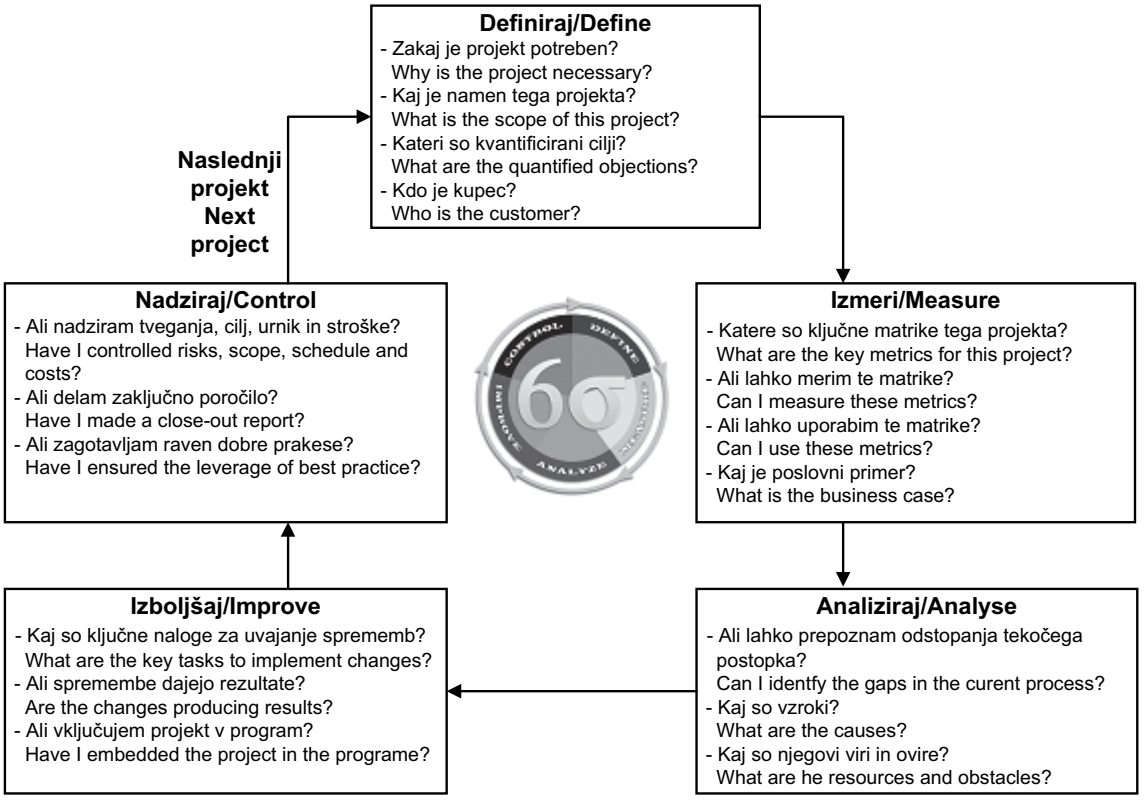

Sl. 6. *Krog DMAIC kot osnova metodologije Šest Sigma*
Fig. 6. *The DMAIC cycle as a methodology for Six Sigma*

Kot povzetek pri uporabi tehnike DMAIC lahko zapišemo: če *ne morete definirati* vašega postopka, ga tudi ne *morete meriti*. To tudi pomeni, če ne morete opisati podatkov ne boste sposobni upeljati DMAIC v vaše razvojne dejavnosti. Zaradi tega ne morete izboljšati ali vzdrževati kakovosti ([8] in [9]).

DMAIC je, kakor je že bilo omenjeno, sestavni del Šest Sigem. Je sistematičen in temelji na dejstvih ter zagotavlja strogi okvir za projektno vodenje, usmerjeno na rezultate. Metodologija naj bi se pojavila kot linearna in izrecno definirana, toda treba je opozoriti, da se najboljše rezultate z DMAIC doseže, če je postopek prilagodljiv, prav tako izločanje slabih korakov. Dober je kot iterativni postopek, če je potrebno, še posebej, ko so člani skupine še začetniki na področju uporabe orodij in tehnik.

3 DFSS

3.1 Definicija

DFSS (Načrtovanje za Šest Sigem) je sistematičen in strukturiran postopek načrtovanja novega izdelka ali postopka, ki se osredotoči na *"preprečevanje problema"*. To opravi z namenom doseči ali preseči vse potrebe kupca ter *CTQ (kritične značilke kakovosti)* kot izhodne zahteve, ko se izdelek izdela prvič. Osrednji cilj DFSS je *"oblikovati stvari pravilno prvič"*.

Sistem sestoji iz vrste orodij za zbiranje potreb, inženirstva in statističnih metod, ki se uporabljajo med razvojem izdelka. DFSS zahteva natančno uporabo orodij in najboljših praks za izpolnjevanje zahtev kupca in prinaša finančne koristi pri zadovoljevanju zahtev kupca [10].

Temeljna značilka DFSS je preverjanje, ki jo razlikuje od Šest Sigem. Zagovorniki priporočajo DFSS bolj kot *celovit pristop* re-inženiringa in manj kot tehniko dopolnilno k Šest Sigmam.

3.2 Uporaba

Primarna uporaba DFSS kot tehnike je v stopnji načrtovanja in razvoja izdelka, postopka ali storitve. Načrtovanje novega izdelka ali postopka z uporabo postopka DFSS *ne nadomešča* sedanjih inženirskih metod, niti ne olajša organizaciji potrebo po skrbnem pregledovanju odličnosti v inženiringu in razvoju izdelka. To daje še dodatno vrednost pri razvoju izdelka. Pomaga v postopku inoviranja,

As a summary of the application of the DMAIC technique, if you *cannot define* your process you *cannot measure* it. This means if you cannot express the data you are not able to utilize DMAIC in your development actions. Therefore, you cannot improve and sustain the quality ([8] and [9]).

DMAIC is an integral part of Six Sigma. It is systematic and fact based and provides a rigorous framework of results-oriented project management. The methodology may appear to be linear and explicitly defined, but it should be noted that the best results from DMAIC are achieved when the process is flexible, thus eliminating unproductive steps. An iterative approach may be necessary as well, especially when the team members are new to the tools and techniques.

3 DFSS

3.1 Definition

DFSS (Design for Six Sigma) is a systematic and structured approach to new products or processes design that focuses on *"problem prevention"*. This is done with the aim of meeting or exceeding all the needs of the customer and the *CTQ (critical to quality)* output requirements when the product is first released. The major objective of DFSS is to *"design things right the first time"*.

The system consists of the set of tools, needs-gathering, engineering and statistical methods to be used during the product's development. DFSS requires the rigorous use of tools and best practices to fulfil customer requirements and brings financial benefits by satisfying customer requirements [10].

One fundamental characteristic of DFSS is the verification, which differentiates it from Six Sigma. The proponents of DFSS are promoting it as a *holistic approach* to re-engineering rather than a technique to complement Six Sigma.

3.2 Application

The primary application of DFSS as a technique is in the design and development stage of a product, process or service. Designing new products or processes using DFSS approach does *not replace* current engineering methods, nor does it relieve an organization of the need to peruse excellence in engineering and product development. It adds another dimension to product development. It helps in the

razvijanja, optimiranja in prenosa nove tehnologije v program načrtovanja izdelka. Omogoča tudi zaporedje poddejavnosti zasnove razvoja, načrtovanja, optimiranja in ovrednotenja novega izdelka pred njegovim uvajanjem na zahteven trg ([11] in [12]). DFSS metodologija prinaša kakovostne in merljive rezultate pri obvladovanju kritičnih parametrov v nasprotju od tipične vrste zahtev za izdelek, ki temelji na g*lasu kupca (VOC).*

DFSS je primerna znotraj zamisli ključnega poslovnega postopka, a to je razvoj izdelka; zajema številna orodja in najboljše prakse, ki jih lahko selektivno razvija skozi faze postopka razvoja izdelka. Posebnost DFSS je v integraciji treh ključnih taktičnih elementov za dosego zahtevanih poslovnih ciljev - nizkih stroškov, visoke kakovosti in krajših časov v razvojnem krogu izdelka [10]:

- o Jasen in prilagodljiv postopek razvoja izdelka.
- o Uravnotežena zbirka orodij za razvoj in načrtovanje ter dobrih praks.
- o Disciplinirana uporaba metod vodenja projektov.

DFSS se izogiba štetju napak in mest, na katerih se inženirski tim osredotoči na merjenje dejanskih delovanj. Dobljeni temeljni model se lahko preigra, analizira in ovrednoti statistično skozi simulacije Monte Carlo in načrtovanje poizkusov (DoE).

Napake in časi zastoja niso poglavitne metrike pri DFSS. DFSS uporablja zvezne spremenljivke, ki vodijo kazalnike nevarnosti za napake in poškodbe, meri in optimira kritične delovne odgovore ob določenih vzrokih za variiacije v proizvodnji, dostavi in uporabi okolja. Preprečevati je treba probleme – ne čakati, da se ti pojavijo in se potem odzivati na njih.

Osnovni razlog za izvajanje DFSS je finančni. To ustvarja vrednost delničarjem, ki temelji na dobavni vrednosti za kupca na trgu. DFSS pomaga izpolniti *zahteve poslovanja* z izpolnjevanjem *glasu kupca*.

Najbolj pogosto omenjena metodologija za uvajanje DFSS v prakso sta **DMADV** (definiraj, meri, analiziraj, načrtuj in overi) in **IDOV** (identificiraj, načrtuj, optimiraj in validiraj). DMADV je pogosto opisana kot naslednja stopnja DMAIC (Šest Sigem) in tako lahko vodi k rodovnemu postopku [1]. Z namenom da bi poudarili določene značilke DFSS, smo vzeli postopek IDOV, da bi ponazorili osnovne korake postopka (sl. 7) [2].

Zagovorniki DFSS verjamejo, da bodo v nekaj naslednjih letih izkušnje naraščale, DFSS pa bo

process on inventing, developing, optimizing and transferring new technology into product design program. It also enables sub-sequent conceptual development, design, optimization and verification of new products prior to launch into their respective market ([11] and [12]). DFSS methodology delivers qualitative and quantitative results by managing critical parameters against the clear set of product requirements based on *Voice of customer (VOC).*

Design for Six Sigma fits within the context of the key business process, namely the product development process; encompasses many tools and best practices that can be selectively deployed during the phases of a product development process. Specifically, DFSS integrates three major tactical elements to help attain the ubiquitous business goals of low cost, high quality and rapid cycle-time from product development [10]:

- o A clear and flexible product development process.
- o A balanced portfolio of development and design tools and best practices.
- o Disciplined use of project management methods.

DFSS avoids counting failures and places the engineering team's focus on measuring real functions. The resulting fundamental model can be exercised, analyzed and verified statistically through Monte Carlo simulations and the sequential design of experiment (DoE).

Defects and time-to-failure are not the main metrics of DFSS. DFSS uses continuous variables that are leading indicators of impending defects and failures to measure and optimize critical functional responses against assignable causes of variation in the production, delivery and use environment. We need to prevent the problems – not wait until they occur and then react to them.

The reason for using DFSS is ultimately financial. It generates shareholder value based on delivering customer value in the marketplace. DFSS helps fulfil the *voice of the business* by fulfilling the *voice of the customer*.

Most frequently reported methodologies for putting DFSS into practice are **DMADV** (**D**efine, **M**easure, **A**nalyze, **D**esign and **V**erify) and **IDOV** (**I**dentify, **D**esign, **O**ptimise and **V**alidate). DMADV is often described as the next stage of DMAIC (Six Sigma) and thus may lead to a generic approach [1]. In order to emphasize the distinctive characteristic of DFSS we have adapted IDOV to show the basic steps of the process, Figure 7 [2].

The proponents of DFSS believe that within the next few years, as experience grows, DFSS will

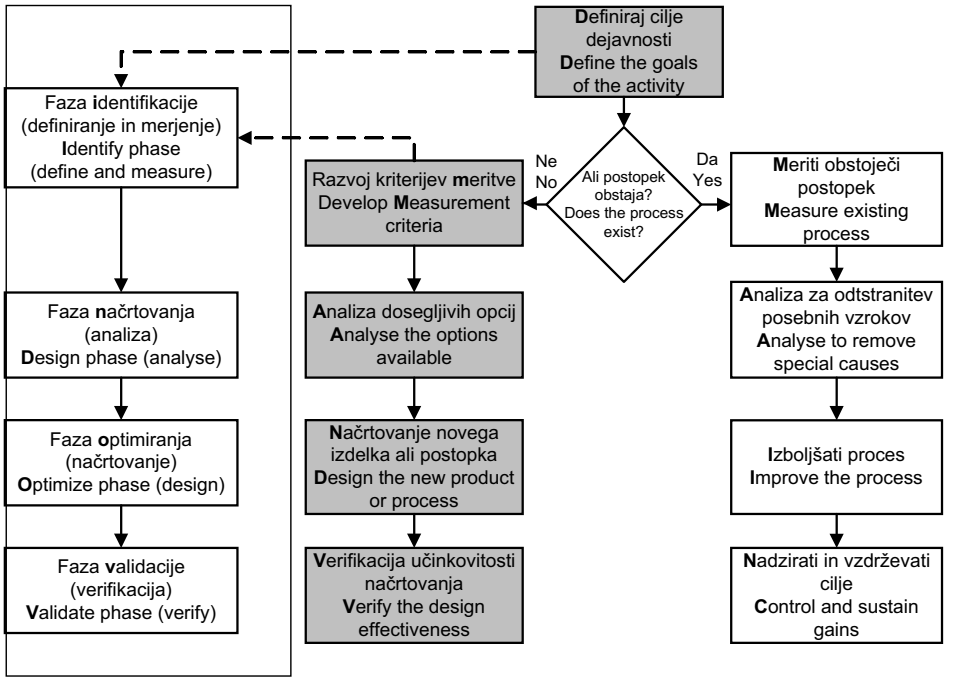

Sl. 7. *Zveza med DMADV (DFSS) in običajnim DMAIC (Šest Sigem) - dodan je tudi novi postopek IDOV [2]*
Fig. 7. *The relationship between DMADV (DFSS) and classical DMAIC (Six Sigma) - a new approach IDOV is also added [2]*

uporabljena pri načrtovanju v podjetjih z enakim zaupanjem kakor v standarde ISO (ISO 9001, ISO 14001, ISO/TS 16949 in ISO OHSAS 18001).

DFSS je dolgotrajen in drag postopek, ki terja obsežne vire. Zato naj bi bil skrbno uporabljen samo na nekaj bistvenih projektih in še posebej usmerjen k razvoju novih izdelkov. Ne začenjajte projektov DFSS brez kupcev, vključevanja prodaje, zavezanosti vrhovnega vodstva in ustrezne skupine, po možnosti usposobljene za Šest Sigem. DFSS je močna tehnika in njena moč naj bi bila primerno uporabljena.

4 SKLEPNE UGOTOVITVE

Metodologija uvajanja nenehnih izboljšav kakovosti se lahko razlikuje v različnih organizacijah. Ne glede na metodologijo in program nenehnih izboljšav vsaka organizacija potrebuje izbiro orodij in tehnik kakovosti v svojem postopku izvajanja izboljšav. Pomembno je to, da so orodja in tehnike izbrane za ustrezno skupino in da se pravilno uporabljajo v ustreznem postopku.

PDCA (Demingov) krog je več kakor le orodje kakovosti. PDCA je zasnova postopka nenehnih izboljšav, vgrajen v kulturo

be used in design houses with the same familiarity as the ISO standards (ISO 9001, ISO 14001, ISO/TS 16949, and ISO OHSAS 18001).

DFSS is a longer-term, resource-hungry process and it is expensive. Therefore, it should be deployed with care and on just a few vital projects, and specifically targeted towards the development of new products. Do not start a DFSS project without the customer, sales involvement, top-management commitment and a team, preferably one with Six Sigma training. DFSS is a powerful technique and its power should not be abused.

4 CONCLUSIONS

The methodology for implementing continuous quality improvement can be varied in different organizations. Regardless of the methodology of the continuous-improvement programmes, each organization needs to use a selection of quality tools and techniques in their implementation process. It is vital that the tools and techniques are selected for the appropriate team and applied correctly to the appropriate process.

The PDCA cycle (Deming's circle) is more than just a quality tool. The PDCA cycle is a concept of

organizacije. Je preprost za razumevanje in naj bi ga uporabljala širša skupina ljudi v podjetju (tudi skozi standard ISO 9001:2000). Najpomembnejši vidik PDCA leži v stopnji *"ukrepaj"* po izpolnitvi projekta, ko krog ponovno zavrtimo za nadaljnje izboljšanje.

Metodologija DMAIC (kot sestavni del Šest Sigem) je sistematična in temelji na dejstvih; zagotavlja natančen okvir za „na rezultate" usmerjeno vodenje projekta. Pripomniti je treba, da so najboljše rezultate z DMAIC dosegli pri prilagodljivih postopkih in izločanju slabih korakov. Kot ponovitveni postopek je primeren zlasti, ko so člani skupine še začetniki na področju uporabe orodij in tehnik.

Metodologija DFSS je sistematičen in discipliniran postopek načrtovanja izdelka ali postopka, vključujoč vse funkcije organizacije od samega začetka, z namenom *oblikovati stvari pravilno že prvič*. Glas kupca (VOC) in Razvoj funkcije kakovosti (QFD) sta orodji za razpoznavo zahtev kupca, prevajanje le-teh v tehnične zahteve za načrtovanje izdelka in njihovo uvrstitev glede na pomembnost za izpolnitev temeljnih zahtev kupca. Ne začenjajte projektov DFSS brez kupcev, vključevanja prodaje, zavezanosti vrhovnega vodstva in ustrezne skupine, po možnosti usposobljene za Šest Sigem. DFSS je izjemno močna tehnika in njena moč naj ne bi bila zlorabljena. Vendar prav tako ne smemo pozabiti: DFSS je dolgotrajen in drag postopek, ki zahteva obsežne vire. Iz teh razlogov naj bi bil skrbno uporabljen samo na nekaj bistvenih projektih in še to usmerjen predvsem k razvoju novih izdelkov.

continuous-improvement processes embedded in the organization's culture. It is simple to understand and should be used by a large number of people in the company (also throughout standard ISO 9001:2000). The most important aspect of PDCA lies in the *"act"* stage after the completion of a project when the cycle starts again for the further improvement.

The methodology DMAIC (an integral part of Six Sigma) is systematic and fact based and provides a rigorous framework of results-oriented project management. It should be noted that the best results from DMAIC are achieved when the process is flexible, thus eliminating unproductive steps. An iterative approach may be necessary as well, especially when the team members are new to the tools and techniques.

DFSS methodology is a systematic and disciplined approach to product or process design, including all organizational functions from the early beginning, with the objective to *design things right from the first time*. Voice of the customer (VOC), to gather customer requirements, and Quality Function deployment (QFD) are tools to identify customer requirements, translate them into the product's technical design requirements and prioritize them according to weighted importance to meet customers' basic requirements. Do not start a DFSS project without the customer, sales involvement, top-management commitment and a team, preferably one with Six Sigma training. DFSS is a powerful technique and its power should not be abused, and do not forget: DFSS is a longer-term, resource-hungry process and it is very expensive. For this reason it should be deployed with care and on just a few vital projects, and specifically targeted towards the development of new products.

5 LITERATURA
5 REFERENCES

[1] Basu, R. (2004) Implementing quality – a practical guide to tools and techniques, *Thomson Learning*, London.

[2] Soković, M. (2006) PDCA cycle *vs.* DMAIC and DFSS, *Proceedings of the International Conference ICQME 2006,* 13. – 15. September 2006, Miločer, Montenegro.

[3] Seaver, M. (2003) Gower handbook of quality management, Third Edition, *Gower Publishing Ltd*, England.

[4] Soković, M., et al. (2005) Quality management - Seminar, Educational material, *Faculty of Mechanical Engineering*, Ljubljana, Slovenia (in Slovene).

[5] Kondo, Y. (1995) Companywide quality control*, 3A Corporation*, Tokyo.

[6] Lesjak, M. and J. Kusar (2006) Optimisation of working place, Diploma thesis, *Faculty of Mechanical Engineering*, Ljubljana, Slovenia (in Slovene).

[7] Breyfogle III, F. W., et al. (2001) Managing Six Sigma, *John Wiley & Sons, Inc.*, New York.

[8] Pavletić, D. and M. Soković (2002) Six Sigma - a complex quality initiative, *J. of Mech. Eng.*, Vol. 48 (2002) 3, pp. 158-168.
[9] Pavletić, D., Fakin, S. and Soković M. (2004) Six Sigma in process design, *J. of Mech. Eng.*, Vol. 50 (2004), Nr. 3, pp. 157-167.
[10] Mesec, A. (2005) Designing new products using DFSS, *Proceedings of the 7th Conference IAT '05*, 21.-22. April 2005, Bled, Slovenia.
[11] Crevelin, C. M., et al. (2003) Design for Six Sigma in technology and product development, *Prentice Hall PTR*, London.
[12] Yang, K., et al. (2003) Design for Six Sigma – a roadmap for product development, *Mc Graw Hill*, London.

Naslova avtorjev:
prof. dr. Mirko Soković
Univerza v Ljubljani
Fakulteta za strojništvo
Aškerčeva 6
1000 Ljubljana
mirko.sokovic@fs.uni-lj.si

doc. dr. Duško Pavletić
Univerza v Rijeki
Tehnična fakulteta
Vukovarska 58
HR-51000 Rijeka, Hrvaška
duskop@riteh.hr

Authors' Addresses:
Prof. Dr. Mirko Soković
University of Ljubljana
Faculty of Mechanical Engineering
Aškerčeva 6
SI-1000 Ljubljana, Slovenia
mirko.sokovic@fs.uni-lj.si

Doc. Dr. Duško Pavletić
University of Rijeka
Faculty of Engineering
Vukovarska 58
HR-51000 Rijeka, Croatia
duskop@riteh.hr

Prejeto: 6.2.2007
Received:
Sprejeto: 25.4.2007
Accepted:
Odprto za diskusijo: 1 leto
Open for discussion: 1 year

Strojniški vestnik - Journal of Mechanical Engineering 53(2007)6, 379-385
UDK - UDC 621.941.025:620.178.16
Kratki znanstveni prispevek - Short scientific paper (1.03)

Učinki kemične sestave orodja na njegovo delovanje pri struženju Inconela 718 s keramičnimi vstavki

The Effects of a Tool's Chemical Composition on Its Performance when Turning Inconel 718 with Ceramic Inserts

Abdullah Altin[1] - Ahmet Taskesen[2] - Muammer Nalbant[2] - Ulvi Seker[2]
([1]Yuzuncu Yil University, Turkey; [2]Gazi University, Turkey)

Raziskovali smo učinke kemične sestave rezalnega orodja na obrabo in dobro trajanja orodja. Izvedli smo serijo preizkusov z uporabo keramičnih orodij na osnovi silicij-nitrita (Si, Al, O, N) in ojačanih z dodatki (Al_2O_3+SiC_w), z dvema različnima geometrijskima oblikama (kvadrat in krog) in tremi različnimi kakovostmi ISO. Pri keramičnem orodju sta veliki vsebnosti aluminija in germanija povzročili oblikovanje roba, medtem ko sta obrabo zarez pri keramičnem orodju ojačanem z dodatkom povzročili veliki vsebnosti bakra in kisika. Z uporabo štirih različnih orodij dveh kakovosti smo ugotovili najboljše delovanje pri rezalni hitrosti 200 m/min. Dejstvo, da je keramično orodje, kvadratne oblike, ojačano z dodatkom podvrženo plastičnim deformacijam, lahko pripišemo veliki vsebnosti kisika v sestavi rezalnega orodja.

(Ključne besede: rezalna orodja, kemične lastnosti, superzlitine, obraba orodij)

The effects of a cutting tool's chemical composition on wear and tool life are investigated. A series of experiments was carried out using silicon-nitrite-based (Si, Al, O, N) and whisker-reinforced ceramic tools (Al_2O_3+SiC_w) that have two different geometries (square and circular) and three different ISO qualities. For the ceramic tools, a high level of aluminum and germanium caused built-up edge (BUE) formation, while notch wear is considered as a cause of high copper and oxygen levels in whisker-reinforced ceramic tools. Four different tools with two qualities showed the best performance at a cutting speed of 200 m/min. The fact that the whisker-reinforced square-type ceramic tools are subjected to plastic deformation is attributed to the high oxygen level in the cutting tool's structure.

(Keywords: cutting tools, chemical properties, superalloys, tool wears)

0 INTRODUCTION

Inconel 718, a nickel-based super-alloy, has been widely used in the aircraft and nuclear industries due to its exceptional thermal resistance and the ability to retain its mechanical properties at elevated temperatures over 700°C ([1] to [3]). Nickel-based super-alloys are classified as difficult-to-cut materials due to their high shear strength, work hardening tendency, highly abrasive carbide particles in the microstructure, a strong tendency to weld and form a built-up edge, and a low thermal conductivity ([4] and [5]). They have a strong tendency to maintain their strength at the high temperatures generated during machining [6].

The short tool life and surface quality problems during the machining of nickel-based superalloys are the main subjects that must be investigated. Residual stresses formed at the workpiece surface during machining negatively affect the mechanical strain and corrosion properties of the workpiece ([2] and [5]).

The main factors that affect the performance of a cutting tool while machining super-alloys are ([6] and [7]): (i) high hardness, (ii) wear resistance, (iii) chemical inertness and (iv) fracture toughness. Ceramic tools are suitable with regard to the first three properties, even at high cutting speeds. With the introduction of sialon materials, Inconel 718 can be machined using whisker-reinforced aluminum-sili-

con-carbide tools at higher cutting speeds. However, their fracture toughness is much lower than that of other tool materials, such as carbide inserts.

The cutting speed is an important factor that influences the tool wear and tool life when cutting nickel-based alloys. Nickel-based super-alloys can be machined successfully at high cutting speeds between 200 m/min and 750 m/min ([1], [8] and [9]). In previous studies, whisker-reinforced ceramic tools were found to be very suitable for the machining of Inconel 718 ([9] and [10]). In this study, for the machining of Inconel 718 with ceramic inserts, cutting-speed experiments of tool wear are carried out to investigate the effects of the tool's chemical structure on tool wear and tool life.

1 MATERIALS AND METHOD

1.1 Test specimens

The workpiece material used in the experiments was a cylinder with a size of Ø50×500 mm mm. The diameter and volume of the Inconel 718 workpiece material after the machining were measured as 408 mm and 273 cm^3, respectively. The chemical composition and mechanical properties of the Inconel 718 workpiece materials used in the experiments are shown in Table 1 and Table 2. Typical SEM analyses and the metallurgical structure of the machined workpiece material are shown in Fig. 1.

1.2 Machining parameters

The cutting-tool inserts were chosen as the square and round types that are widely used in manufacturing industry, having two different geometries and three different ISO qualities. The materials and properties of the cutting tools used are shown in Table 3. These inserts are tested by cutting Inconel 718 under a constant feed rate of 0.20 mm/rev, a constant depth of cut equal to 2 mm and different cutting speeds of 150 m/min, 200 m/min, 250 m/min and 300 m/min, taking into consideration ISO 3685 and the manufacturer's recommendations. For each experiment, 273 cm^3 workpiece material was cut and the mean flank wear values were measured.

An OKUMA LB-45II type CNC turning machine was used for the machining experiments. The general specifications of the machine tool can be seen in Table 4.

2 RESULTS AND DISCUSSION

A reference flank wear value of $V_B = 0.3$ mm was chosen as the wear criterion, according to ISO 3685 [11]. The cutting tool was rejected and further machining stopped based on one or a combination of the following rejection criteria, based on ISO Standard 3685 for tool-life testing:

- Average flank wear = 0.3 mm.
- Maximum flank wear = 0.4 mm.
- Nose wear = 0.5 mm.
- Notching at the depth-of-cut line = 0.6 mm.
- Excessive chipping (flaking) or catastrophic fracture of the cutting edge.

The whisker-reinforced aluminum insert ($Al_2O_3 + SiC_w$) KYON 4300 SNGN and the silicon-nitrite-based ceramic KYON 2100 SNGN insert remained below the reference value at 150 m/min, as seen in Fig. 2. The other two round-type inserts

Table 1. *Chemical composition of Inconel 718 (wt. %)*

C	Mn	Si	P	S	Cr	Ni	Co	Mo	Nb+Ta	Ti
0.040	0.08	0.08	<0.015	0.002	18.37	53.37	0.23	3.04	5.34	0.98
Al	B	Ta	Cu	Fe	Ca	Mg	Pb	Bi	Se	Nb
0.50	0.004	0.005	0.04	17.80	<0.01	<0.01	0.0001	.00001	<.0001	5.33

Table 2. *Mechanical properties of Inconel 718*

Temperature (°C)	Yield Strength MPa	Tensile Strength MPa	%Elongation	%Contraction
RT(Room Temp)	807.08	673.20	23.3	42.1
648 °C	641.70	555.10	22.2	30.8

Table 3. *Geometry and material of the cutting tool inserts*

	Material	Grade	Catalog No	Tool holders	Approach angle	Rake Angle (Degree)
Ceramic tools	Sialon ceramic	KYON 2000	RNGN 12 07 00	CRSN R 2525 M12-MN4	75°	– 7
	Sialon ceramic	KYON 2100	SNGN 12 07 12	SSBC R 2525 M 12	75°	+5
	Whisker-reinforced ceramic ($Al_2O_3 + SiC_w$)	KYON 4300	SNGN 12 07 12	SSBC R 2525 M 12	75°	+5
	Whisker-reinforced ceramic ($Al_2O_3 + SiC_w$)	KYON 4300	RNGN 12 07 00	CRSN R 2525 M12-MN4	75°	– 7

Table 4. *General specifications of the CNC turning machine tool used in the experiments*

Phase number	3
Frequency	50 Hz
Load capacity	60.9 kW
Serial number	0046
Chuck	N15 A11
Cylinder	Y2050 Re
Max. revolution number	2800 rpm.
Max. pressure	3 MPa

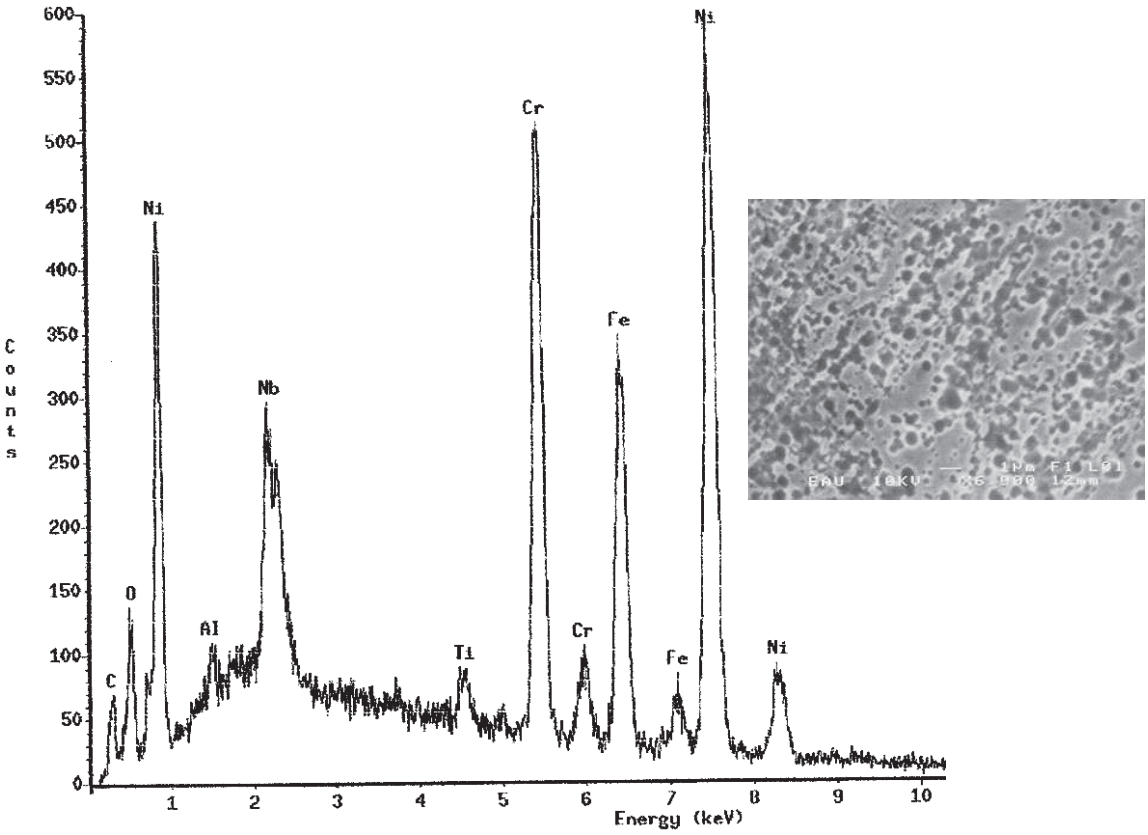

Fig. 1. *Typical SEM (scanning electron microscope) analysis and metallurgical structure of the machined workpiece material*

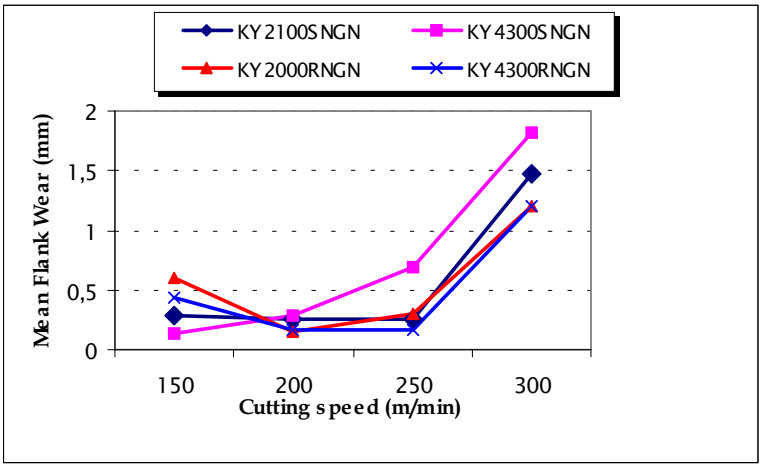

Fig. 2. *Relationship between the mean flank wear (VB) and the cutting speed (V) when machining Inconel 718 (f = 0.2mm/rev, d = 2 mm)*

exceeded the reference case and they were not suitable for cutting Inconel 718 at this cutting speed (Fig. 2). The EDS (electron-dispersion spectroscopy) analyses were obtained using a scanning electron microscope in order to determine the chemical elements present in the cutting tools (Fig.3, Fig. 4, and Table 5). From the EDS results we can see that the composition contains mainly Si, Al and C for the KYON 2100 SNGN tool, and that this cutting tool is subjected to general BUE and crater wear. The KYON 4300 SNGN cutting tool, having Al, O and Si in its structure, showed better performance at low cutting speeds, as shown in Fig. 2. The other inserts, KYON 2000 RNGN 12 07 00 and KYON 4300 RNGN 12 07 00, did not show a satisfactory performance. The KYON 2000 RNGN ceramic tool showed excessive wear compared to the other inserts (Fig. 2 and Fig.5). From the EDS analysis of this cutting tool, one can see that the levels of Si and Al are very high (Fig. 3), which contributes to the notch formation.

From Fig. 2 it is clear that the round-type cutting inserts wore out more quickly than the square-type inserts at low cutting speeds. This can be attributed to the tool geometry, and when the cutting speed increased the tool-wear value decreased. Generally good agreement was observed between these experimental results and the existing literature studies ([6], [7] and [10]).

All the inserts wore out beyond the reference value at a cutting speed of 300 m/min. At this speed, the round-type cutting inserts exhibited better performance than the square-type tools.

As a result, the KYON 4300 SNGN insert resisted only at low cutting speeds. At high cutting speeds both the KYON 4300 RNGN and KYON 2000 RNGN inserts showed good performance compared to the other inserts. The recommendation for tool inserts for the cutting of Inconel 718 was the KYON 4300 square type at low cutting speeds and the KYON 2000 round type at high cutting speeds. The

Table 5. *Element analysis of ceramic cutting tools under SEM equipment*

KYON 4300 RNGN 12 07 00

Element	k-ratio (calc.)	ZAF	Atom %	Element Wt %	Wt % Err. (1-Sigma)
Zr-L	0.0319	1.320	4.42	4.21	+/- 1.87
Ti-K	0.0174	0.890	3.09	1.55	+/- 0.83
V -K	0.0072	0.889	1.21	0.64	+/- 1.36
W -M	0.3776	1.212	23.81	45.75	+/- 2.95
Cr-K	0.0954	0.857	15.03	8.17	+/- 1.87
Ni-K	0.1893	0.807	24.91	15.28	+/-10.63
Fe-K	0.0420	0.832	5.99	3.50	+/- 3.70
Nb-L	0.1674	1.248	21.53	20.90	+/- 2.53
As-L	0.0000	1.476	0.00	0.00	+/- 0.00
Ta-M	0.0000	1.285	0.00	0.00	+/- 0.00
Total			100.00	100.00	

KYON 4300 SNGN 12 07 12

Element	k-ratio (calc.)	ZAF	Atom %	Element Wt %	Wt % Err. (1-Sigma)
Zr-L	0.0000	1.393	0.00	0.00	+/- 0.00
Ti-K	0.0000	0.829	0.00	0.00	+/- 0.00
V -K	0.0000	0.818	0.00	0.00	+/- 0.00
W -M	0.7437	1.049	62.21	77.99	+/- 2.36
Cr-K	0.0000	0.781	0.00	0.00	+/- 0.00
Ni-K	0.0448	0.711	7.95	3.18	+/- 4.77
Fe-K	0.0017	0.746	0.33	0.13	+/- 1.88
Nb-L	0.1459	1.282	29.51	18.70	+/- 1.78
As-L	0.0000	1.133	0.00	0.00	+/- 0.00
Ta-M	0.0000	1.065	0.00	0.00	+/- 0.00
Total			100.00	100.00	

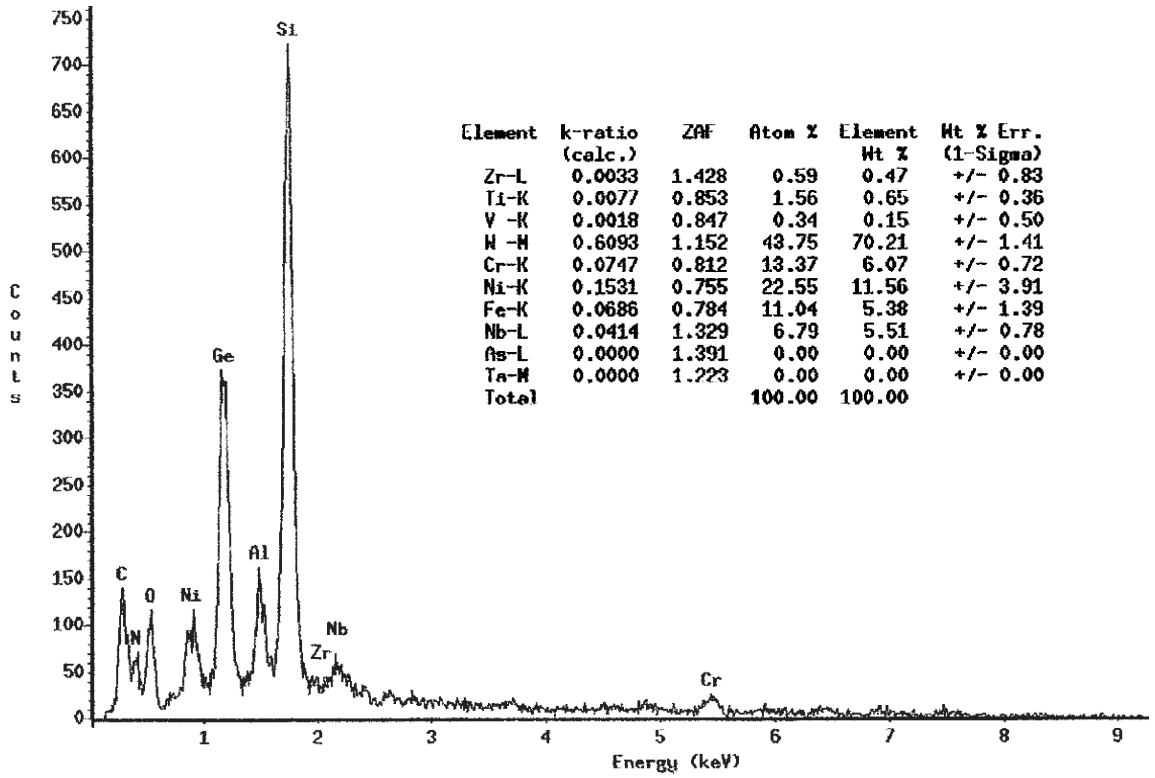

Element	k-ratio (calc.)	ZAF	Atom %	Element Wt %	Wt % Err. (1-Sigma)
Zr-L	0.0033	1.428	0.59	0.47	+/- 0.83
Ti-K	0.0077	0.853	1.56	0.65	+/- 0.36
V -K	0.0018	0.847	0.34	0.15	+/- 0.50
W -M	0.6093	1.152	43.75	70.21	+/- 1.41
Cr-K	0.0747	0.812	13.37	6.07	+/- 0.72
Ni-K	0.1531	0.755	22.55	11.56	+/- 3.91
Fe-K	0.0686	0.784	11.04	5.38	+/- 1.39
Nb-L	0.0414	1.329	6.79	5.51	+/- 0.78
As-L	0.0000	1.391	0.00	0.00	+/- 0.00
Ta-M	0.0000	1.223	0.00	0.00	+/- 0.00
Total			100.00	100.00	

Fig. 3. *Element analysis of KYON 2000 RNGN ceramic cutting tool*

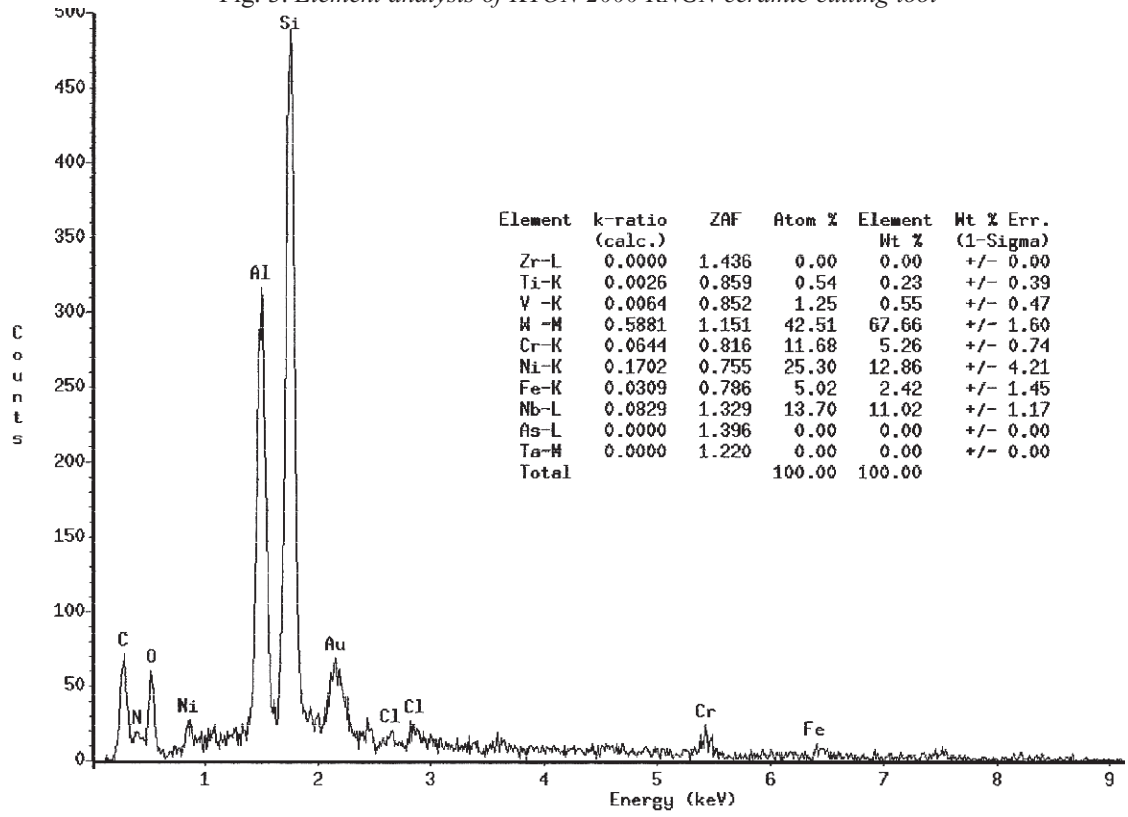

Element	k-ratio (calc.)	ZAF	Atom %	Element Wt %	Wt % Err. (1-Sigma)
Zr-L	0.0000	1.436	0.00	0.00	+/- 0.00
Ti-K	0.0026	0.859	0.54	0.23	+/- 0.39
V -K	0.0064	0.852	1.25	0.55	+/- 0.47
W -M	0.5881	1.151	42.51	67.66	+/- 1.60
Cr-K	0.0644	0.816	11.68	5.26	+/- 0.74
Ni-K	0.1702	0.755	25.30	12.86	+/- 4.21
Fe-K	0.0309	0.786	5.02	2.42	+/- 1.45
Nb-L	0.0829	1.329	13.70	11.02	+/- 1.17
As-L	0.0000	1.396	0.00	0.00	+/- 0.00
Ta-M	0.0000	1.220	0.00	0.00	+/- 0.00
Total			100.00	100.00	

Fig. 4. *Element analysis of KYON 2100 SNGN ceramic cutting tool*

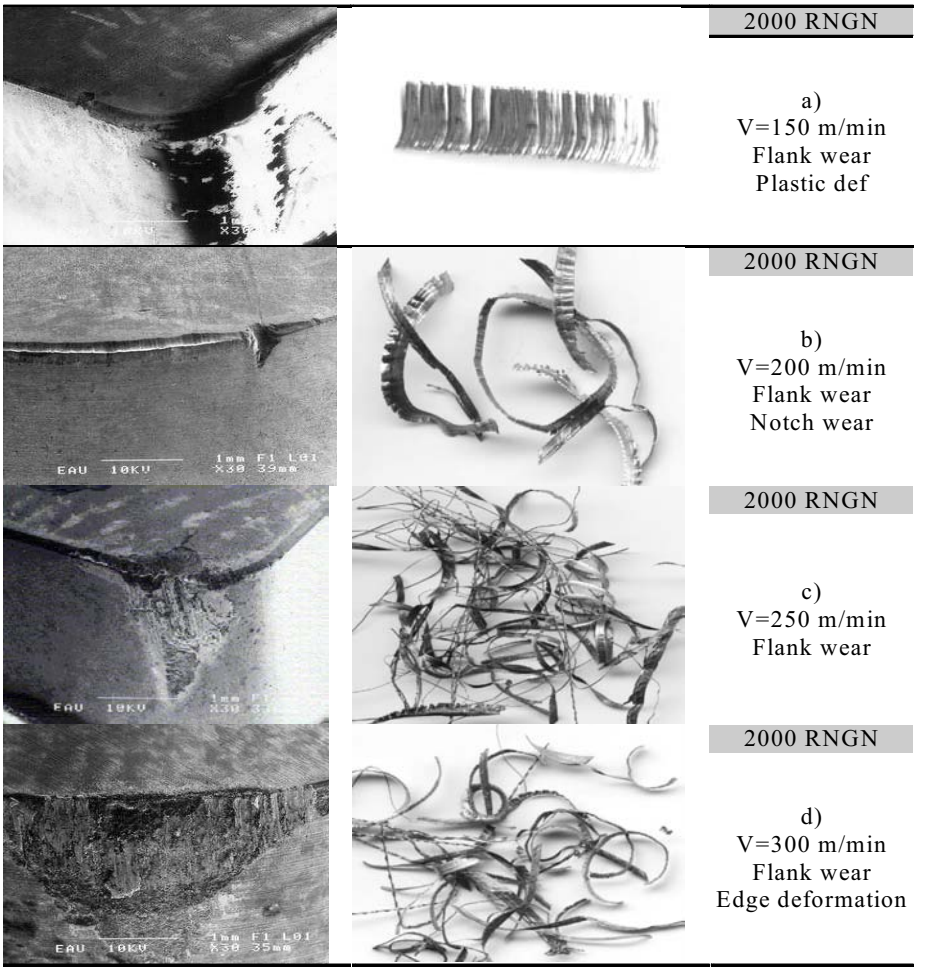

Fig. 5. *Typical wear types and chip formation of the ceramic tools under test*

KYON4300 SNGN insert was not suitable for cutting Inconel at high speeds.

3 CONCLUSIONS

Generally speaking, flank wear, cratering, notching and plastic deformation are the wear mechanisms observed with ceramic inserts when machining Inconel 718. The dominant wear mechanisms seen for round-type inserts are notch wear, while flank wear and cratering are the major wear types for the square-type inserts. Based on the experimental results, the optimum cutting speed was found to be 250 m/min, with the tool life being negatively affected above this speed. The major wear types for the ceramic inserts are flank wear, chipping and plastic deformation.

Acknowledgements

The authors thank Kennametal TR A.S., especially Ilhan Eryener, Sales Manager and Taner Cinar, Europe representative, for their financial support and for the cutting tools.

4 REFERENCES

[1] D. Dudzinski a, A. Devillez a,et.al. (2004) A review of developments towards dry and high speed machining of Inconel 718 alloy, *International Journal of Machine Tools & Manufacture*, 44, 439–456.

[2] Coudhury, I.A., El-Baradie, M.A. (1998) Machinability of nickel-base super alloys : a general review, *Journal of Materials Processing Technology*, Volume 77, Issues 1-3, Pages 278-284.

[3] E.O. Ezugwua, J. Bonney a, D.A. Fadare b, W.F. Sales (2005) Machining of nickel-base, Inconel 718, alloy with ceramic tools under finishing conditions with various coolant supply pressures, *Journal of Materials Processing Technology*, 162, 609–614.
[4] S. Lo Casto, E. Lo Valvo, E. Lucchini et. al.(1999) Ceramic materials wear mechanisms when cutting nickel-based alloys, *Wear*, 225–229, 227–233.
[5] R.T. Coelho, L.R. Silva, A. Braghini, Jr., A.A. Bezerra (2004) Some effects of cutting edge preparation and geometric modifications when turning INCONEL 718TM at high cutting speeds, *Journal of Materials Processing Technology*, 148, 147–153.
[6] M. Soković, J. Mikuła, L.A. Dobrzanski et.al. (2005) Cutting properties of the Al2O3 + SiC(w) based tool ceramic reinforced with the PVD and CVD wear resistant coatings, *Journal of Materials Processing Technology,* 164, 924–929.
[7] E.O. Ezugwu, Z.M. Wang, A.R. Machado (1999) The machinability of nickel-based alloys: a review, *Journal of Materials Processing Technology*, 86 1–16.
[8] Richards, N., Aspinwall, D. (1989) Use of ceramic tools for machining nickel-based alloys, *Int. J. Mach. tools Manuf,* 294, pp. 575-588.
[9] Khamsehzadeh, H. (1991) Behaviour of ceramic cutting tools when machining superalloys, *Ph.D. Thesis*, University of Warwick, pp125.
[10] Bhattacharya, S. K., Pashby, I. R., Ezugwu, E. O. (1987) Machining of INCO 718 and INCO 901 superalloys with Sic-whisker reinforced Al_2O_3 composite ceramic tools, *Prod. Eng*, Osaka, 176-181.
[11] A. Altin, M. Nalbant, A. Taskesen (2006) The effects of cutting speed on tool wear and tool life when machining Inconel 718 with ceramic tools , *Materials & Design*, In Press, Corrected Proof, Available online 2 November 2006.

Authors' Addresses:
Dr. Abdullah Altin
Yuzuncu Yil University
Technical High School
65080 Van, Turkey

Dr. Ahmet Taskesen
Prof. Dr. Muammer Nalbant
Prof. Dr. Ulvi Seker
Gazi University
Technical Education Faculty, Besevler
Ankara, 06500, Turkey
taskesen@gazi.edu.tr

Prejeto: 8.9.2006
Received:
Sprejeto: 25.4.2007
Accepted:
Odprto za diskusijo: 1 leto
Open for discussion: 1 year

Strojniški vestnik - Journal of Mechanical Engineering 53(2007)6, 386-398
UDK - UDC 534.12:519.61/.64
Strokovni članek - Speciality paper (1.04)

Prenos vibracij po ukrivljenih cevovodih v prostoru

Vibrations of a 3-Dimensional Piping System

Matej Tadina - Miha Boltežar
(Fakulteta za strojništvo, Ljubljana)

V prispevku je na kratko predstavljena metoda prenosnih matrik za modeliranje prenosa vibracij preko cevovoda v prostoru. Na temelju točne rešitve gibalnih enačb je na novo definirana prenosna matrika krožnega loka s tekočino, pri katerem upoštevamo tudi osno deformljivost. Osredotočili se bomo na ustaljeno stanje odziva ob harmonski vzbujevalni motnji. Poznavanje prenosne matrike ravne cevi in krožnega loka omogoča modeliranje prenosa vibracij po poljubnem cevovodu, kjer upoštevamo učinke pretakajoče se tekočine in nadtlaka v cevi. V numeričnem preizkusu je potrjeno pravilno delovanje metode na podlagi primerjave rezultatov prenosa sile, določene z metodo prenosnih matrik in metodo končnih elementov. Enako je potrjeno tudi s preizkusom. Izkaže se tudi, da je čas preračuna pri uporabi metode prenosnih matrik občutno krajši v primerjavi z metodo končnih elementov.

(Ključne besede: cevovodni sistemi, prenos vibracij, modeliranje, metode prenosnih matrik)

This paper briefly presents the transfer-matrix method (TMM) for the vibration analysis of a 3-dimensional piping system. The transfer matrix of a curved pipe with fluid was derived based on the exact solution of the governing equations, where the axial deformability was also taken into account. Only the steady-state response for the case of harmonic excitations was analyzed. With the formulation of the transfer matrix for a straight pipe and for a curved pipe, a 3-dimensional complex piping system can be easily modeled. The inviscid fluid-dynamic forces were derived according to the plug-flow approximation and the slender-body theory. As shown in a numerical example of a 3-dimesional piping system the comparison of the transfer function obtained with the finite-element method (FEM) and the TMM is quite good. On the basis of a comparison of the experimental results and the results obtained with the TMM, the correctness of the method was confirmed. It was also shown that the TMM is significantly faster than the FEM.

(Keywords: piping systems, vibration analysis, modeling, transfer-matrix method)

0 UVOD

V zadnjem času ima vedno več avtomobilov klimatske naprave, pri čemer so posamezni deli povezani s cevovodi. Ti cevovodi so izpostavljeni vibracijam kompresorja in vibracijam, ki se prenašajo po karoseriji. Nihajoči cevovod povzroča nezaželen hrup, prav tako pa lahko privede do odpovedi posameznih sklopov klimatskega sistema zaradi prenesenih vibracij. V izogib temu si prizadevamo pri snovanju cevovoda za čim manjši prenos vibracij. Običajno lahko to dosežemo s pravilnim načinom in mestom vpetja, s kombinacijo več cevi različnih materialov, z geometrijskimi lastnostmi cevovoda ter optimalnim potekom cevovoda.

0 INTRODUCTION

Nowadays, more and more cars have integrated air conditioners, where the individual parts are connected with a piping system. These piping systems are exposed to the vibrations of the compressor and the vibrations of the car body, caused by irregularities in the road surface. The vibrations of the piping system cause undesirable noise and the system may subsequently fail due to fatigue. In the designing of the piping system attention is focused on the minimization of the vibrations. This can be achieved with the proper types and positions of the supports, with a combination of pipes of different materials and the optimal shape of the pipe system in space.

Zaradi izredno širokega področja uporabe cevovodov, npr. kot izmenjevalniki toplote, pri hidravličnih inštalacijah, klimatskih napravah ipd. so se v zadnjih letih zahteve in želje po modeliranju prenosa vibracij po cevovodu zelo povečale. Pri pregledu literature zasledimo, da se večina avtorjev osredotoča na modeliranje bodisi ravne cevi ([1] in [2]), pri katerih poskušajo čim bolj natančno upoštevati interakcijo med tekočino in steno cevi, bodisi krožnega loka ([1], [3] in [4]), kjer pa fizikalni modeli še niso povsem dodelani. Zasledimo le nekaj virov, ki obravnavajo prenos vibracij po zapletenem prostorskem cevovodu ([5] in [6]). Avtorji običajno popišejo celoten cevovod z ravnimi končnimi elementi, pri katerih je upoštevan preprost model interakcije med tekočino in steno cevi.

V prispevku se bomo osredotočili na modeliranje prenosa vibracij po prostorskem cevovodu. Predpostavili smo, da lahko poljubno obliko cevovoda v prostoru popišemo s kombinacijo ravnih cevi in krožnih lokov. Uporabili bomo metodo prenosnih matrik (MPM), ki je v literaturi dobro poznana in velikokrat uporabljena metoda. Huang [7] je metodo uporabil za izračun kritične pretočne hitrosti, Walsh [8] je z MPM računal prenos moči po nosilcu in Koo [9] je uporabil MPM za določitev prenosa vibracij po cevovodu v prostoru, sestavljenem iz ravnih cevi.

Glavni namen prispevka je uporaba prenosnih matrik za modeliranje prenosa vibracij po prostorskem cevovodu. V ta namen so v drugem poglavju predstavljene gibalne enačbe in izpeljana prenosna matrika krožnega loka s tekočino. Nato je v tretjem poglavju podana primerjava rezultatov prenosa sile po cevovodu, dobljenih s prenosnimi matrikami in končnimi elementi za analizirani cevovod. Sledi poglavje eksperimentalnega ovrednotenja uporabljena modela krožnega loka. Kot zadnje sledi poglavje s sklepi.

1 METODA PRENOSNIH MATRIK

Zaradi celovitosti prispevka bomo najprej predstavili metodo prenosnih matrik. Metoda prenosnih matrik je uporabna za linijske sisteme, pri katerih nas zanima predvsem odziv sistema v končni točki *K* glede na harmonsko motnjo v začetni točki *Z*, primer tega je prikazan na sliki 1. Sistem najprej diskretiziramo na podelemente, katerih prenosne matrike **PM** poznamo. Celotno prenosno matriko sistema $\mathbf{PM}_S$ v nadaljevanju dobimo z verižnim množenjem posameznih prenosnih matrik, kakor to prikazuje enačba (1).

Vibration analyses of a piping system with a conveying fluid have received considerable attention in recent decades due to widespread applications in areas such as heat-exchanger tubes, hydraulic pipelines, air conditioners, etc. Extensive investigations have been carried out either on the subject of the vibrations of straight pipes conveying fluid ([1] and [2]), where the authors try to couple the motion of the pipe and the fluid accurately, or on curved pipes, conveying fluid ([1], [3] and [4]). Fewer studies have been made for the response analysis of a 3-dimensional complex piping system conveying fluid ([5] and [6]). The vibrations of the whole pipeline are usually studied by using conventional finite-element formulations.

This paper proposes a computational method to analyze the response of a 3-dimensional piping system. It has been assumed that the 3-dimensional piping system can be composed of a combination of straight and curved pipes. The transfer-matrix method (TMM) was applied to calculate the vibrations of the piping system. In [7] the method is used to calculate the critical flow velocity, the analysis of the power flow in beams is shown in [8], and in [9] the model for analyzing the vibrations of the straight pipe conveying the fluid is shown.

In Section 2 the governing equations are presented and the transfer matrix of the curved pipe including the fluid is derived. In Section 3 the comparison of the force transfer over the piping system is given using the derived transfer matrix and the finite-element method. The result for the curved pipe is verified by experiment. At the end the conclusions are presented.

1 TRANSFER-MATRIX METHOD

For the purposes of completeness this section gives a brief review of the transfer-matrix method. The TMM is mainly useful for one-dimensional systems, where only the response of the system at the end point K due to harmonic excitation at the start point Z is of interest, Fig 1. The system is initially discretized on the sub-elements, where the transfer matrices (**PM**) of those sub-elements are known. The global $\mathbf{PM}_S$ of the system can be further computed with the chain-product of the individual **PM**, Eq. 1.

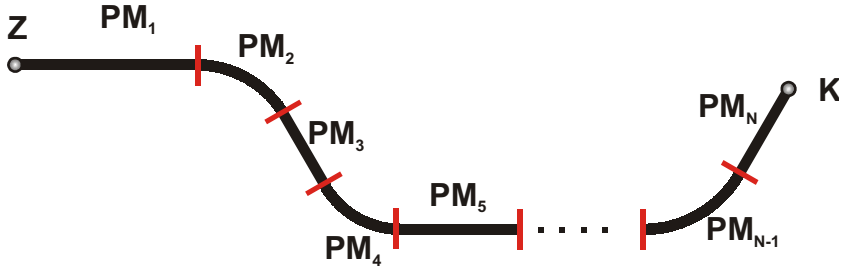

Sl. 1. *Elementi cevne sestave in njihove prenosne matrike*
Fig. 1. *Elements of the piping system and their transfer matrices*

$$\mathbf{PM}_S = \mathbf{PM}_N \cdot \mathbf{PM}_{N-1} \cdots \mathbf{PM}_1 \tag{1}.$$

Poznavanje prenosne matrike cevovoda $\mathbf{PM}_S$ omogoča določitev vektorja stanja na koncu cevovoda, točka *K*, če poznamo vektor stanja na začetku cevovoda, točka *Z*, kakor prikazuje enačba (2). Vektor stanja vsebuje vse pomike in elastične sile v izbranem krajišču:

Knowing the global transfer matrix of the piping system $\mathbf{PM}_S$ enables us to represent the piping system with pipe-end state vectors at points *Z* and *K*, Eq 2. In the pipe-end state vector all the elastic restoring forces and the displacements that influence the pipe-element end are introduced.

$$\mathbf{Z}_{SZ} = \mathbf{PM}_S \mathbf{Z}_{SK} \tag{2}.$$

1.1 Prenosna matrika ravne cevi

Diferencialne enačbe, ki popisujejo nihanje ravne cevi s preprostim modelom tekočine, so podane v [1]. Enačbi, ki popisujeta prečni nihanji, sta dobljeni na temelju Euler-Bernoullijeve teorije upogiba nosilca, pri čemer je upoštevan tudi vpliv pretakajoče se tekočine. Tekočina je modelirana kot nestisljiva in neviskozna, kar je upravičeno v primerih obravnave dolgih cevovodov, pri katerih je razmerje dolžina/premer cevovoda veliko. Posledica takšnih predpostavk za tekočino je, da ne moremo modelirati tlačnih nihanj in dinamičnih učinkov tekočine v cevi. Za popis torzijskega nihanja je uporabljena Saint-Venantova teorija torzije, medtem ko je za osna nihanja uporabljena splošna teorija osnega nihanja nosilca, pri katerem upoštevamo tudi vpliv pretakajoče se tekočine. Na podlagi enačb, podanih v [1], je definirana prenosna matrika za ravno cev v [10].

1.2 Prenosna matrika krožnega loka

Gibalne enačbe, ki popisujejo nihanje krožnega loka s tekočino, prikazanega na sliki 2, so izpeljane v [10]. Enačbe so izpeljane ob predpostavki neupoštevanja učinka debelina-ukrivljenost oziroma upoštevamo linearni potek napetosti po prerezu, kar približno velja za krožne loke z razmerjem $R/D \geq 4$, kjer sta *D* premer cevovoda in *R* radij ukrivljenosti krožnega loka. Upoštevana pa je raztegljivost

1.1 Transfer matrix of a straight pipe

The governing differential equations for the vibrations of a uniform straight pipe with the plug-flow model of a fluid are given in [1]. The transverse vibrations are described with the Euler-Bernoulli beam theory, where the additional fluid effect is taken into account. The inviscid fluid-dynamics forces were derived according to the plug-flow approximation and the slender-body theory. The slender-body theory is valid for pipes with a large length-to-radius ratio. The drawback of such assumptions for the fluid is that the fluid effects cannot be modeled. The torsional vibrations are governed by the Saint-Venant theory. On the basis of the equations in [1], the transfer matrix for a straight pipe with a fluid was defined in [10].

1.2 Transfer matrix of a curved pipe

The governing equations for a curved pipe conveying a fluid, Figure 2, are given in [10]. The equations were governed by disregarding the thickness-curvature effect, which is valid for circular pipes with a ratio $R/D \geq 4$, where *D* is the diameter of the pipe and *R* is the radius of the curvature of the curved pipe. The extensibility conditions are taken into account. The inviscid fluid-dynamics forces were

nevtralne črte. Uporabljen je enak model tekočine kakor pri ravni cevi, torej nestisljiva in neviskozna. Ker ima cev kolobarjasti prerez, ki je simetričen, dobimo le delno sklopljene gibalne enačbe.

Sklopljeni gibalni enačbi krožnega loka s tekočino, ki popisujeta nihanje znotraj ravnine ukrivljenosti, sta [10]:

derived according to the plug-flow approximation and the slender-body theory. Based on the Euler-Bernoulli hypothesis and because the cross-section is uniform and doubly symmetrical, the out-of-plane and the in-plane vibrations are uncoupled.

The governing differential equations for the in-plane vibrations are [10]:

$$\ddot{u}\left(m_p+m_f\right)+2m_f c\left(\dot{u}'+\frac{\dot{v}'}{R}\right)+m_f c^2\left(u''+2\frac{v'}{R}-\frac{u}{R}\right)+\frac{EI}{R}\left(v'''-\frac{u''}{R}\right)-EA_p\left(u''-\frac{v'}{R}\right)-A_f p_f\left(\frac{u}{R}-v'\right)\frac{1}{R}=q_s \quad (3)$$

$$\ddot{v}\left(m_p+m_f\right)+2cm_f\left(\dot{v}'-\frac{\dot{u}}{R}\right)+m_f c^2\left(v''-2\frac{u'}{R}-\frac{v}{R^2}\right)$$
$$+EI\left(v^{\mathrm{IV}}-\frac{u'''}{R}\right)+\frac{EA_p}{R}\left(u'+\frac{v}{R}\right)-A_f p_f\left(\frac{u'}{R}-v''\right)=\frac{1}{R}\left(c^2 m_f+A_f p_f\right)+q_r\ , \quad (4),$$

za nihanje zunaj ravnine ukrivljenosti [10]:

and for the out-of-plane vibrations are [10]:

$$\ddot{w}\left(m_p+m_f\right)+2m_f c\dot{w}'+EI\left(w^{\mathrm{IV}}-\frac{\phi''}{R}\right)-GI_0\left(\phi''+w''\right)+A_f p_f w''=q_z \quad (5)$$

$$\rho_p I_0\ddot{\phi}+\frac{EI}{R}\left(\frac{\phi}{R}-w''\right)-GI_0\left(\phi''+\frac{w''}{R}\right)=q_t \quad (6),$$

kjer so: m_p, m_f dolžinski masi cevi in tekočine, c hitrost tekočine, A_p, A_f prečna prereza cevi in tekočine, u, v, w in ϕ so pomiki v osni smeri, v obeh prečnih smereh in zasuk okoli nevtralne osi, EA_p, EI in GI_0 so osna, prečna in torzijska togost, R polmer ukrivljenosti loka, p_f nadtlak tekočine, ρ_p gostota cevi in q_s, q_r, q_z zvezne obtežbe vzdolž cevi.

Nihanje krožnega loka bomo v nadaljevanju reševali ločeno, in sicer kot nihanje krožnega loka znotraj ravnine ukrivljenosti ter nihanje loka zunaj ravnine ukrivljenosti. Gibalni enačbi (3) in (4), ki popisujeta nihanje krožnega loka v ravnini sta sklopljeni parcialni diferencialni enačbi. V primeru,

where m_p and m_f are the masses per unit length for the pipe and the fluid, c is the fluid velocity, and A_p and A_f are the cross-sections of the pipe and the fluid. u, v and w denote the displacements of the pipe in the s, r and z directions and ϕ is the twist angle. The coefficients EA_p, EI in GI_0 represent the axial, the flexural and the torsional stiffnesses of the curved pipe, R is the radius of the curvature of the curved pipe, p_f is the internal pressure, ρ_p is the density of the pipe and q_s, q_r, q_z are the distributed excitation forces.

Because the in-plane and out-of-plane vibrations are uncoupled, the governing equations

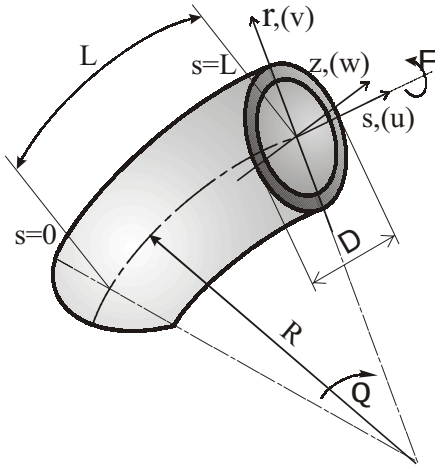

Sl. 2. *Geometrijska oblika krožnega loka*
Fig. 2. *Geometry of the curved pipe*

da sta člena q_s in q_r enaka nič, je enačba (3) homogena, medtem ko je enačba (4) nehomogena. Nehomogeni člen v enačbi (4) predstavlja statično deformacijo krožnega loka, ki je posledica pretakajoče tekočine in nadtlaka v cevi. Izkaže se, da statična deformacija ne vpliva na prenos vibracij, zato lahko enačbo (4) nadalje obravnavamo kot homogeno.

Zanima nas le ustaljeno stanje nihanja loka glede na harmonično vzbujanje, zato iščemo le partikularni del rešitve gibalnih enačb (3) in (4). Za določitev partikularnih rešitev gibalnih enačb (3) in (4) izberemo nastavka, ki ju podajata enačbi (7) in (8):

are solved separately. The governing differential equations (3) and (4) for the in-plane vibrations are coupled and inhomogeneous. If there is no distributed load, Equation (3) becomes homogenous and Equation (4) inhomogeneous. The inhomogeneous part of Equation (4) is due to fluid effects and can be neglected, because only the steady-state vibrations are of interest.

Of most interest is the steady-state behavior, so consequently only the particular solution of Equations (3) and (4) is computed. For the harmonic excitation, the solutions for *u(s,t)* and *v(s,t)* of Equations (3) and (4) are written in the form:

$$u(s,t) = U(s)e^{j\omega t} \tag{7}$$

$$v(s,t) = V(s)e^{j\omega t} \tag{8},$$

kjer funkciji *U(s)* in *V(s)* podajata neznani obliki nihanja pri krožni frekvenci vzbujanja ω. Z vstavitvijo izrazov (7) in (8) v enačbi (3) in (4) in preurejanju dobimo naslednjo neskloplјeno diferencialno enačbo 6. reda v odvisnosti od spremenljivke *s*:

where *U(s)* and *V(s)* are the amplitudes of vibration and ω is the excitation frequency. After substituting Equations (7) and (8) into Equation (3) and (4), and after some mathematical manipulating of the equations, it is possible to obtain a sixth-order ordinary differential equation for *U(s)*:

$$K_6U^{\mathrm{VI}} + K_5U^{\mathrm{V}} + K_4U^{\mathrm{IV}} + K_3U''' + K_2U'' + K_1U' + K_0U = 0 \tag{9},$$

kjer so koeficienti K_6,...,K_0 enaki:

where the coefficients K_6,...,K_0 are:

$$K_0 = A_pE\left[c^2m_f + A_fp_f + \left(m_f + m_p\right)R^2\omega^2\right] - R^2\omega^2\left[c^2m_f\left(m_p - m_f\right) + \left(m_f + m_p\right)\left(A_fp_f + \left(m_f + m_p\right)R^2\omega^2\right)\right] \tag{10}$$

$$K_1 = jm_fcR^2\omega\left[2A_pE - c^2m_f - A_fp_f + 3\left(m_f + m_p\right)R^2\omega^2\right] \tag{11}$$

$$\begin{aligned} K_2 = {} & R^2\left[-EI\left(m_f + m_p\right) + \left(c^2m_f\left(3m_f + m_p\right) + A_f\left(m_f + m_p\right)p_f\right)R^2\right]\omega^2 \\ & + A_pE\left[EI - R^2\left(-2c^2m_f - 2A_fp_f + \left(m_f + m_p\right)R^2\omega^2\right)\right] \end{aligned} \tag{12}$$

$$K_3 = -jcm_fR^2\left[\left(c^2m_f + A_fp_f\right)R^2 + E\left(I - 2AR^2\right)\right]\omega \tag{13}$$

$$K_4 = ER^2\left[A_p\left(2EI + \left(c^2m_f + A_fp_f\right)R^2\right) + I\left(m_f + m_p\right)R^2\omega^2\right] \tag{14}$$

$$K_5 = jcEI\,\mathrm{m}_f\,R^4\omega \tag{15}$$

$$K_6 = A_pE^2IR^4 \tag{16}.$$

Splošno rešitev enačbe (9) lahko zapišemo v naslednji obliki:

As is well known, the solution to equation (9) can also be written as:

$$U(s) = \sum_{i=1}^{6} D_ie^{\lambda_i s} \tag{17},$$

kjer so D_i neznani koeficienti, λ_i pa so koreni karakteristične enačbe (9). Ob znanem *U(s)*, pa lahko

where D_i are the unknown coefficients and λ_i are the roots of the characteristic equation (9). By knowing

zapišemo, zaradi sklopljenosti enačb (3) in (4), še *V(s)* kot:

the *U(s)* due to the coupled governing equations (3) and (4), *V(s)* can also be obtained:

$$V(s)=\sum_{i=1}^{6}\Gamma_i D_i e^{\lambda_i s} \tag{18}$$

kjer so koeficienti Γ_i enaki:

where the coefficients Γ_i are:

$$\Gamma_i=\frac{jm_f cR\omega+\lambda_i\left(A_f p_f+c^2 m_f-EA_p\right)R+\lambda_i^3 EIR}{c^2 m_f+A_f p_f+\left(m_f+m_p\right)R^2\omega^2-jm_f cR^2\lambda_i\omega+E\left(I+A_p R^2\right)\lambda_i^2}\qquad i=1,\ldots,6 \tag{19}$$

Z uporabo enačb (17) in (18) zapišemo primarne spremenljivke na krajiščih krožnega loka v matrični obliki kot:

Using equations (17) and (18) the displacements of the pipe end can be written in matrix form:

$$\begin{Bmatrix} U_Z \\ V_Z \\ -V_Z' \\ U_K \\ V_K \\ -V_K' \end{Bmatrix}=\begin{bmatrix} \alpha_{11} & \cdots & \alpha_{16} \\ \vdots & \ddots & \vdots \\ \alpha_{61} & \cdots & \alpha_{66} \end{bmatrix}\begin{Bmatrix} D_{V1} \\ \vdots \\ D_{V6} \end{Bmatrix} \tag{20}$$

kjer so:

where the coefficients a are:

$$\alpha_{1i}=\Gamma_i,\ \alpha_{2i}=1,\ \alpha_{3i}=-\lambda_i,\ \alpha_{4i}=\Gamma_i e^{\lambda_i L},\ \alpha_{5i}=e^{\lambda_i L},\ \alpha_{6i}=-\lambda_i e^{\lambda_i L}$$

Primarne spremenljivke so *U* osni pomik, *V* prečni pomik in *V'* zasuk. Indeksa *Z* in *K* primarnih spremenljivk pa ponazarjata začetno in končno krajišče. Enačbo (20) lahko v skrajšani obliki zapišemo kot:

The displacements are as follows: *U* is the axial displacement, *V* is the transversal displacement and *V'* is the slope. The letters Z and K indicate the start node and the end node, respectively. Equation (20) can be expressed further as:

$$\mathbf{W}_{in}=\mathbf{Q}_1\mathbf{D} \tag{21}$$

kjer je $\mathbf{W}_{in}$ vektor primarnih spremenljivk na krajiščih loka, **D** pa vektor neznanih koeficientov. Podobno kakor smo to zapisali v matrični enačbi (20) za primarne spremenljivke, zapišemo še sekundarne spremenljivke za krožni lok. Zveze med deformacijami in sekundarnimi spremenljivkami so podane v [8]. Matrična oblika je naslednja:

where $\mathbf{W}_{in}$ is the vector of the pipe-end displacements and **D** is the vector of the unknown coefficients. Using the Euler-Bernoulli theory for a curved pipe, the elastic restoring forces can be obtained with the equations given in [8]. Using these equations the elastic restoring forces at the end of the curved pipe are obtained with:

$$\begin{Bmatrix} -N_Z \\ -M_Z \\ -S_Z \\ N_K \\ M_K \\ S_K \end{Bmatrix}=\begin{bmatrix} \beta_{11} & \cdots & \beta_{16} \\ \vdots & \ddots & \vdots \\ \beta_{61} & \cdots & \beta_{66} \end{bmatrix}\begin{Bmatrix} D_{V1} \\ \vdots \\ D_{V6} \end{Bmatrix} \tag{22}$$

kjer so:

where the terms β are:

$$\beta_{1i}=-A_p E\left(\frac{1}{R}+\lambda_i\Gamma_i\right),\ \beta_{21}=-EI\left(\frac{\lambda_i\Gamma_i}{R}-\lambda_i^2\right),\ \beta_{3i}=-EI\left(\frac{\lambda_i^2\Gamma_i}{R}-\lambda_i^3\right)$$

$$\beta_{4i}=A_p E e^{\lambda_i L}\left(\frac{1}{R}+\lambda_i\Gamma_i\right),\ \beta_{5i}=EIe^{\lambda_i L}\left(\frac{\lambda_i\Gamma_i}{R}-\lambda_i^2\right),\ \beta_{6i}=EIe^{\lambda_i L}\left(\frac{\lambda_i^2\Gamma_i}{R}-\lambda_i^3\right).$$

Enačbo (22) zapišemo krajše v matrični obliki kot:

Equation (22) can be written as:

$$\mathbf{F}_{in}=\mathbf{Q}_2\mathbf{D} \tag{23}$$

kjer je $\mathbf{F}_{in}$ vektor neznanih sekundarnih spremenljivk z elementi: *N* osna sila, *M* upogibni moment in *S* prečna sila.

Razvidno je, da se vektor neznanih koeficientov **D** pojavlja tako v enačbi (21) kakor tudi v enačbi (23). Nepoznavanju vektorja **D** se lahko izognemo tako, da zapišemo neposredno povezavo med primarnimi in sekundarnimi spremenljivkami kot:

where $\mathbf{F}_{in}$ is the vector of the elastic restoring forces with the axial force *N*, the bending moment *M* and the shear force *S*.

The vector of the unknown coefficients appears in Equation (21) and also in Equation (23). To avoid the calculation of the unknown vector **D**, equation (21) is substituted into equation (23) and the relation between the elastic restoring forces and the displacements is obtained as:

$$\mathbf{F}_{in} = \mathbf{Q}_2\mathbf{Q}_1^{-1}\mathbf{W}_{in} \tag{24},$$

kjer $\mathbf{Q}_2\mathbf{Q}_1^{-1} = \mathbf{TM}_{in}$ pomeni togostno matriko velikosti 6×6, ki je funkcija frekvence. Togostno matriko $\mathbf{TM}_{in}$ je treba razširiti še za prostostne stopnje nihanja loka zunaj ravnine ukrivljenosti. Postopek določanja togostne matrike za nihanje loka izven ravnine je enak, kakor je prikazan za nihanje loka v ravnini. Tako dobimo togostno matriko krožnega loka $\mathbf{TM}^L$ velikosti 12×12, ki je definirana za krajevni koordinatni sistem krožnega loka in podaja povezavo med primarnimi in sekundarnimi spremenljivkami na začetnem in končnem krajišču, enačba (25):

where $\mathbf{Q}_2\mathbf{Q}_1^{-1} = \mathbf{TM}_{in}$ is the 6×6 dynamic stiffness matrix as a function of frequency. The dynamic stiffness matrix of the curved pipe has to be expanded for the out-of-plane vibration. The procedure for obtaining the dynamic stiffness matrix for the out-of-plane vibration is the same as was shown for the in-plane vibrations. Using this procedure, the final 12×12 dynamic stiffness matrix $\mathbf{TM}^L$ is obtained for the curved pipe. The relation between the displacement vector **W** and the vector of the elastic restoring forces **F** is given by the equation:

$$\mathbf{F} = \mathbf{TM}^L\mathbf{W} \tag{25}.$$

Metodologija prenosnih matrik vključuje v končni fazi verižno množenje prenosnih matrik posameznih elementov v rezultirajočo prenosno matriko $\mathbf{PM}_S$. Zaradi različne usmerjenosti posameznih elementov cevovoda je treba obravnavo prevesti na kinematične spremenljivke (primarne in sekundarne spremenljivke), definirane v absolutnem koordinatnem sistemu. Za spremembo vpeljemo transformacijsko matriko koordinatnih sistemov **Tc**. Enačbo (25) lahko sedaj zapišemo v absolutnem koordinatnem sistemu v obliki:

With this dynamic stiffness matrix and the dynamic stiffness matrix for the straight pipe, the final dynamic stiffness matrix for the complex 3-dimensional piping system using the global assembly techniques can be constructed. To assemble the dynamic stiffness matrix of a pipe element in a local coordinate system into the global coordinate system the transformation matrix **Tc** is introduced, so Equation (25) can be transformed into the global coordinate system as:

$$\mathbf{Tc}^{\mathrm{T}} \cdot \mathbf{F} = \mathbf{Tc}^{\mathrm{T}} \cdot \mathbf{TM}^{\mathrm{L}} \cdot \mathbf{Tc} \cdot \mathbf{W} \tag{26}$$

in v skrajšani obliki kot:

Or simply:

$$\mathbf{F}_G = \mathbf{TM}_G^L\mathbf{W}_G \tag{27}.$$

Indeks *G* ponazarja zapis enačbe v absolutnem koordinatnem sistemu. Na podlagi togostne matrike $\mathbf{TM}_G^L$ sedaj definiramo prenosno matriko $\mathbf{PM}_G^L$. Določimo jo s pomočjo delnega obrata dinamične togostne matrike tako, da v levem vektorju zberemo le spremenljivke, ki se pojavljajo na končnem krajišču in v desnem vektorju le spremenljivke, ki se pojavljajo v začetnem krajišču. Po delnem obratu dobimo:

The subscript *G* indicates that Equation (27) is defined in the global coordinate system. To obtain the transfer matrix from Equation (27) a partial inversion of the dynamic stiffness matrix is needed and further leads to the transfer matrix as:

$$\begin{Bmatrix} \mathbf{W}_{KG} \\ \mathbf{F}_{KG} \end{Bmatrix} = \begin{bmatrix} \mathbf{PM}_1 & \mathbf{PM}_2 \\ \mathbf{PM}_3 & \mathbf{PM}_4 \end{bmatrix} \begin{Bmatrix} \mathbf{W}_{ZG} \\ \mathbf{F}_{ZG} \end{Bmatrix} \tag{28}.$$

Enačbo (28) zapišemo kratko v obliki:

$$\mathbf{Z}_K = \mathbf{PM}_G^L \mathbf{Z}_Z \quad (29),$$

kjer sta $\mathbf{Z}_K$ in $\mathbf{Z}_Z$ vektorja stanja na končnem in začetnem krajišču. $\mathbf{PM}_G^L$ je prenosna matrika krožnega loka.

V gibalnih enačbah krožnega loka dušenje ni vpeljano izrecno, ker upoštevamo le strukturno dušenje, preko vpeljanega kompleksnega modula elastičnosti.

2 NUMERIČNI PREIZKUS

Na primeru cevovoda (sl. 3), smo s predstavljeno metodo določili prenosnost sile in jo primerjali s prenosnostjo, določeno z MKE, v programskem paketu ANSYS. Cevovod je sestavljen iz treh ravnih cevi (1, 3 in 5) ter treh krožnih lokov (2, 4 in 6). Podatki, ki smo jih uporabili pri analizi so naslednji: E=210 GPa, D=0,03 m, d=0,025 m, m_f=0,49 kg/m, m_p=1,695 kg/m. Dolžine ravnih cevi so: l_1=1 m, l_3=0,6 m in l_5=0,4 m in radiji lokov R_2=0,3 m, R_4=0,2 m in R_6=0,4 m. Uporabljeni programski paket ANSYS ne omogoča analize cevovoda s pretakajočo tekočino, zato je za analizirani primer vzeto, da tekočina miruje, c=0 m/s in ni pod nadtlakom. Z obravnavo po metodi prenosnih matrik smo celoten cevovod popisali s 6 elementi, medtem ko je v modelu KE cevovod modeliran s 60 ravnimi elementi *PIPE 16*. V obeh primerih smo analizirali prenos sile po cevi, iz točke *A* do točke *B*, v frekvenčnem področju od 10 do 250 Hz.

Prenos sile smo določevali z linearno prenosno funkcijo *TF*, ki je definirana kot $TF(\omega)=F_B(\omega)/F_A(\omega)$, kjer sta $F_A(\omega)$ amplituda vzbujevalne sile, $F_B(\omega)$ pa amplituda odzivne sile v

Equation (28) can be represented as:

$$\mathbf{Z}_K = \mathbf{PM}_G^L \mathbf{Z}_Z \quad (29),$$

where $\mathbf{Z}_K$ and $\mathbf{Z}_Z$ are the state vectors at the pipe-element ends.

The governing equations of the curved pipe are un-damped, because damping is modeled using the complex modulus of elasticity.

2 NUMERICAL EXPERIMENT

In this section the frequency-response analysis was carried out using the proposed transfer-matrix method and the FEM for the 3-dimensional piping system conveying a fluid, Fig. 3. The piping system was composed of three straight pipes (1,3 and 5) and three curved pipes (2, 4 and 6). The data used in the analyses were as follows: E=210 GPa, D=0.03 m, d=0.025 m, m_f=0.49 kg/m, m_p=1.695 kg/m. The lengths of the straight pipes were as follows: l_1=1 m, l_3=0.6 m and l_5=0.4, and the radii of curvature were R_2=0.3 m, R_4=0.2 m and R_6=0.4 m. The commercial package used for the FEM (Ansys) is not able to model the vibrations of pipes with a moving fluid. Consequently, only the case of a non-moving fluid was analyzed, c=0. The number of elements used in the transfer matrix approach was only 6, but with the finite-element method 60 straight pipe elements (PIPE 16) were used. The force transmissibility over the piping system, from point *A* to point *B*, was analyzed in both cases for the frequency range from 10 to 250 Hz.

For the computation of the force transmissibility, the transfer response function (*TF*) was defined as $TF(\omega)=F_B(\omega)/F_A(\omega)$, where $F_A(\omega)$ and $F_B(\omega)$ represent the forces at the points A and B

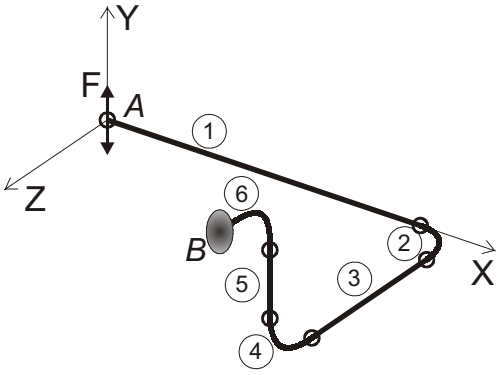

Sl. 3. *Primer 3D analiziranega cevovoda*
Fig. 3. *Analyzed numerical example*

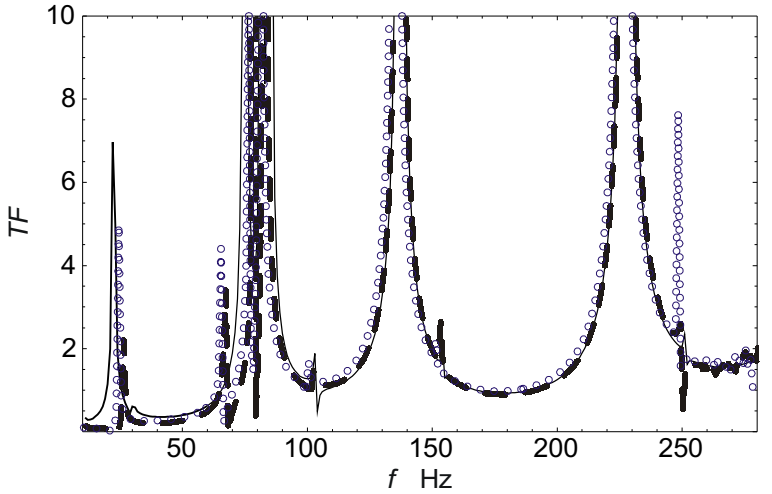

Sl. 4. *Prenosna funkcija TF v smeri y; (a) MPM, c=0 (---), (b) MKE, c=0 (—) in (c) MPM, c=2,5m/s (ooo)*
Fig. 4. *Transfer function TF in the y direction: (a) MPM, c=0 (---), (b) MKE, c=0 (—) and (c) MPM, c=2.5m/s (ooo)*

točki *B* v odvisnosti od frekvence. Prenosna funkcija je prikazana na sliki 4. Iz grafa je razvidno, da prihaja do neujemanja vrednosti prenosnosti, kakor tudi lastnih frekvenc, med prenosnima funkcijama, določenima z MPM in MKE v nizkem frekvenčnem področju, medtem ko je ujemanje v višjem frekvenčnem področju boljše. Razhajanje prenosa sile, določene z MPM in MKE v nizkem frekvenčnem področju, je posledica sklopljenih nihanj krožnega loka. To nakazuje dodatna resonančna frekvenca v področju med 60 Hz in 90 Hz v primeru obravnave z MPM, ki se v primeru obravnave z MKE ne pojavi. Glede na to, da je prenosna matrika izpeljana na temelju točne rešitve gibalnih enačb, medtem ko pri končnih elementih je rešitev približna z izbranimi oblikovnimi funkcijami, sklepamo, da podaja metoda prenosnih matrik bolj natančne rešitve. S slike 4 je tudi razvidno, da se v primeru upoštevanja hitrosti pretoka tekočine v cevi *c*=2,5 m/s potek prenosne funkcije nekoliko spremeni, iz enakega vzroka pa se spremeni tudi lega resonančnih frekvenc.

3 PREIZKUS

Izbrani matematični model za popis vibracij krožnega loka cevi smo ovrednotili s preizkusom. V prvi fazi nas je zanimala pravilnost uporabljenega modela na primeru krožnega loka, v drugi fazi pa njegova primernost za napoved prenosa vibracij po krožnem loku. Pravilnost modela smo ovrednotili na kompozitni gumeni cevi znanih geometrijskih lastnosti. Za določitev prenosa prečnih vibracij in lastnih

at the discrete frequencies. The transmissibility of the force obtained with the transfer-matrix method and the finite-element method is shown in Fig. 4. The finite-element method gives similar results to the transfer-matrix method in the higher-frequency regions but in the lower-frequency regions the difference is greater. The differences in the force transmissibility at low frequencies are believed to be due to the uncoupled axial and flexural vibration in the finite-element formulation. This shows in the additional resonance frequency that occurs from 60 Hz to 90 Hz in the transfer-matrix approach but not with the finite-element method. However, in the transfer-matrix approach the dynamic properties are derived exactly from the governing equations for the straight pipe and the curved pipe; therefore, the results from the transfer-matrix method are exact within the range of validity of the assumed governing equations and the plug-flow model. As can be seen from Fig. 4, example (c), the fluid effects can not be neglected.

3 EXPERIMENAL STUDY

The suitability and verification of the mathematical model used for the prediction of the vibration transmissibility over the curved pipes was tested with an experiment. The verification of the mathematical model was made on a curved rubber hose. The hose was excited with a sweep-sine signal in the frequency range from 15 to 300 Hz. At the excited end of the hose the amplitude

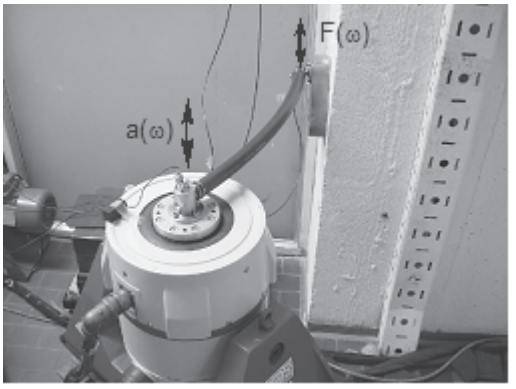

Sl. 5. *Preizkus za merjenje prenosnosti sile krožnega loka*
Fig. 5. *Experimental setup for measuring the vibration of the curved pipe*

frekvenc smo sistem vzbujali s sinusnim signalom v območju od 15 Hz do 300 Hz (prelet frekvenc). Pri meritvi smo zajemali amplitudo vzbujevalnega pospeška $a(\omega)$ na enem krajišču, na drugem pa preneseno amplitudo sile $F(\omega)$, kakor je prikazano na sliki 5.

Na temelju teh dveh merjenih spremenljivk smo definirali prenosno funkcijo kot:

of the acceleration $a(\omega)$ was measured and at the end the amplitude of the transferred force $F(\omega)$ was measured. The experimental set-up is shown in Fig 5.

The vibration transmissibility of the curved pipe is derived from the ratios of the measured excitations and responses as:

$$TF_M(\omega) = \frac{F(\omega)}{a(\omega)} \tag{30},$$

ki bo rabila za ugotavljanje ustreznosti uporabljenega matematičnega modela.

Za določitev prenosa vibracij preko loka z uporabo matematičnega modela je treba poznati poleg geometrijskih tudi snovne lastnosti gradiva. Geometrijski podatki so preprosto izmerljivi, medtem ko je določitev elastičnega modula E nekoliko večji problem. Obravnavani lok je namreč kompozit več plasti gume in ojačan z vlakni. Glede na prevladujoči delež gume v kompozitu le-ta izkazuje viskoelastične lastnosti. Lastnosti viskoelastičnega gradiva lahko v primeru harmonskih pomikov podajamo s kompleksnim elastičnim modulom, ki je funkcija frekvence. Imaginarni del kompleksnega modula elastičnosti predstavlja dušilne lastnosti materiala. Običajnega testa statičnega določanja elastičnega modula v tem primeru ne moremo uporabiti. Wei [11] navaja možnost ocenitve povprečnega elastičnega modula prereza na podlagi resonančne tehnike. Podal je zvezo za oceno modula elastičnosti, če poznamo izmerjene lastne frekvence ter geometrijske in snovne lastnosti gradiva:

Equation (30) will be used for the assessment of the suitability of the mathematical model.

For the calculation of the vibration transmissibility with the derived mathematical model, the proper geometrical and material characteristics need to be identified. Geometrical data can be easily obtained, while a measurement of the elastic modulus represents a slightly larger problem. The analyzed hose is made from different layers of rubber and is reinforced with a cord. This hose has viscoelastic properties because of the overall composition of the rubber. The viscoelastic properties can be described under harmonic load with a complex elastic modulus, which in many cases is frequency dependent. The imaginary part of the complex elastic modulus relates to the energy dissipation. The conventional static method for measuring the elastic modulus cannot be used in this case. Wei [11] proposed the resonance technique for determining the average elastic modulus for composite structures. The relation between the modulus of elasticity and the resonance frequencies is determined by means of the formula:

$$E_i = CWf_i^2 \tag{31},$$

kjer so: W masa preizkušanca, f_i^2 i-ta lastna frekvenca in C faktor oblike, definiran kot:

where W is the mass of the specimen, f_i^2 is the resonant frequency and C is the factor that can be written in the form:

$$C = \frac{4\pi^2 L^3}{n^4 I} \quad (32),$$

kjer so: L dolžina, n koeficient robnega pogoja in I vztrajnostni moment prereza. Elastični modul obravnavanega loka smo določili pri štirih lastnih frekvencah. Za popis elastičnega modula čez celotno obravnavano frekvenčno območje smo dobljene vrednosti interpolirali s kubičnim polinomom. Imaginarni del elastičnega modula smo ocenili po literaturi [12] in ga nato popravili glede na ujemanje prenosnih funkcij v okolici resonance. Ovrednotenje tako dobljenega elastičnega modula je bila izvedena na krožnem loku in ravni cevi različnih dolžin. Izmerjena in izračunana krivulja prenosnosti sile preko krožnega loka sta prikazani na sliki 6. Razvidno je, da je ujemanje med meritvami in rezultatom numeričnega modela zadovoljivo. Iz grafa je razvidno, da so amplitude funkcije prenosnosti določene z numeričnim modelom nekoliko manjše kakor pa to pokažejo meritve. Predvidevamo, da je razlika posledica izbranega poenostavljenega modela za določitev snovnih lastnosti cevovoda.

4 SKLEPI

V prispevku predstavljena metoda prenosnih matrik se izkaže za učinkovito metodo pri modeliranju prenosa vibracij preko poljubnega cevovoda v prostoru. Izpeljana prenosna matrika v drugem poglavju z uporabo prenosne matrike za ravno cev, definirane v [10], omogoča dodatno upoštevanje vpliva pretakajoče se tekočine in nadtlaka na prenos vibracij preko cevovoda.

where L is the length of the specimen, n is a factor that depends on the boundary conditions, and I is the second area moment of the cross-section. The elastic modulus of the hose was estimated from the first four resonant frequencies. The values of the elastic modulus were interpolated above the entire frequency range of interest with a cubic polynomial. The imaginary part of the elastic modulus was assessed on the basis of the literature [12] and then corrected to fit the transmissibility function at the resonant region. The measured values of the elastic modulus were verified for the straight pipes of different lengths. The measured and calculated transfer functions are shown in Fig. 6. It is clear from Fig. 6 that the agreement between the transfer functions is good. The amplitudes of the transmissibility function obtained with the TMM are shown to be a little smaller than the amplitudes of the measured transfer function. We believe that the difference in the amplitudes of the transfer functions is due to the simplified model used for the material properties.

4 CONCLUSIONS

The paper presents the use of the transfer-matrix method for modeling the vibration transmission over an arbitrary piping system in space. With the help of the derived matrix in Section 2 and the matrix for straight piping, which is shown in [10], we can consider the additional influence of the fluid flow and the fluid pressure on the vibration transmission over the piping system. The fluid model used in the analysis

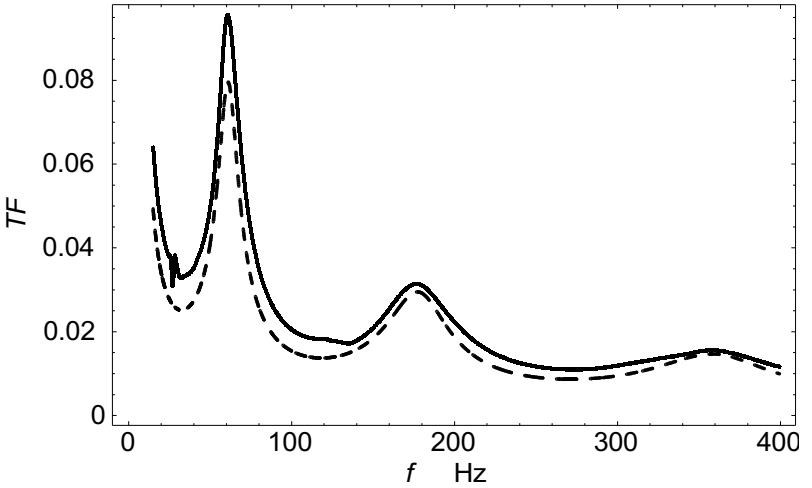

Sl. 6. *Graf izmerjene in numerično dobljene prenosne funkcije: izmerjeno (—), MPM (---)*
Fig. 6. *Measured and calculated transfer functions: measurement (—) and TMM (---)*

Uporabljen model tekočine je preprost, zato omogoča le analizo vpliva tekočine na prenos vibracij, medtem ko dinamičnih učinkov tekočine s takšnim modelom ne moremo analizirati.

Iz analiziranega numeričnega primera vidimo, da dobimo po MPM podobne rezultate kakor po MKE, kar pomeni, da metoda s teoretičnega vidika deluje pravilno. Na podlagi analiziranega primera, pri katerem upoštevamo pretakajočo se tekočino, lahko sklepamo, da tega vpliva ne smemo zanemariti, predvsem za večje hitrosti tekočine.

Primerjava eksperimentalno in numerično določene prenosnosti potrdi pravilnost uporabljenega postopka, saj je ujemanje vrednosti prenosnosti kakor tudi vrednosti lastnih frekvenc precej dobro. Uporabljeni kompleksni elastični modul za popis snovnih lastnosti se izkaže v primeru harmonskega obremenjevanja viskoelastičnega gradiva za primernega.

Predstavljena metoda torej lahko uspešno rabi za iskanje optimalne sestave cevi različnih gradiv in geometrijske oblike, z namenom zmanjševanja prenosa vibracij po cevovodu. Omogoča tudi analizo že obstoječih cevovodov, pri katerih lahko spreminjamo režim delovanja (hitrost in tlak tekočine), z namenom zmanjševanja prenosa vibracij. V prihodnje bi bilo primerno preveriti prenos vibracij preko spojev dveh cevi, saj v obravnavanih numeričnih primerih predpostavljamo, da se vibracije prenašajo preko spojev brez dodatnih ojačitev ali izgub.

can only account for the influence of the fluid on the vibration transmission, while the additional observation of the dynamic effect of the fluid is not possible.

It is clear from Figure (4) that the results obtained with the TMM model and the FEM model give similar values regarding the vibration transmission function. From this we can conclude that the presented method gives the correct results from the theoretical point of view. The results obtained from the case study showed that the consideration of the fluid's influence on the piping system is very important, especially for high flow velocities.

The comparison of the experimental and numerical results for the vibration transmission verifies the correctness of the used approach, because the vibration transmissions function and the values of the natural frequencies give a satisfactory agreement. The use of the complex modulus of elasticity was found to be suitable for the purposes of accounting the viscoelastic material properties and the harmonic excitation of the piping system.

In general, the presented method proves to be very useful for the optimization of the shape of a piping system with different material properties and geometries, with the objective of minimizing the vibration transmission. The model can also be used for an analysis of an existing piping system, where the influence of the fluid velocity and the fluid pressure can be observed and varied for the purposes of minimizing the vibration transmission. In future work the joints of the piping substructures could be modeled and analyzed, because in the present paper the assumption of an ideal vibration transmission over the joint is made, which means there are no additional increases in the vibrations because of joints.

5 LITERATURA
5 LITERATURE

[1] Paidoussis, M. P., 1st edition, ed. (1998) Fluid-structure interactions, *Academic Press*.

[2] Gorman, D. G., Reese, J. M. & Zhang, Y. L. (2000) Vibration of a flexible pipe conveying viscous pulsating fluid flow, *Journal of Sound and Vibration* 230(2), 379-392.

[3] Kim, M. Y.; Kim, N. I. & Min, B. C. (2002) Analytical and numerical study on spatial free vibration of non-symmetric thin-walled curved beams, *Journal of Sound and Vibration* 258(4), 595-618.

[4] Lee, S. Y. & Chao, J. C. (2000) Out-of-plane vibrations of curved non-uniform beams of constant radius, *Journal of Sound and Vibrations* 238(3), 443-458.

[5] Sreejith B., Jayaray K., N. Ganesan, Padmanabhan D., Chellapandi P. & Selvaray P. (2004) Finite element analysis of fluid-structure interaction in pipeline system, *Nuclear Engineering and Design* 227, 313-322.

[6] Mattheis A., Trobitz M., Kussmaul K., Kerkhof K., Bonn R. & Beyer K. (2000) Diagnostics of piping by ambient vibration analysis, *Nuclear Engineering and Design* 198, 131-140.

[7] Huang Y., Zeng G. & Wei W. (2002) A new matrix method for solving vibration and stability of curved pipes conveying fluid, *Journal of Sound and Vibration* 251(2), 215-225.

[8] Walsh A. & White R. G. (2000) Vibrational power transmission in curved beams, *Journal of Sound and Vibration* 233(3), 455-488.
[9] Koo G. H. & Park Y. (1996) Vibration analysis of a 3-dimensional piping system conveying fluid by wave approach, *International Journal of Pressure Vessels and Piping* 67, 249-256.
[10] Tadina M. (2005) Prenos vibracij preko armiranih gumenih cevi, Diplomska naloga, *Univerza v Ljubljani.*
[11] Wei C.Y. & Kureka S. N. (2000) Evaluation of damping and elastic properties of composites and composite structure by resonance technique, *Journal of Material Science* 35, 3785-3792
[12] Lakes R. S.: High damping composite materials: Effect of structural hierarchy, *Journal of Composite Materials* 36(3)

Naslov avtorjev: Matej Tadina
prof. dr. Miha Boltežar
Univerza v Ljubljani
Fakulteta za strojništvo
Aškerčeva 6
1000 Ljubljana
matej.tadina@fs.uni-lj.si
miha.boltezar@fs.uni-lj.si

Authors' Address: Matej Tadina
Prof. Dr. Miha Boltežar
University of Ljubljana
Faculty of Mechanical Eng.
Aškerčeva 6
SI-1000 Ljubljana, Slovenia
matej.tadina@fs.uni-lj.si
miha.boltezar@fs.uni-lj.si

Prejeto: 13.3.2007
Received:
Sprejeto: 25.4.2007
Accepted:
Odprto za diskusijo: 1 leto
Open for discussion: 1 year

Strojniški vestnik - Journal of Mechanical Engineering 53(2007)6, 399-408
UDK - UDC 534.83:621.512
Strokovni članek - Speciality paper (1.04)

Vpliv okrova na hrup batnega kompresorja

The Influence of the Housing on the Noise Emitted by a Reciprocating Compressor

Anže Jerič - Janez Gradišek - Igor Grabec - Edvard Govekar
(Fakulteta za strojništvo, Ljubljana)

V prispevku analiziramo vpliv okrova na hrup tipičnega batnega kompresorja za gospodinjske aparate. Analiza lastnosti hrupa kompresorja z okrovom in brez njega temelji na meritvah zvočnega tlaka in zvočne intenzivnosti. Eksperimentalno ugotovljene elastične lastnosti okrova kompresorja primerjamo s teoretičnim izračunom, ki temelji na metodi končnih elementov. Rezultati izkazujejo dobro ujemanje glavnih frekvenc hrupa z lastnimi frekvencami okrova. V prispevku pokažemo, kako lahko s preprosto ojačitvijo okrova zmanjšamo amplitudo in spremenimo frekvenčno vsebino hrupa, izmerjenega zunaj kompresorja.

(Ključne besede: gospodinjski aparati, batni kompresorji, hrup, intenzivnost hrupa)

The influence of the housing on the noise emitted by a typical reciprocating compressor for domestic appliances is analyzed. Sound-pressure and sound-intensity measurements were conducted to analyze the properties of the noise emitted by the compressor with and without the housing. The experimentally determined elastic properties of the compressor housing were compared with calculations based on a finite-element model. The results show that the dominant noise frequencies correspond to the eigen frequencies of the housing. Simple stiffening of the housing is shown to reduce the amplitude and modify the frequency content of the noise recorded outside the compressor.

(Keywords: domestic appliances, reciprocating compressors, noise, sound intensity)

0 UVOD

Pri izbiri kompresorjev za gospodinjske aparate na današnjem trgu je hrup eno najpomembnejših meril. Z namenom zmanjšanja hrupa kompresorja je treba raziskati tako vire hrupa kakor tudi poti prenosa hrupa ([3] in [2]). V splošnem so viri hrupa odvisni od načina stiskanja hladilnega medija, prenosne poti hrupa pa od konstrukcije kompresorja [2].

V pričujočem prispevku raziskujemo hrupnost enobatnega kompresorja, ki vsebuje v okrov vgrajeno kompresorsko enoto. Izkaže se, da so glavni viri hrupa v kompresorski enoti utripanje hladilnega medija vzdolž cevi in komor ter vibracije sesalnega in izpušnega ventila. Hrup oddan znotraj okrova, se prek okrova prenese v okolico, kjer ga sliši uporabnik gospodinjskega aparata z vgrajenim kompresorjem. Ker hrup v okolico oddaja okrov, pričakujemo, da njegove elastične lastnosti vplivajo na lastnosti hrupa zunaj kompresorja.

0 INTRODUCTION

Noise is one of the most important selection criteria in today's market for the compressors in domestic appliances. In order to reduce the noisiness of a compressor, one has to investigate both the noise sources and the noise transmission paths ([3] and [2]). In general, noise sources depend on the physical principle employed for compression, while the transmission paths depend on the design of the compressor [2].

In this article the noisiness of a single-piston reciprocating compressor is investigated. The compressor consists of a compressor unit mounted in a housing. The dominant noise sources within the compressor unit appear to include the cooling-media pulsations in the muffler and along the pipes and chambers, the inlet/outlet valve vibration, etc. The noise emitted within the housing is then transmitted through the housing to the outside, where it is heard by the owner of the domestic appliance in which the compressor is used. Since the housing acts as a noise transmitter, it is expected that its elastic properties affect the properties of the noise outside the compressor.

Cilj tega prispevka je preučiti vpliv okrova na hrup zunaj kompresorja. V ta namen smo izmerili in primerjali zvočni tlak in prostorsko porazdelitev zvočne intenzivnosti kompresorja z okrovom in brez njega. Prenosno funkcijo okrova smo ugotovili eksperimentalno in teoretično z modelom končnih elementov. Analiza je pokazala, da se glavne frekvence hrupa kompresorja z okrovom ujemajo z lastnimi frekvencami nihanja okrova. Preprosta ojačitev okrova kompresorja spremeni frekvenčno vsebino hrupa in zmanjša amplitudo glavnih frekvenc hrupa.

1 PREIZKUSI

Da bi ugotovili vpliv okrova na oddani hrup kompresorja, smo pri preizkusih uporabili dva kompresorja: enega z okrovom in enega brez okrova. Kompresor v okrovu je deloval v enakih razmerah kakor v gospodinjskem aparatu. Pri kompresorju brez okrova sta bili sesalna in izpušna cev odprti, kar je preprečevalo normalno delovanje. Prevzeli smo, da odprte cevi nepomembno spremenijo lastnosti hrupa, ki je oddan med delovanjem kompresorja. Preizkuse smo opravili v sobi za standardno merjenje ravni zvočne moči kompresorjev za gospodinjske aparate.

Z uporabo mikrofona in zvočne sonde smo pri obeh kompresorjih izmerili zvočni tlak in zvočno intenzivnost. Mikrofon je bil nameščen navpično nad kompresorjem, približno 25 cm nad pokrovom okrova kompresorja. Znotraj 2 min periode delovanja kompresorja smo izmerili po 10 signalov zvočnega tlaka pri frekvenci vzorčenja 16 kHz. Dolžina signalov

The aim of the article is to examine the influence of the housing on the noise outside the compressor. For this purpose, the sound pressure and the spatial distribution of the sound intensity are recorded and compared for a reciprocating compressor with and without a housing. The transfer function of the housing is determined experimentally and theoretically using a finite-element model. The analysis shows that the dominant frequencies of the noise from the compressor with the housing mainly correspond to the eigen frequencies of the housing, and that a simple reinforcement of the compressor housing modifies the frequency content of the noise and reduces the amplitudes of the dominant noise frequencies.

1 EXPERIMENTS

In order to determine the influence of the housing on the noise emitted by the compressor, experiments were conducted using two reciprocating compressors: one with a housing and one without. The compressor with a housing was operated under realistic conditions. In the compressor without a housing the suction and exhaust pipes had to be opened, which prevented normal operating conditions. However, it was assumed that the open pipes did not significantly change the properties of the noise emitted during the operation of the compressor. The experiments were conducted in a room designed for standard measurements of the sound-power level for the compressors of domestic appliances.

Sound pressure and sound intensity were recorded for both compressors using a microphone and a sound-intensity probe. The microphone was mounted directly above the compressor at a distance of approximately 25 cm from the compressor surface. During a 2-min period of compressor operation, 10 sound-pressure signals were recorded at a sampling

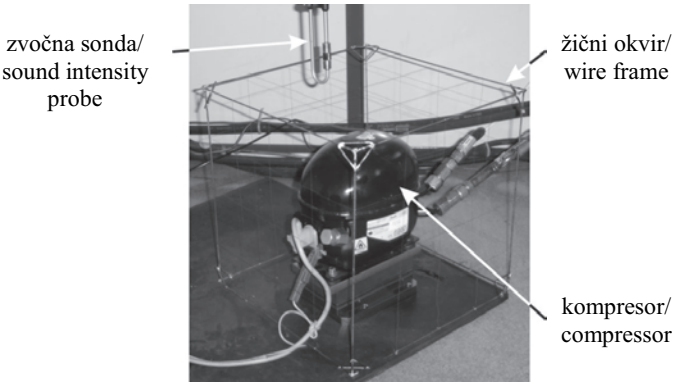

Sl. 1. *Eksperimentalno mesto za meritve zvočne intenzivnosti*
Fig. 1. *Experimental setup for sound-intensity measurement*

je bila 4 s. Signale smo shranili za poznejšo frekvenčno analizo.

Za merjenje zvočne intenzivnosti smo uporabili sondo z dvema mikrofonoma, obrnjenima čelno drug proti drugemu. Med mikrofonoma je bil nameščen 12 mm debel distančnik, ki omogoča kakovostne meritve signalov s frekvencami do 5 kHz. Pri meritvah prostorske porazdelitve zvočne intenzivnosti smo zvočno sondo postavljali na navidezno kocko, ki jo je predstavljal okvir iz tanke žice.

Vsaka od petih primerjalnih ravnin kocke je vsebovala 16 naključno razporejenih primerjalnih točk. Razdalja med primerjalnimi ravninami in površino kompresorja je bila približno 15 cm. Na vsaki primerjalni točki smo izmerili 6 parov 4 s dolgih signalov zvočnega tlaka pri frekvenci vzorčenja 20 kHz. Zvočno intenzivnost smo nato izračunali iz imaginarnega dela križnega spektra parov signalov zvočnega tlaka ([1] in [4]). Zvočna sonda je bila vedno usmerjena pravokotno na primerjalno ravnino. Tako izračunana in analizirana zvočna intenzivnost je bila komponenta vektorja zvočne intenzivnosti pravokotno na površino kompresorja.

Modalne lastnosti okrova kompresorja smo ugotovili eksperimentalno in teoretično. Eksperimentalni način vključuje impulzno vzbujanje okrova z instrumentalnim kladivom na več naključno razporejenih točkah vzdolž pokrova okrova (sl. 2). Odziv okrova smo izmerili s pospeškomerom nameščenim na vrh pokrova. Na vsaki točki vzbujanja

frequency of 16 kHz, lasting 4 sec each. The signals were stored for subsequent frequency analysis.

For the sound-intensity measurement a probe with a face-to-face arrangement of the pressure microphones was employed. A 12-mm solid spacer was used between the microphones, allowing high-quality measurements of signals with frequencies up to 5 kHz. To determine the spatial distribution of the sound intensity the outer form of the compressor was modelled with a virtual square block represented by a thin wire frame.

Each of the five reference planes of the block contained 16 evenly distributed reference points. The distance between the reference planes and the compressor surface was approximately 15 cm. At each reference point, six pairs of sound pressure signals were recorded at a sampling frequency of 20 kHz, lasting 4 sec each. The sound intensity was then calculated from the imaginary part of the cross-spectrum of a pair of sound pressure signals ([1] and [4]). The sound-intensity probe was always oriented perpendicularly to the reference plane, and thus the sound-intensity calculated and analyzed in this article is in fact a component of the sound-intensity vector normal to the reference plane.

The modal properties of the compressor housing were determined experimentally and theoretically using a finite-element (FE) model. The experiments involved impact excitation of the housing using an instrumented hammer at several points evenly distributed along the housing cover (Fig. 2). The response of the housing was recorded by an accelerometer mounted on top of the cover. At each excitation point, 10 excita-

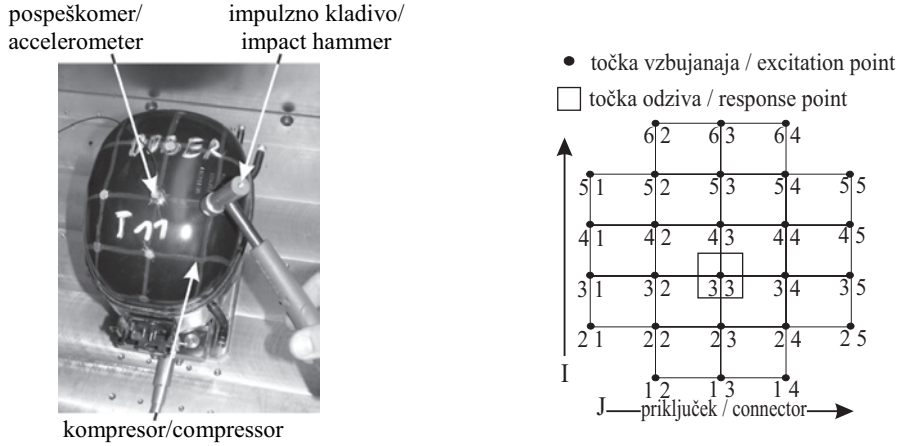

Sl. 2. *Eksperimentalno mesto za merjenje prenosne funkcije (levo) in porazdelitev točk vzbujanja in točke odziva*

Fig. 2. *Experimental setup for transfer-function measurement (left), and the distribution of the excitation points and the response point*

smo izmerili po 10 parov 1 s dolgih signalov vzbujanja in odziva pri frekvenci vzorčenja 25 kHz. Izmerjene signale smo nato uporabili za izračun prenosne funkcije pokrova okrova [5].

Lastne frekvence in lastne oblike okrova smo izračunali tudi prek modela končnih elementov z uporabo ustreznega tržnega programa.

2 REZULTATI

2.1 Zvočni tlak

Najprej obravnavajmo zvočni tlak hrupa, ki ga odda kompresor z okrovom in brez njega. Slika 3 prikazuje povprečna amplitudna spektra izmerjenih signalov v logaritemski skali za oba kompresorja. Povprečna amplituda hrupa kompresorja z okrovom je približno dva reda velikosti nižja od tiste pri kompresorju brez okrova. Opazimo lahko tudi razliko v frekvenčni vsebini hrupa obeh kompresorjev. V hrupu kompresorja z okrovom so glavni spektralni vrhovi pri frekvencah 4,2 KHz, 5,3 kHz in 5,7 kHz. V spektru hrupa kompresorja brez okrova pomembnih vrhov pri teh frekvencah ne opazimo, glavni vrhovi so na območju od 50 Hz do 2 kHz. V obeh primerih so

tion-response signal pairs were recorded at a sampling frequency of 25 kHz, lasting 1 sec each. The recorded signals were then used to calculate the transfer function of the housing cover [5].

The eigen frequencies and eigen modes of the housing were also calculated using an FE model with a commercial FE solver.

2 RESULTS

2.1 Sound Pressure

Let us first consider the sound pressure of the noise emitted by the compressor with and without the housing. The average amplitude spectra of the recorded sound-pressure signals for the two compressors are shown in Fig. 3. It is obvious that the average amplitude of the noise emitted by the compressor with the housing is much lower than without the housing. A difference in the frequency content of the two noises can also be observed. In the noise of the compressor with the housing, the dominant spectral peaks are found at frequencies of 4.2 kHz, 5.3 kHz and 5.7 kHz. In the noise of the compressor without the housing, these spectral peaks are not observed at all, although there are several dominant peaks in the range from 50 Hz to 2

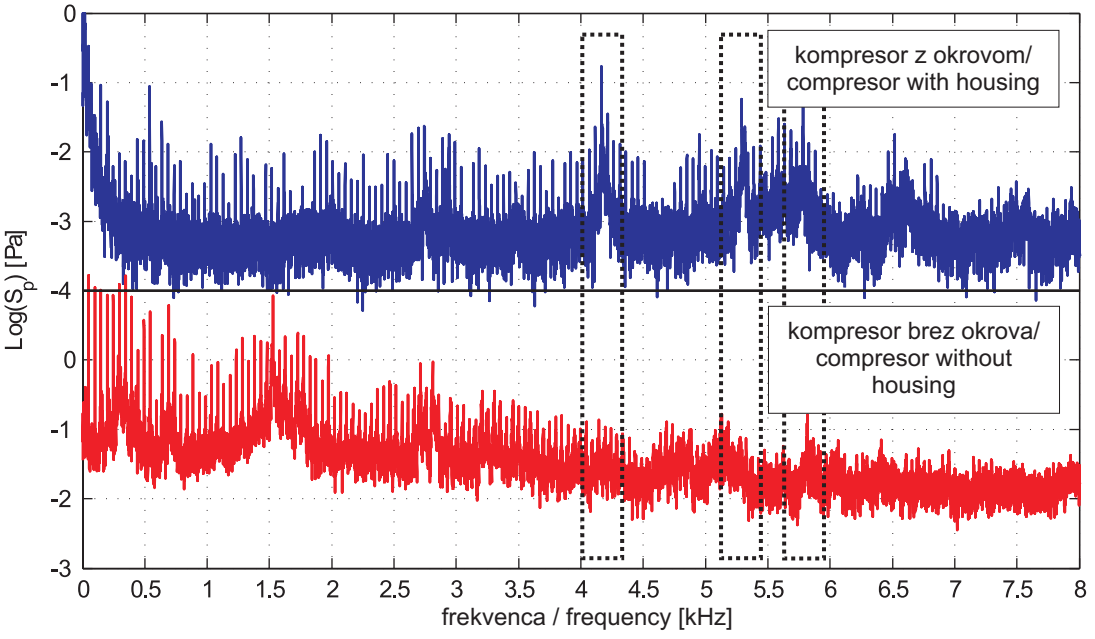

Sl. 3. *Povprečni amplitudni spekter zvočnega tlaka za kompresor z okrovom (zgoraj) in brez njega (spodaj)*

Fig. 3. *Average amplitude spectra of the sound pressure of the noise emitted by the compressor with (top) and without the housing (bottom)*

spektralni vrhovi večinoma pri večkratnikih frekvence 50 Hz, ki se ujema z osnovno frekvenco delovanja kompresorja. Ti rezultati dokazujejo, da okrov ne samo zmanjša amplitudo hrupa oddanega znotraj okrova kompresorja, temveč tudi izrazito spremeni frekvenčno vsebino hrupa. Analiza prostorske porazdelitve zvočne intenzivnosti, ki jo bomo predstavili v naslednjem razdelku, pokaže nekatere dodatne vplive okrova na lastnosti hrupa.

2.2 Zvočna intenzivnost

Slika 4 prikazuje prostorsko porazdelitev zvočne intenzivnosti za kompresor z okrovom in brez njega. Vsak od petih polj s 16 kvadrati ustreza eni od petih referenčnih ravnin okrog kompresorja, tako kakor je prikazano v desnem zgornjem kotu slike. Na vsakem od 16 kvadratov posamezne ravnine je povprečna amplituda in usmerjenost zvočne intenzivnosti predstavljena v osenčeni skali. Negativna vrednost povprečne zvočne intenzivnosti tako predstavlja obratno smer širjenja zvoka. Ravni zvočne moči L_{Wi} nad petimi polji pa pomenijo moč hrupa, oddanega skozi posamezno referenčno ravnino. Uokvirjena vrednost L_W pomeni celotno raven zvočne moči iz vseh primerjalnih ravnin.

Kompresor z okrovom odda največ hrupa skozi vrhnjo (5) in desno (2) primerjalno ravnino. Največje amplitude zvočne intenzivnosti smo opazili na vrhnji ravnini (5). Prostorska porazdelitev zvočne intenzivnosti za kompresor brez okrova je precej drugačna. Ta večino hrupa odda skozi spodnjo desno (2) in zadnjo (3) ravnino, kjer so dušilnik ter sesalna in izpušna cev. Celotna raven zvočne moči, ki jo odda kompresor z okrovom in brez okrova, je 34,1 dB in 79,3 dB. To označuje močan dušilni učinek okrova. Razlika med prostorsko porazdelitvijo zvočne intenzivnosti kompresorja z okrovom in brez okrova kaže, da poleg zmanjšanja amplitude hrupa in spremembe njegove frekvenčne vsebine okrov tudi prostorsko prerazporedi oddani hrup.

Rezultati analize zvočnega tlaka in zvočne intenzivnosti kažejo, da okrov močno popači hrup kompresorja zunaj okrova. Da bi vpliv okrova na hrup bolje razumeli, bomo v naslednjem razdelku predstavili analizo modalnih lastnosti okrova.

kHz. In both cases the spectral peaks are mostly located at multiples of 50 Hz, which corresponds to the fundamental operating frequency of the compressor. These results therefore indicate that the housing not only reduces the amplitude of the noise emitted by the compressor, but it also markedly changes the frequency content of the noise. The analysis of the spatial distribution of the sound intensity presented in the next section shows some additional influences of the housing on the properties of the noise.

2.2 Sound intensity

Fig. 4 shows the spatial distribution of the sound intensity for the compressor with and without the housing. The five fields with 16 squares each correspond to the five reference planes around the compressor, as illustrated in the top-right-hand corner of the figure. On every square of each reference plane the average sound-intensity amplitude and its orientation are represented on a colour scale. In this way a negative value of the average sound intensity denotes the opposite sound-propagation direction. The sound-power levels L_{Wi} above the five fields denote the noise power emitted through the five reference planes. The boxed sound-power level L_W stands for the total sound-power level from all the reference planes.

The compressor with a housing emits most of the noise through the top (5) and right (2) reference planes. The highest sound-intensity amplitudes are found at the top plane (5). The spatial distribution of the sound intensity for the compressor without the housing is significantly different. Most of the noise is emitted from the bottom-right-hand (2) and back (3) planes, where the muffler and inlet and outlet pipes are located. The total sound-power levels emitted by the compressor with and without the housing are 34.1 dB and 79.3 dB, respectively, indicating the tremendous damping effect of the housing. However, the differences between the spatial distributions of the sound intensity of the compressors with and without the housing also show that, apart from decreasing the noise amplitude and modifying its frequency content, the housing also spatially rearranges the noise emitted by the compressor.

The results of the sound-pressure and sound-intensity analyses therefore indicate that the compressor noise recorded outside the housing is significantly affected by the housing. In order to better understand the influence of the housing on the noise it is necessary to determine the modal properties of the housing.

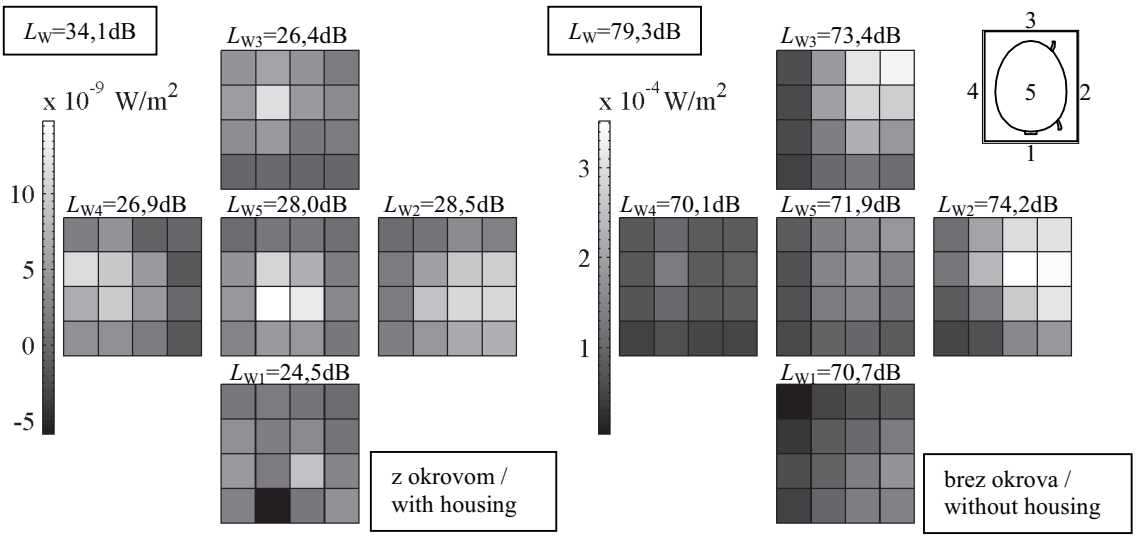

Sl. 4. *Prostorska porazdelitev zvočne intenzivnosti v frekvenčnem območju od 200 Hz do 8 kHz za kompresor z okrovom (levo) in brez njega (desno); amplitudni skali se razlikujeta za več velikostnih redov.*

Fig. 4. *Spatial distribution of the sound intensity in the frequency range from 200 Hz to 8 kHz emitted by the compressor with (left) and without housing (right). Note that the amplitude scales differ by several orders of magnitude.*

2.3 Prenosna funkcija pokrova okrova

Prenosno funkcijo pokrova okrova smo ugotovili eksperimentalno z merilnikom pospeškov nameščenim na vrh pokrova kompresorja in teoretično z modelom končnih elementov. Slika 5 kaže amplitudo izmerjene prenosne funkcije na vrhu pokrova okrova (mesto označuje točka 33 na sl. 2). Najvišji spektralni vrhovi, ki predstavljajo lastne frekvence okrova, so pri frekvencah 4,2 kHz, 5,2 kHz, 5,6 kHz in 6,5 kHz. Omenjene frekvence so zelo blizu frekvencam glavnih spektralnih vrhov v spektru hrupa, ki ga odda kompresor z okrovom (sl. 3).

2.3 Transfer function of the housing cover

The transfer function of the housing cover was determined experimentally using the accelerometer mounted on the top of housing cover and theoretically by the finite-element (FE) method. Fig. 5 shows the amplitude of the recorded transfer function at the top of the housing cover (point 33 in Fig. 2). The highest spectral peaks appear at frequencies of 4.2 kHz, 5.2 kHz, 5.6 kHz and 6.5 kHz, which represent the eigen frequencies of the housing. Similar frequencies were obtained using the FE method. These frequencies closely match those of the dominant spectral peaks in the spectrum of the noise emitted by the compressor with the housing (Fig. 3).

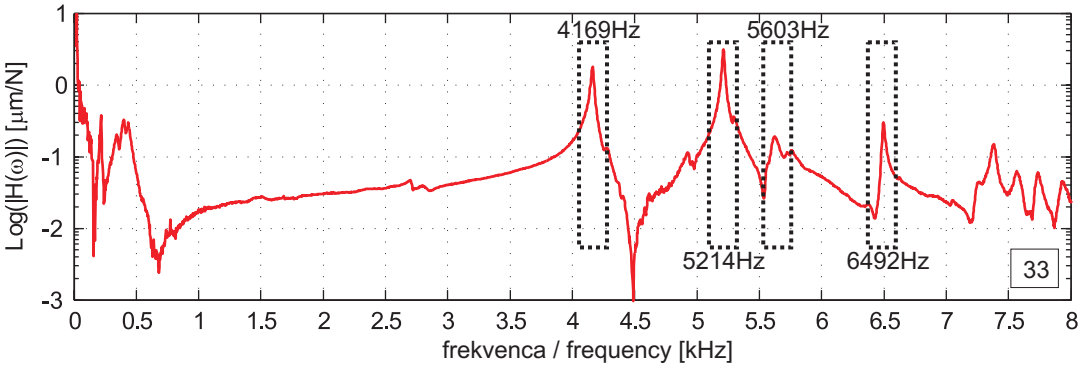

Sl. 5. *Amplituda prenosne funkcije pokrova okrova na vrhu pokrova*

Fig. 5. *Amplitude of the transfer-function amplitude of the housing cover at the cover top*

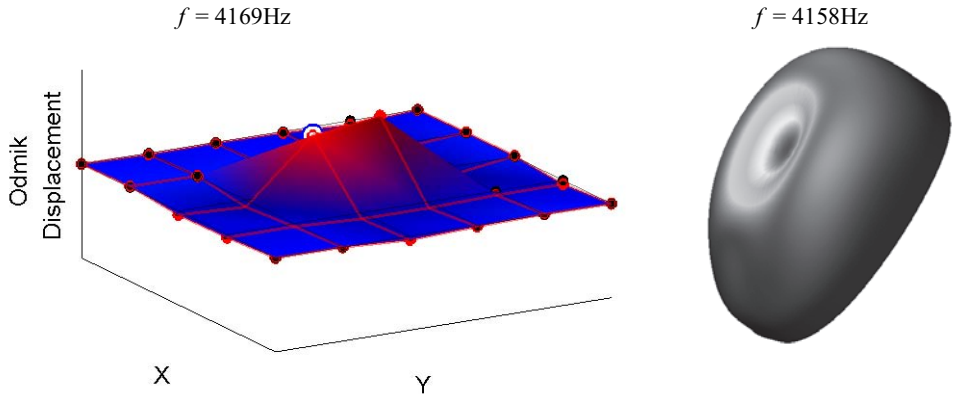

Sl. 6. *Rekonstruirana (levo) in z metodo končnih elementov izračunana (desno) glavna lastna oblika pri frekvenci 4169 Hz*
Fig. 6. *The reconstructed (left) and the FE-calculated (right) shapes of the dominant eigen mode at a frequency of 4169 Hz*

Slika 6 kaže meritev rekonstruirane in z metodo končnih elementov izračunane oblike izrazitejših lastnih oblik pokrova okrova. Lastne oblike po obeh metodah se zelo dobro ujemajo. Iz lastnih oblik lahko razberemo, da se mesta največjih odmikov okrova ujemajo z mesti največjih amplitud zvočne intenzivnosti (sl. 6). Za zmanjšanje amplitude hrupa kompresorja, ki se prenese skozi okrov, se tako zdi najbolj logična rešitev ojačitev okrova [2].

3 PREPROSTA SPREMEMBA OKROVA

Obstaja več načinov ojačanja okrova. Na primer sprememba oblike okrova, povečanje njegove debeline ali pritrditev ojačitvenih reber. V naši raziskavi smo izbrali zadnji način in na vrh okrova navarili dve prekrižani rebri (sl. 7). Mesto reber smo določili na podlagi analize lastnih oblik in porazdelitve zvočne intenzivnosti, medtem ko smo za obliko reber izbrali kar najpreprostejši profil vara. Vpliv spremenjenega okrova smo vrednotili z analizo zvočnega tlaka in porazdelitve zvočne

Fig. 6 shows the reconstructed and FE-calculated shapes of the dominant eigen mode of the housing cover. The two mode shapes agree very well. It is clear from the mode shapes that the location of the maximum housing displacement corresponds to the location of the highest sound-intensity amplitudes (Fig. 6). It therefore seems reasonable to stiffen the housing in order to decrease the amplitude of the noise emitted by the compressor through the housing [2].

3 SIMPLE MODIFICATION OF THE HOUSING

There are several ways to stiffen the housing, such as modifying its design, increasing its thickness or attaching stiffening ribs to it. For this investigation, the last of these methods was chosen, and two crossed ribs were welded to the top of the housing (Fig. 7). The location of the ribs was determined based on the analysis of the eigen-mode shapes and the spatial distribution of the sound intensity, while the shape of the ribs was chosen to be as simple as possible. The influence of such a modification was evaluated by an analysis of the sound pres-

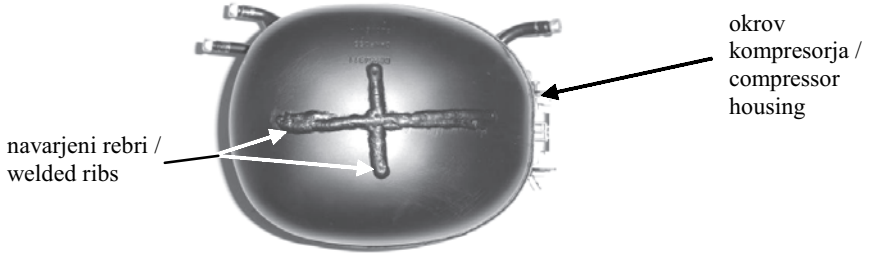

Sl. 7. *Kompresor s spremenjenim okrovom*
Fig. 7. *Compressor with modified housing*

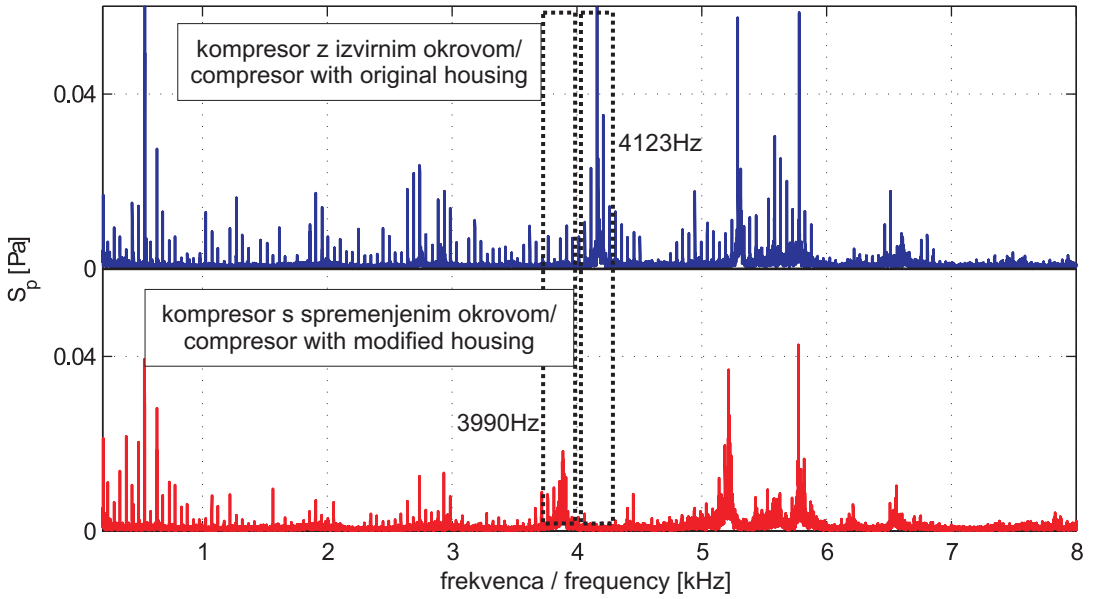

Sl. 8. *Povprečni amplitudni spekter zvočnega tlaka za kompresor z izvirnim (zgoraj) in spremenjenim okrovom (spodaj)*

Fig. 8. *Average amplitude spectra of the sound pressure of the noise emitted by the compressor with the original (top) and modified housings (bottom)*

intenzivnosti hrupa kompresorja s spremenjenim okrovom.

Slika 8 primerja amplitudni spekter zvočnega tlaka hrupa kompresorja z izvirnim in spremenjenim okrovom. Sprememba okrova zmanjša amplitudo in spremeni frekvenco glavnih spektralnih vrhov hrupa. Glavni spektralni vrh se s 4,1 kHz za izvirni okrov premakne na 3,9 kHz za spremenjeno okrov, medtem ko se njegova amplituda opazno zmanjša. Analiza prenosne funkcije spremenjenega okrova tudi potrdi, da frekvence glavnih spektralnih vrhov hrupa še vedno ležijo blizu lastnih frekvenc okrova.

Slika 9 primerja prostorsko porazdelitev zvočne intenzivnosti za kompresor z izvirnim in spremenjenim okrovom. Sprememba okrova je zmanjšala ravni zvočne moči na desni (2), levi (4) in vrhnji (5) primerjalni ravnini, medtem ko celotna raven zvočne moči pade s 34,1 dB na 33,1 dB. Natančnejša analiza je pokazala, da raven moči najbolj pade na območju od 3,5 kHz do 4,3 kHz [6], ki vsebuje glavne spektralne vrhove hrupa.

4 SKLEP

V prispevku smo analizirali vpliv okrova na hrup batnega kompresorja. Analize

sure and the sound-intensity distribution of the noise emitted by the compressor with a modified housing.

Fig. 8 compares the amplitude spectra of the sound pressure for noise emitted by the compressors with the original and modified housings. The modification of the housing decreases the amplitudes and changes the frequency of the dominant spectral peaks of the noise. The dominant spectral peak is shifted from 4.1 kHz for the original housing to 3.9 kHz for the modified housing, while its amplitude is significantly decreased. An analysis of the transfer function of the modified housing also confirms that the frequencies of the dominant spectral peaks of noise still lie close to the eigen frequencies of the housing.

The spatial distributions of the sound intensity emitted by the compressors with original and modified housings are compared in Fig. 9. The housing modification decreased the sound-power levels at the right (2), left (4) and top (5) reference planes, while the total sound-power level decreased from 34.1 dB to 33.1 dB. A detailed analysis revealed that the largest decrease in the power level occurs in the frequency range from 3.5 kHz to 4.3 kHz [6], which contains the dominant spectral peak of the noise.

4 CONCLUSION

In this paper we analysed the influence of the housing on the noise emitted by a reciprocating

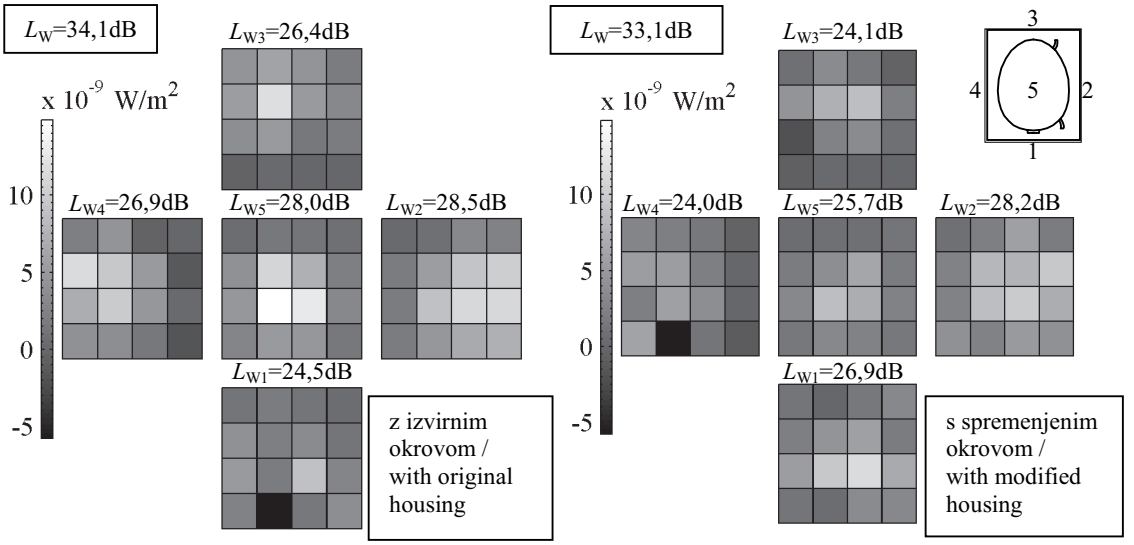

Sl. 9. *Prostorska porazdelitev zvočne intenzivnosti v frekvenčnem območju od 200 Hz do 8 kHz za kompresor z izvirnim (levo) in s spremenjenim okrovom (desno)*

Fig. 9. *Spatial distribution of the sound intensity in the frequency range from 200 Hz to 8 kHz emitted by the compressor with the original (left) and with the modified housing (right)*

izmerjenega zvočnega tlaka in prostorske porazdelitve zvočne intenzivnosti za kompresor z okrovom in brez njega so pokazale, da je vpliv okrova na hrup oddan znotraj kompresorja ter prenesen skozi okrov zelo velik. Okrov ne samo zaduši amplitudo hrupa, temveč tudi spremeni njegovo frekvenčno vsebino in prostorsko porazdelitev okrog kompresorja.

Glavni spektralni vrhovi hrupa kompresorja z okrovom so blizu lastnih frekvenc okrova. Mesta največjih amplitud zvočne intenzivnosti se ujemajo z mesti največjih odmikov, ki smo jih ugotovili prek lastnih oblik okrova. Za ojačanje okrova kompresorja smo na vrh pokrova okrova navarili dve rebri. Ta sprememba je zmanjšala amplitudo hrupa in spremenila frekvence glavnih spektralnih vrhov hrupa, medtem ko je raven zvočne moči hrupa kompresorja se je znižala s 34,1 dB na 33,1 dB. Ti rezultati kažejo, da hrup kompresorja lahko zmanjšamo s spremembo okrova. Prepričani smo, da naprednejša a še vedno cenovno ugodna sprememba okrova lahko vodi do znatnega zmanjšanja hrupa batnega kompresorja za gospodinjske aparate.

compressor. An analysis of the recorded sound pressure and the spatial distribution of the sound intensity emitted by the compressor with and without the housing revealed that the housing significantly affects the noise emitted inside and transmitted through the housing. The housing not only dampens the noise amplitude, but it also modifies its frequency content and the spatial distribution around the compressor.

The dominant spectral peaks of the noise emitted by the compressor with the housing are located close to the eigen frequencies of the housing. The locations of the dominant sound-intensity amplitudes match the locations of the displacement maxima determined by the eigen modes of the housing. In order to stiffen the housing, two ribs were welded to the top of the housing cover. This modification decreased the noise amplitude and changed the frequencies of the dominant spectral peaks of the noise, while the sound-power level of the noise radiating from the compressor was decreased from 34.1 dB to 33.1 dB. These results show that a reduction of the compressor noise can be achieved by modifying the housing. We believe that more advanced, yet inexpensive, housing modifications could lead to considerable reductions in the noise emitted by a reciprocating compressor in domestic appliances.

5 LITERATURA
5 REFERENCES

[1] M.J. Crocker, J.P. Arenas (2003) Fundamentals of the direct measurement of sound intensity and practical applications, *Acoustical Physics* 2(2003), pp.163–175.
[2] S. Le Moyne, J.-L. Tebec, I. Tawfiq (2005) Acoustical influence of stiffeners on acoustic radiation of plates, *Mechanical Systems and Signal Processing* (2005), pp. 195–212.
[3] M.P. Norton (2003) Fundamentals of noise and vibration analysis. *Cambridge University Press*.
[4] F.J. Fahy (1995) Sound intensity, Second edition. *E & FN Spon*.
[5] D. J. Ewins (2000) Modal testing: theory, practice and application. *Research Studies Press*, Philadelphia.
[6] A. Jerič (2005) Acoustic emission analysis of a compressor for domestic appliances (in Slovene), Undergraduate thesis. *University of Ljubljana, Faculty of Mechanical Engineering*, Ljubljana.
[7] "ISO 9614-1 – Acoustics – Determination of sound power levels of noise sources using sound intensity – Part 1: Measurement at discrete points".

Naslov avtorjev: Anže Jerič
doc. dr. Janez Gradišek
prof. dr. Igor Grabec
prof. dr. Edvard Govekar
Univerza v Ljubljani
Fakulteta za strojništvo
Aškerčeva 6
1000 Ljubljana
anze.jeric@gmail.com
edvard.govekar@fs.uni-lj.si

Authors' Address: Anže Jerič
Doc. Dr. Janez Gradišek
Prof. Dr. Igor Grabec
Prof. Dr. Edvard Govekar
University of Ljubljana
Faculty of Mechanical Eng.
Aškerčeva 6
1000 Ljubljana, Slovenia
anze.jeric@gmail.com
edvard.govekar@fs.uni-lj.si

Prejeto: 12.2.2007
Received:
Sprejeto: 25.4.2007
Accepted:
Odprto za diskusijo: 1 leto
Open for discussion: 1 year

Strojniški vestnik - Journal of Mechanical Engineering 53(2007)6, 409-419
UDK - UDC 532.58
Strokovni članek - Speciality paper (1.04)

Dinamično odzivanje valjaste cevi na gibajoči se tlak

The Dynamic Response of a Cylindrical Tube under the Action of a Moving Pressure

Bahador Saranjam[1] - Kambiz Bakhshandeh[1] - Mohammad-Hassan Kadivar[2]
([1]MUT University, Iran; [2]Shiraz University, Iran)

V predstavljeni raziskavi smo z metodo končnih elementov preučili dinamično odzivanje valjastih cevi na notranji gibajoči se tlak, ki potuje s stalno hitrostjo. V prispevku predpostavljamo, da je debelina sten cevi povsod enaka in majhna v primerjavi s povprečnim polmerom cevi. Moč gibajočega se tlaka in hitrosti čela tlaka je stalna. Izračunali smo dinamično obnašanje različnih valjev z različnimi razmerji med dolžino in premerom. Glede na ugotovitve naše raziskave ima analiza dinamike bistven pomen za hitrost visokega tlaka. V naši raziskavi smo določili dve novi zasnovi: faktor radialne dinamične povečave in dolgi del. Pokazali smo, da sta vrednost in obnašanje faktorja radialne dinamične povečave odvisna od razmerja med dolžino in premerom ter ju lahko razdelimo na tri območja.V primeru dolgega valja lahko obnašanje faktorja radialne dinamične povečave razdelimo na podkritično, prehodno in nadkritično območje. Po izsledkih naše raziskave se faktor radialne dinamične povečave giblje med 1,8 in 2,55 in je odvisen od dolžine valjev. Za analizo končnih elementov smo uporabili računalniški program Msc/Nastran.

(Ključne besede: gibanje tlaka, analize končnih elementov, faktor radialne dinamične povečave, valjaste cevi)

In this study the dynamic response of cylindrical tubes subjected to an internal moving pressure, travelling at a constant velocity, has been investigated with the finite-element method. In this paper the tube's wall thickness is considered to be uniform throughout and small compared to the mean radius of the tube. The intensity of the moving pressure as well as the velocity of the front is constant. The dynamic behaviour of various cylinders with different length-to-diameter ratios is calculated. Based on this study, we believe a dynamic analysis is essential for a high pressure velocity. In this study, two new concepts are defined: the radial dynamic magnification factor and the long member. We show that the value and behaviour of the radial dynamic magnification factor are dependent on the length-to-diameter ratio and can be divided into two or three regions. For a long cylinder the behaviour of the radial dynamic magnification factor is divided into the under-critical, transition and overcritical regions. According to this study, the radial dynamic magnification factor changes from 1.8 to 2.55, depending on the length of the cylinders. The Msc/Nastran software package was used for the finite-element analysis.

(Keywords: moving pressure, finite element analysis, dynamic magnification factor, cylindrical tube)

0 UVOD

Različne konstrukcije, od mostov do cest in cevovodov, so neprestano izpostavljene gibajočim se silam ali tlakom. Določanje dinamičnega učinka gibajočega se bremena na elastične konstrukcije, posebno na cevi, je zelo zapletena naloga. Vemo, da je dinamični učinek obremenitve na steno cevi velik, kadar se čelo tlaka z veliko hitrostjo giblje vzdolž cevi. Analiza mirovanja stene cevi je smiselna, kadar se čelo tlaka giblje z majhno hitrostjo. Za velike

0 INTRODUCTION

Various structures, ranging from bridges and roads to pipes, are constantly acted upon by moving forces or pressures. Determining the dynamic effects of moving loads on elastic structures and, particularly, on pipes, is a very complicated problem. It is known that the dynamic effect of the stresses on the tube's wall is large when a pressure front with high velocity moves down a tube. A static analysis of the tube wall is valid when the pressure front moves with low velocity.

hitrosti pa analiza mirovanja ne zadošča in je treba izvesti analizo dinamike.

Problem sestavov, ki so izpostavljeni različnim obremenitvam, se pogosto pojavlja v sodobnem inženirstvu. Primeri takšnih struktur so: mostovi, žerjavi in letališke steze [1]. Večinoma so bili doslej ti sistemi pri uporabi tramov in plošč oblikovani z uporabo metod analize in približka ([2] do [4]). Nekaj avtorjev je sicer pripravilo podlage za izpeljavo dinamičnih enačb, ki bi veljale za splošna ogrodja, ki nosijo potujoča bremena, a so v praksi upoštevali le modele tramov ali plošč. Zato so nerešeni problem splošnih ogrodij, še posebej ogrodij iz valjastih plošč, ki so izpostavljeni gibajočemu se tlaku, spregledali, ali mu posvetili premalo pozornosti. Tang [5] je raziskoval dinamično odzivanje polzaprte valjaste cevi, ki je izpostavljena notranjemu gibajočemu se tlaku. Tudi Faria [6] je z metodo končnih elementov analiziral tresenje lupine valja, na katerega deluje gibajoča se sila ali masa. Preučeval je učinek krivine valja. Opravljenih je bilo nekaj raziskav gibajočega se tlaka, še posebej za primer končnega valja.

V naši raziskavi smo preučili dinamično obnašanje različnih valjastih cevi, na katere deluje gibajoči se tlak. Predpostavili smo, da se čelo tlaka giblje s stalno hitrostjo vzporedno z osjo cevi, in da je moč tlaka povsod enaka. Upoštevali smo različne valje z različnimi razmerji med dolžino in premerom. Dinamično obnašanje vsakega valja smo izračunali za širok razpon mogočih hitrosti. Definirali smo dve novi zasnovi, faktor radialne dinamične povečave in dolgi del.

Faktor radialne dinamične povečave (FRDP) je razmerje med radialnim dinamičnim upogibom in radialnim statičnim upogibom. Izpeljali in primerjali smo faktorje radialne dinamične povečave za različna razmerja med dolžino in premerom. S faktorjem radialne dinamične povečave smo uvedli še eno zamisel, dolgi del. Tega smo definirali kot valj, pri katerem je dinamična povečava stalna glede na določen razpon hitrosti tlaka. Za analizo končnih elementov smo uporabili računalniški program Msc/Nastran.

1 POSTOPEK DOLOČITVE FAKTORJA RADIALNE DINAMIČNE POVEČAVE

Postopek, ki smo ga uporabili za določitev faktorja radialne dinamične povečave, je vključeval

However, for high velocities a static analysis is not enough and a dynamic analysis must be used.

The problem of structures subjected to varying loads is often encountered in modern engineering. A few examples of such structures are bridges, overhead cranes and airport runaways [1]. However, most studies to date have modelled these systems using analytical and approximate methods for the cases of beams or plates ([2] to [4]). A few authors have provided a basis for the derivation of the dynamic governing equations of general shells carrying moving loads but have, in practice, implemented beam or plate models only. Hence, the important problem of general shells, in particular cylindrical panels, subjected to a moving pressure has been overlooked or received little attention. Tang [5], investigated the dynamic response of a semi-finite cylindrical tube under an internal moving pressure. Also, Faria [6] analyzed the vibration of a cylinder's panel resulting from a moving force or mass using the finite-element method. The studies focused on the cylinder's curvature effect. There have been few studies on moving pressures in cylinders, especially for finite cylinders.

In this study, the dynamic behaviour of various cylindrical tubes under the action of a moving pressure is investigated. The pressure front is assumed to be moving with constant velocity, parallel to the axis of the tube, and the pressure intensity is assumed to be uniform. Various cylinders with different length-to-diameter ratios are considered. The dynamic behaviour of each cylinder is calculated for a wide range of speeds. Two new concepts are defined: the radial dynamic magnification factor and the long member.

The radial dynamic magnification factor (RDMF) is the ratio of the radial dynamic deflection to the radial static deflection. The radial dynamic magnification factor for various length-to-diameter ratios is extracted and compared. Also, with use of RDMF behaviour another concept is defined, i.e., the long member. The long member is defined as a cylinder for which the dynamic magnification has a constant behaviour in a part of the pressure speed range. The Msc/Nastran software package was used for the finite-element analysis.

1 PROCEDURE FOR DETERMINING THE RADIAL DYNAMIC MAGNIFICATION FACTOR

The procedure employed in this study consisted of determining the radial dynamic magnification

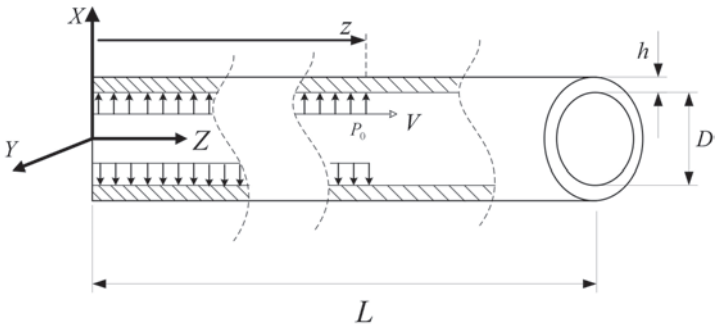

Sl. 1. *Valj, izpostavljen gibajočemu se tlaku*
Fig. 1. *Cylinder subjected to a moving pressure*

metodo končnih elementov. Faktor radialne dinamične povečave smo izračunali za valj, ki je izpostavljen gibajočemu se tlaku (Sl. 1). Čelo tlaka se giblje od leve strani valja s stalno hitrostjo V in velikostjo P_0.

Faktor radialne dinamične povečave smo določili kot radialni dinamični upogib valja deljen z radialnim statičnim upogibom na sredini dolžine valja.

Pri naši raziskavi smo obravnavali različne valje s stalnim razmerjem med debelino in premerom (h/D) in različne vrednosti razmerja med dolžino in premerom (L/D). Dolžina valjev L se spreminja od $L = D$ do $L = 20D$. Za vsak valj smo izračunali statični radialni upogib. Izračune smo izvedli za različne vrednosti razmerja med dolžino in premerom (L/D) ter stalno razmerje med debelino stene in premerom ($h/D = 0{,}05$).

Izračunali smo radialne dinamične upogibe valjev za različne hitrosti gibajočega se tlaka. Z delitvijo dinamičnih upogibov valjev z izračunanim statičnim upogibom dobimo FRDP za različne valje in za določen razpon hitrosti gibajočega se tlaka. Slika 2 prikazuje analizni algoritem, ki smo ga uporabili v raziskavi. V tem postopku smo upoštevali širok razpon hitrosti, da smo lahko prepoznali obnašanje faktorja FRDP za vsak valj posebej.

Izračun končnih elementov smo izvedli z računalniškim programom Msc/Nastran [7]. Izračun linearne elastičnosti prehoda smo izvedli za potrebe izračuna odziva sestava na gibajoči se tlak bremena. Pri vseh izračunih smo v smislu izotropne elastičnosti ravninske napetosti uporabili metodo končnih elementov s standardnim 8-vozliščnim izoparametričnim elementom s štirimi stranicami.

Za doseganje primerne gostote mreže, potrebne za izboljšanje natančnosti rezultatov, smo

factor using the finite-element (FE) method. The radial dynamic magnification factor is calculated for a cylinder subjected to a moving pressure (Figure 1). The pressure front begins to move from the left-hand side of cylinder with a constant speed V and magnitude P_0.

The radial dynamic magnification factor is defined as the radial dynamic deflection of the cylinder divided by the radial static deflection of the cylinder at mid-length.

In this study various cylinders with a constant thickness-to-diameter ratio (h/D) and various values of the length-to-diameter (L/D) ratio are considered. The length L of the cylinders changes from $L = D$ to $L = 20D$. For each cylinder the static radial deflection is calculated. The computations were performed for different values of the length-to-diameter (L/D) ratio and a constant thickness-to-diameter ratio ($h/D = 0.05$).

The radial dynamic deflections of the cylinders were calculated for various moving pressure speeds. With dividing these dynamic deflections by the calculated radial static deflection, the RDMF for various cylinders was obtained for a particular moving pressure speed range. The analysis algorithm that was used is shown in Figure 2. This procedure was performed for a wide range of velocities in order to investigate the RDMF behaviour of each cylinder.

The finite-element calculation was made with the Msc/Nastran software package [7]. A transient linear elastic calculation was carried out to calculate the structural response to a moving pressure load. The FE method with a standard 8-node quadrilateral iso-parametric element was used in the context of plane-stress isotropic elasticity for all the computations.

Various mesh densities in the longitudinal direction of each cylinder were used to achieve a suit-

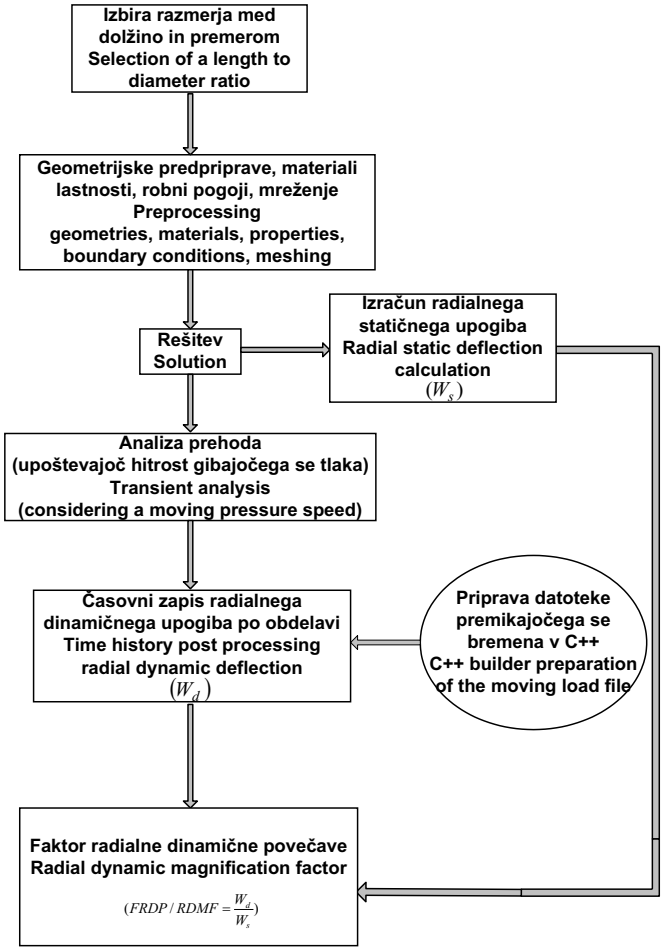

Sl. 2. *Analizni algoritem*
Fig. 2. *Analysis algorithm*

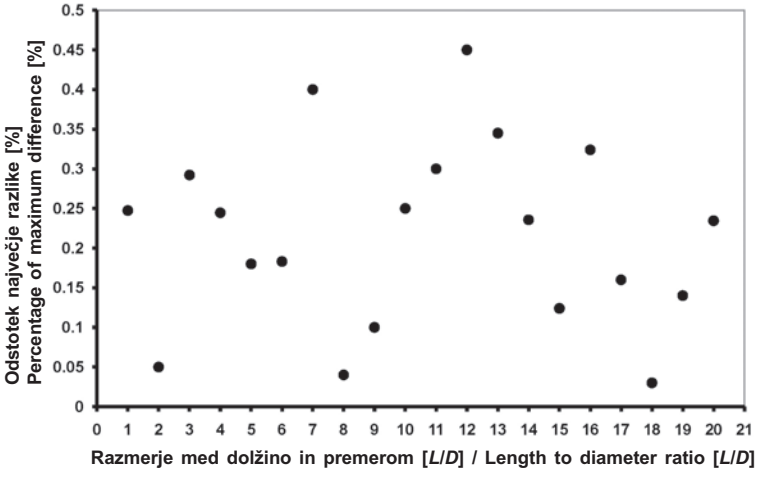

Sl. 3. *Rezultati študije konvergence*
Fig. 3. *Convergence study results*

uporabili različne gostote mreže po dolžini vsakega valja. Zgoščevanje mreže smo ponavljali, dokler ni postala razlika med zaporednimi rezultati manjša od 0,5%. Slika 3 prikazuje končna odstopanja faktorjev dinamične povečave pri različnih razmerjih med dolžino in premerom.

Gostoto radialne mreže smo izbrali tako, da je razmerje med stranicami elementov približno 1. Slika 4 prikazuje tipični model končnih elementov, ki smo ga uporabili v naši raziskavi. Model vsebuje 27.662 vozlišč in 9.073 elementov, pri katerih je $L/D = 1$ ter 304.254 vozlišč in 100.801 elementov, pri katerih je $L/D = 20$. Vsako vozlišče ima šest prostostnih stopenj.

Valji so preprosto podprti in jih lahko analiziramo z uporabo naslednjih robnih pogojev:
Začetni pogoj:

able mesh density to improve the accuracy of the results. Densifying the mesh was iteratively repeated until the difference between consecutive results became less than 0.5%. In Figure 3 the final discrepancy of the dynamic magnification factor for various length-to-diameter ratios is shown.

The radial mesh density was chosen so that elements' aspect ratios become about 1. Figure 4 shows a typical FE model used in this study. The FE model consists of 27,662 nodes and 9,073 elements for $L/D = 1$ to 304,254 nodes and 100,801 elements for $L/D = 20$. Each node has six degrees of freedom.

The cylinders were simply supported and could be analyzed by employing the following boundary conditions:
Initial condition:

$$w(z,0) = \dot{w}(z,0) = 0 \tag{1}$$

Robni pogoj:

Boundary condition:

$$\begin{aligned} w(0,t) &= w(L,t) = 0 \\ M(0,t) &= M(L,t) = 0 \end{aligned} \tag{2},$$

kjer sta:
$w(z,t)$ - radialni pomik v točki z in času t,
$M(z,t)$ - upogibni moment v točki z in času t.

Najpomembnejši del simulacijske metode končnih elementov je oblikovanje oblike gibajočega se tlaka bremena in pogojev za njegovo delovanje. Prehodno breme smo prikazali z določitvijo tlaka v odvisnosti od časa v vsaki posamezni točki. Slika 5 prikazuje spreminjanje tlaka v točki z_i.

where:
$w(z,t)$ - the radial displacement at point z and time t,
$M(z,t)$ - the bending moment at point z and time t.

The most important part of the FE method simulation was the modelling and preconditioning of a moving pressure load with the required profile. Transient loading was represented by describing the pressure as a function of time at each point. Figure 5 shows the pressure history at point z_i.

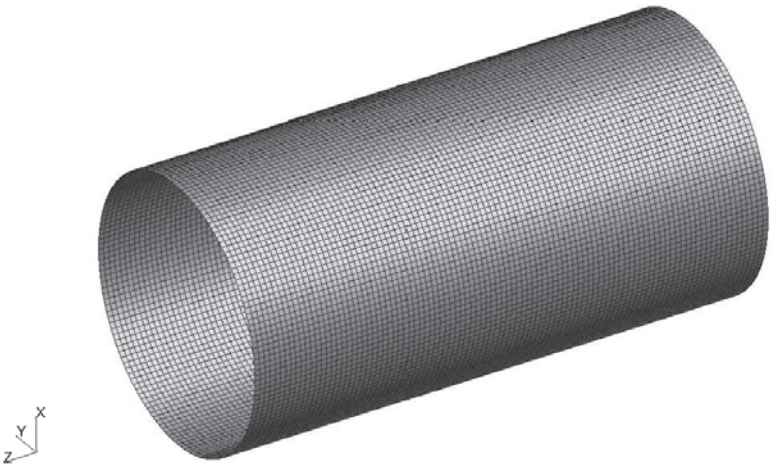

Sl. 4. *Model končnih elementov*
Fig. 4. *Finite-element model*

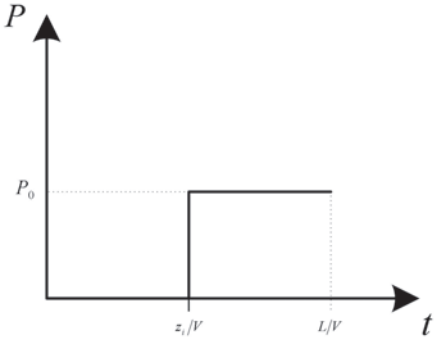

Sl. 5. *Porazdelitev tlaka*
Fig. 5. *Pressure distribution*

Prikaz sprememb tlaka v vsaki točki valja je določen kot:

This pressure history for each point of the cylinder was defined as:

$$P(z,t) = P_0 u(t - z/V) \tag{3}$$

kjer so:
P_0 - velikost tlaka,
u - skočna funkcija,
V - hitrost gibajočega se tlaka.

where:
P_0 - pressure magnitude
u - step function
V - travelling speed of the pressure

Ta tlak smo uporabili pri modelu končnih elementov s približno 1000 odseki v razdobju L/V, ki je enako trajanju vsake posamezne simulacije.

This pressure was applied to the finite-element model with about 1000 segments over a time period of L/V, equal to the duration of each simulation.

Metodo končnih elementov lahko uporabimo tudi za neenakomerni prerez trama [8]. Analizni algoritem, ki ga uporabimo v tem primeru, je podoben algoritmu iz slike 2. Kakor smo pokazali z našo študijo, ponuja metoda končnih elementov veliko natančnost, zato lahko to metodo uporabimo za izračun gibajočega se tlaka ali sile na različnih sestavih.

The FE method has also been used for a non-uniform cross-sectional beam [8]. The analysis algorithm used for this beam is similar to Figure 2. As shown in that study, the accuracy of the FE method is excellent, and so this method can be used for calculating a moving pressure or force in various structures.

Za potrebe analize prehoda smo uporabili Newmarkovo metodo [7] in z njo izvedli integracijo po času, pri kateri so znani vsi parametri za t_n, hkrati pa lahko t_{n+1} izračunamo z uporabo naslednje enačbe gibanja:

For transient analysis the Newmark [7] method is used to integrate with respect to time; where all the parameters for t_n are known, t_{n+1} can be calculated using the following equation of motion:

$$\mathbf{M}\ddot{q}_{n+1} + \mathbf{C}\dot{q}_{n+1} + \mathbf{K}q_{n+1} = \mathbf{F}_{n+1}^{ext}, \tag{4}$$

kjer so: **M** matrika mase, **C** matrika dušenja, **K** matrika togosti, $\mathbf{F}_{n+1}^{ext}$ vektor zunanjega bremena, $\ddot{q}_{n+1}$ pospešek pri t_{n+1}, $\dot{q}_{n+1}$ hitrost pri t_{n+1} in q_{n+1} pomik pri t_{n+1}.

where **M** is the mass matrix, **C** is the damping matrix, **K** is the stiffness matrix, $\mathbf{F}_{n+1}^{ext}$ is the external load vector, $\ddot{q}_{n+1}$ is the acceleration at t_{n+1}, $\dot{q}_{n+1}$ is the velocity at t_{n+1} and q_{n+1} is the displacement at t_{n+1}.

Ocene vrednosti za q_{n+1}, $\dot{q}_{n+1}$ in $\ddot{q}_{n+1}$ podamo takole:

The estimates of q_{n+1}, $\dot{q}_{n+1}$ and $\ddot{q}_{n+1}$ are given by:

$$\begin{aligned} q_{n+1} &= q_n^* + \beta\ddot{q}_{n+1}\Delta t^2 \\ \dot{q}_{n+1} &= \dot{q}_n^* + \gamma\ddot{q}_{n+1}\Delta t \\ \ddot{q}_{n+1} &= \mathbf{M}^{*-1}\mathbf{F}_{n+1}^{residual} \end{aligned} \tag{5}$$

kjer je Δt časovna razlika, γ in β pa sta stalnici; q_n^*, $\dot{q}_n^*$, matriko $\mathbf{M}^*$ in vektor $\mathbf{F}_{n+1}^{residual}$ izračunamo z naslednjimi enačbami:

where Δt is the time step and γ and β are the constants. The q_n^*, $\dot{q}_n^*$, matrix $\mathbf{M}^*$ and vector $\mathbf{F}_{n+1}^{residual}$ are calculated with these equations:

$$\begin{aligned}\mathbf{F}_{n+1}^{residual} &= \mathbf{F}_{n+1}^{ext} - \mathbf{C}\dot{q}_n^* - \mathbf{K}q_n^* \\ \mathbf{M}^* &= \mathbf{M} + \mathbf{C}\gamma\Delta t + \mathbf{K}\beta\Delta t^2 \\ \dot{q}_n^* &= \dot{q}_n + (1-\gamma)\ddot{q}_n\Delta t \\ q_n^* &= q_n + \dot{q}_n\Delta t + \frac{(1-2\beta)\ddot{q}_n\Delta t^2}{2}\end{aligned} \quad (6),$$

2 REZULTATI

Skupine valjev imajo premer D = 20 mm, debelino h = 1 mm, modul elastičnosti E = 210 GPa, in gostoto ρ = 7800 kg/m^3 (preglednica 1).

Preglednica 1. *Lastnosti materiala*
Table 1. *Material Properties*

	Modul elastičnosti Elastic modulus	Poissonovo število Poisson's ratio	Gostota Density
	E	υ	ρ
	GPa		kg/m^3
jeklo steel	210	0,3	7800

Dolžina L valjev iz te skupine niha med L = D in L = 20D. Račune smo izvedli za različne vrednosti razmerja med dolžino in premerom (L/D) in stalno razmerje med debelino in premerom (h/D = 0,05).

Čelo tlaka se začne gibati na levi strani valja s stalno intenzivnostjo (P_0 = 445 MPa). Na vsaki stopnji izračuna je hitrost čela tlaka stalna.

Sliki 6 in 7 prikazujeta spreminjanje radialnega dinamičnega upogiba na različnih točkah (W_d) valja, deljenega z radialnim statičnim upogibom (W_s) glede na lego gibajočega se tlaka. Analiza mirovanja valja je smiselna le takrat, ko se čelo tlaka giblje z majhno hitrostjo. V primeru velike hitrosti pa moramo uporabiti analizo dinamike. Glede na omenjena diagrama je največji radialni dinamični upogib pri majhni hitrosti tlaka blizu statičnemu upogibu (maksimalni faktor radialne dinamične povečave: Najv. FRDP≈1,0), toda ob zvečani hitrosti faktor dinamične povečave preseže statični upogib.

Kakor kažejo slike, se lega pojava Najv. FRDP spreminja s povečano hitrostjo tlaka in dolžino valja. Pri majhni hitrosti je njegova lega na levi strani valja, pri povečani hitrosti tlaka pa se ta lega premakne proti desni strani valja. Kakor kaže slika 6, je pri hitrosti 5 m/s faktor pri dolžini 0,1 (0,1L), pri hitrosti 80 m/s pa se, v primeru L/D = 3, premakne na levo

2 RESULTS

The cylinder groups have a diameter D = 20 mm, thickness h = 1 mm, elastic modulus E = 210 GPa, and density ρ = 7800 kg/m^3 (Table 1).

The length L of the cylinders in this group changes from $L = D$ to $L = 20D$. The computations were performed for different values of the length-to-diameter ratio (L/D) and a constant thickness-to-diameter ratio (h/D = 0.05).

The pressure front begins to move form the left-hand side of the cylinder with a constant intensity (P_0 = 445 MPa). The velocity of the pressure front is constant at each calculation stage.

Figure 6 and Figure 7 show the variation of the radial dynamic deflection of various points (W_d) of the cylinder divided by the radial static deflection (W_s), with respect to the position of the moving pressure. A static analysis of the cylinder is only valid when the pressure front moves with low velocity. If the velocity is high, a dynamic analysis must be used. According to the figures, for a low pressure velocity the radial maximum dynamic deflection is close to a static deflection (the maximum radial dynamic magnification factor, Max RDMF, ≈1.0) but with increasing velocity the dynamic magnification factor becomes higher than for a static deflection.

As shown in these figures the location of Max RDMF changes with increasing pressure velocity and cylinder length. For a low velocity this location is in the left-hand side of cylinder, but with increasing pressure velocity the location moves towards the right-hand side of the cylinder. As shown in Figure 6, the Max RDMF for a velocity of 5 m/s occurs at a length of 0.1 (0.1L), but this location for

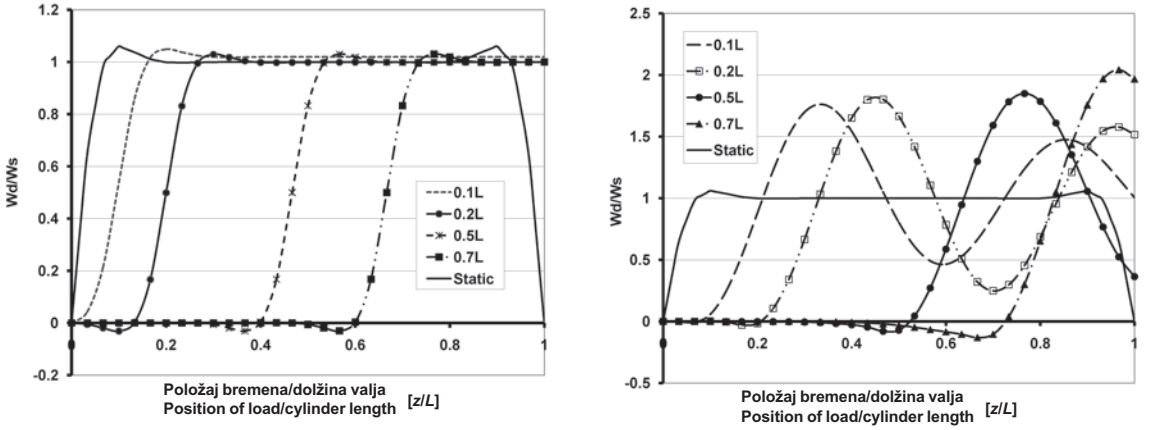

Sl. 6. *Primerjava dinamičnih in statičnih upogibov za L/D = 3 pri hitrosti tlaka: a) 5 m/s; b) 80 m/s*
Fig. 6. *Comparison between dynamic and static deflection for L/D = 3 for a pressure velocity of: a) 5 m/s; b) 80 m/s*

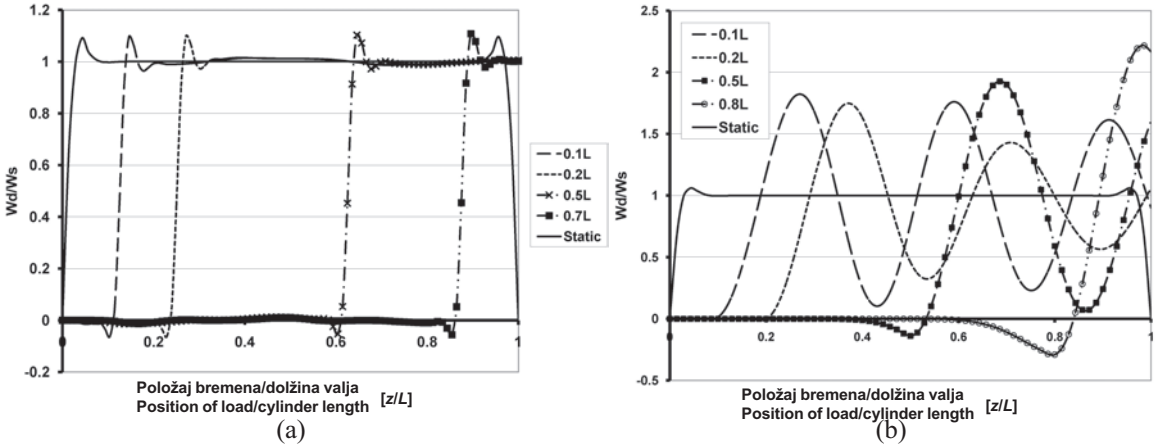

Sl. 7. *Primerjava dinamičnih in statičnih upogibov za L/D = 7 pri hitrosti tlaka: a) 5 m/s, b)120 m/s*
Fig. 7. *Comparison between dynamic and static deflection for L/D = 7 at a pressure velocity of: a) 5 m/s, b) 120 m/s*

stran valja (0,7*L*). V primeru *L/D* = 7 se faktor pojavi pri dolžini 0,8*L* in se nanaša na hitrost 120 m/s. Najv. FRDP se pri nizki hitrosti dejansko približa največjemu statičnemu upogibu, medtem ko ob zvečani hitrosti tlaka ta faktor začne zaostajati za gibajočim se tlakom. To zaostajanje se ob povečani hitrosti poveča.

Kakor vidimo na sliki 8, je spreminjanje največjega faktorja za gibajoči se tlak pri različnih hitrostih odvisno od razmerja *L/D*. Pri majhnem razmerju *L/D* to obnašanje lahko razdelimo na dve območji: podkritično in nadkritično. Pri velikem razmerju *L/D* pa ga razdelimo na tri območja: podkritično, prehodno in nadkritično območje.

a velocity of 80 m/s, for *L/D* = 3, is shifted to the left-hand side of the cylinder (0.7*L*). This value for *L/D* = 7 is 0.8*L* and relates to 120 m/s. Indeed the Max RDMF at low velocity is near to the location of the maximum static deflection, but with increasing the pressure velocity the Max RDMF has a delay with respect to the position of the moving pressure. This delay time increases with increasing velocity.

As can be seen from Figure 8, the variation of Max RDMF for a moving pressure at various speeds is dependent of the *L/D* ratio. For low *L/D* ratios this behaviour can be divided into two regions: under-critical and overcritical. For high *L/D* ratios this is divided into three regions: under-critical, transition and overcritical regions.

V podkritičnem območju se FRDP poveča ob povečani hitrosti in doseže vrh ob koncu tega območja. V nadkritičnem območju se Najv. FRDP zmanjšuje ob povečevanju hitrosti. Ob povečevanju dolžine valja se pojavi še prehodno območje. V prvem delu prehodnega območja se Najv. FRDP rahlo zmanjša. Po tem zmanjšanju pa se Najv. FRDP poveča in ostane stalen pri različnih hitrostih tlaka. Razpon hitrosti tlaka je odvisen od razmerja *L/D*, tako da se le-ta povečuje ob povečevanju razmerja *L/D*. Glede na to območje lahko določimo dolge dele. Dolgi del določimo kot del, ki ima tudi prehodno območje. Tako je, glede na sliko 8, valj prepoznan kot dolgi del, če je $L/D \geq 3$.

In the under-critical region the radial dynamic magnification factor increases with increasing speed and has a maximum peak at the end of this region. In the overcritical region the Max RDMF reduces with increasing velocity. With increasing the cylinder length the transition region is added to previous regions. In the first part of the transition region the Max RDMF reduces slightly. After this reduction the Max RDMF increases and becomes constant for a range of pressure velocities. This pressure velocity range depends on the *L/D* ratio, so that this is extended with increasing *L/D* ratios. Depending on this region, long members can be defined. A long member is defined as a member that has a transition region. Thus, according to Figure 8, a cylinder is considered as a long member if $L/D \geq 3$.

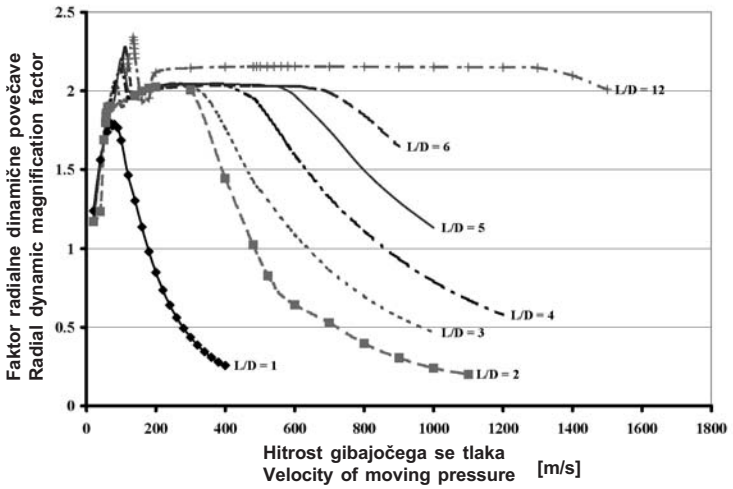

Sl. 8. *Faktor radialne dinamične povečave glede na hitrost gibajočega se tlaka*
Fig. 8. *Radial dynamic magnification factor with respect to moving pressure velocity*

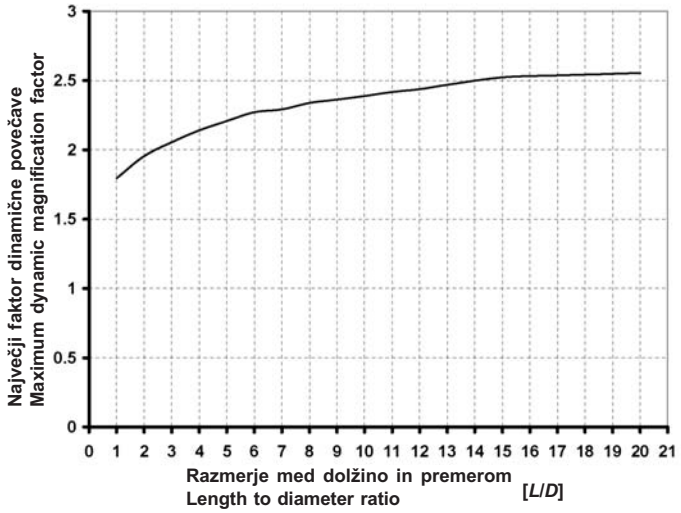

Sl. 9. *Največji faktor radialne dinamične povečave glede na razmerja L/D*
Fig. 9. *Maximum radial dynamic magnification factor with respect to L/D ratios*

Glede na sliko 8 postaja ob povečevanju razmerja med dolžino in premerom prehodno območje daljše in bolj gladko, medtem ko se nadkritično območje zmanjšuje. Obnašanje faktorja radialne dinamične povečave je v primeru majhnega razmerja *L/D* podobno obnašanju v primeru tramov [8]. Pri tramu, izpostavljenemu delovanju gibajočih se bremen, je obnašanje faktorja razdeljeno na dve območji, podkritično in nadkritično, nikjer pa ne zasledimo prehodnega območja.

Slika 9 prikazuje največji faktor radialne dinamične povečave glede na razmerja *L/D*. Pri vseh valjih je dinamični upogib večji od statičnega upogiba. Dinamični upogib je v primeru, ko je *L/D* = 1, približno 1,8 krat večji od statičnega upogiba. Ta vrednost se, ob povečanju razmerja med dolžino in premerom do *L/D* = 20, poveča na 2,55.

3 SKLEP

Pri majhni hitrosti tlaka zadostuje analiza mirovanja, pri povečani hitrosti pa je ključna analiza prehoda.

Faktor radialne dinamične povečave pri valju je odvisen od razmerja med dolžino in premerom. Ob povečevanju razmerja *L/D* se faktor poveča od 1,8 do 2,55.

Pri dolgem valju lahko obnašanje največjega faktorja radialne dinamične povečave razdelimo na tri območja: podkritično, prehodno in nadkritično območje. Nasprotno pa je pri kratkem valju prehodno območje zelo majhno in ga lahko zanemarimo. Treba je še dodati, da ob povečanju dolžine valja nadkritično območje postane majhno v primerjavi z drugima območjema. V primeru, ko je $L/D \geq 3$, ima FRDP stalno obnašanje pri različnih hitrostih in tako lahko dolge dele določimo kot valje, pri katerih je dolžina trikrat daljša od premera. Obnašanje kratkih valjev pa je podobno obnašanju tramov, izpostavljenih delovanju gibajočih se bremen.

According to Figure 8, with an increasing length-to-diameter ratio the transition region becomes longer and smoother, whereas the overcritical region becomes smaller. The behaviour of the RDMF for a low *L/D* ratio is similar to that for beams [8]. For a beam under the action of moving loads the RDMF behaviour consists of two regions, the under-critical and the overcritical, and there is no sign of a transition region.

The Max RDMF with respect to *L/D* ratios is shown in Figure 9. For all cylinders the dynamic deflection is higher than the static deflection. The dynamic deflection for *L/D* = 1 is about 1.8 times greater than the static deflection. This value increases to 2.55 when the length-to-diameter ratio increases up to *L/D* = 20.

3 CONCLUSION

With a low pressure velocity a static analysis is adequate, but with increasing velocity a transient analysis is essential.

The radial dynamic magnification factor in a cylinder depends on the length-to-diameter ratio. With an increasing *L/D* ratio the RMDF changes from 1.8 to 2.55.

In a long cylinder, the Max RDMF behaviour can be divided into three regions: under-critical, transition and overcritical. In contrast, in a short cylinder, the transition region is very small and can be eliminated. However, when increasing the length of the cylinder the overcritical region is small compared to the other regions. For $L/D \geq 3$, the RMDF is constant with a change in the speed, and as such long members are defined as the cylinders where the length is three times the diameter. The short cylinders' behaviour is similar to beams, under the action of moving loads.

4 LITERATURA
4 REFERENCES

[1] Fryba, L. (1999) Vibration of solids and structures under moving loads, *ThomasTelford*, Third edition.

[2] Pesterev A. V., Yang B., Bergman L. A., Tan C. A. (2003) Revisiting the moving force problem , *J of sound and vibration*, 261(2003), pp. 75-91.

[3] Gbadeyan J. A., Oni S. T. (1995), Dynamic behaviour of beams and rectangular plates under moving loads, *J of Sound and Vibration*, 182 (1995), pp. 677-695.

[4] Renard J.,Taazount M. (2002) Transient responses of beams and plates subject to traveling load. Miscellaneous results, *European J of Mechanics A/Solid*, 21(2002), pp. 301-322

[5] Tang S. (1996) Dynamic response of a tube under moving pressure, *Journal of Engineering Mechanics Division*, 91(1996), pp. 96-122
[6] Faria A. R. (2004) Finite element analysis of the dynamic response of cylindrical panels under traversing loads, *European Journal of Mechanics A/Solids*, 23(2004), pp. 677-687
[7] Manual (2004) MSC/NASTRAN for Windows: Quick start guide, *MacNeal-Schwendler Corporation*.
[8] Saranjam B, Bakhshandeh K., Kadivar M. H. (2006) Dynamic behaviour of a beam with non-uniform linear varying cross-section under moving load*, Strojnický Časopis-Journal of Mechanical Engineering*, 57(2006) C. 1, pp. 45-58.

Naslova avtorjev:

Bahador Saranjam
Kambiz Bakhshandeh
Center za zračno-mornariške raziskave
Univerza MUT
Shiraz, Iran
Kambiz@Bakhshandeh.ir

prof. dr. Mohammad-Hassan Kadivar
Oddelek za strojništvo
Šola za tehniške vede
Univerza Shiraz
Shiraz, Iran

Authors' Addresses:

Bahador Saranjam
Kambiz Bakhshandeh
Air Naval Research Center
MUT University
Shiraz, Iran
Kambiz@Bakhshandeh.ir

Prof. Dr. Mohammad-Hassan Kadivar
Department of Mechanical engineering
School of Engineering
Shiraz University
Shiraz, Iran

Prejeto: 18.7.2006
Received:

Sprejeto: 25.4.2007
Accepted:

Odprto za diskusijo: 1 leto
Open for discussion: 1 year

Osebne vesti - Personal Events

Doktorat, magisteriji in diplome - Doctor's, Master's and Diploma Degrees

DOKTORAT

Na Fakulteti za strojništvo Univerze v Ljubljani je z uspehom zagovarjal svojo doktorsko disertacijo:

dne *17. maja 2007*: **Boštjan Pečnik**, z naslovom: "Neporušno določevanje stanja materiala iz magnetnega Barkhausnovega šuma" (mentor: prof. dr. Janez Grum).

S tem je navedeni kandidat dosegel akademsko stopnjo doktorja znanosti.

MAGISTERIJI

Na Fakulteti za strojništvo Univerze v Ljubljani so z uspehom zagovarjali svoja magistrska dela:

dne *8. maja 2007*: **Jare Gačnik**, z naslovom: "Informacijska podpora pri montaži in servisiranju montažnih zgradb" (mentor: prof. dr. Peter Butala);

dne *25. maja 2007*: **Sebastjan Mašera**, z naslovom: "Obvladovanje kvalitete hladnega kovanja jekel" (mentorja: prof. dr. Alojz Sluga, prof. dr. Karl Kuzman) in **Darko Tičič** z naslovom: "Obrabni mehanizmi na orodju za hladno kovanje" (mentorja: doc. dr. Bojan Podgornik, prof. dr. Jože Vižintin).

Na Fakulteti za strojništvo Univerze v Maroboru sta z uspehom zagovarjala svoji magistrski deli:

dne *8. maja 2007*: **Marko Podlesek**, z naslovom: "Nadzor tlaka v hidravličnem sistemu obsekovalnega stroja s hitrostno reguliranim pogonom črpalke" (mentorja: prof. dr. Edvard Kiker, doc. dr. Darko Lovrec);

dne *10. maja 2007*: **Stanko Laković**, z naslovom: "Računalniške simulacije prometnih tokov v avtocestnih predorih" (mentorja: prof. dr. Iztok Potrč, prof. dr. Tomaž Tollazzi)

S tem so navedeni kandidati dosegli akademsko stopnjo magistra znanosti.

DIPLOMIRALI SO

Na Fakulteti za strojništvo Univerze v Ljubljani so pridobili naziv univerzitetni diplomirani inženir strojništva:

dne *4. maja 2007*: Gašper BENEDIK, Aleš DEŽMAN, Uroš ŠKRBE, Jure VETRŠEK;

dne *28. maja 2007*: Blaž BAJŽELJ, Blaž RIHTARŠIČ, Rok RUTAR.

Na Fakulteti za strojništvo Univerze v Mariboru sta pridobila naziv univerzitetni diplomirani inženir strojništva:

dne *31. maja 2007*: Marko GRAČNER, Iztok HAJDNIK.

*

Na Fakulteti za strojništvo Univerze v Ljubljani so pridobili naziv diplomirani inženir strojništva:

dne *11. maja 2007*: Matej HRIBERNIK, Jože JAZBEC, Peter PAŠKULIN, Mihec ŽERDIN.

Na Fakulteti za strojništvo Univerze v Mariboru so pridobili naziv diplomirani inženir strojništva:

dne *31. maja 2007*: Goran OLETIČ, Janez PONIKVAR, Marko POTOČNIK, Janez ŠVENT, Jože VAVH, Rudi VAVH, Uroš ZORKO.

Navodila avtorjem - Instructions for Authors

Članki morajo vsebovati:
- naslov, povzetek, besedilo članka in podnaslove slik v slovenskem in angleškem jeziku,
- dvojezične preglednice in slike (diagrami, risbe ali fotografije),
- seznam literature in
- podatke o avtorjih.

Strojniški vestnik izhaja od leta 1992 v dveh jezikih, tj. v slovenščini in angleščini, zato je obvezen prevod v angleščino. Obe besedili morata biti strokovno in jezikovno med seboj usklajeni. Članki naj bodo kratki in naj obsegajo približno 8 strani. Izjemoma so strokovni članki, na željo avtorja, lahko tudi samo v slovenščini, vsebovati pa morajo angleški povzetek.

Za članke iz tujine (v primeru, da so vsi avtorji tujci) morajo prevod v slovenščino priskrbeti avtorji. Prevajanje lahko proti plačilu organizira uredništvo. Če je članek ocenjen kot znanstveni, je lahko objavljen tudi samo v angleščini s slovenskim povzetkom, ki ga pripravi uredništvo.

VSEBINA ČLANKA

Članek naj bo napisan v naslednji obliki:
- Naslov, ki primerno opisuje vsebino članka.
- Povzetek, ki naj bo skrajšana oblika članka in naj ne presega 250 besed. Povzetek mora vsebovati osnove, jedro in cilje raziskave, uporabljeno metodologijo dela,povzetek rezulatov in osnovne sklepe.
- Uvod, v katerem naj bo pregled novejšega stanja in zadostne informacije za razumevanje ter pregled rezultatov dela, predstavljenih v članku.
- Teorija.
- Eksperimentalni del, ki naj vsebuje podatke o postavitvi preskusa in metode, uporabljene pri pridobitvi rezultatov.
- Rezultati, ki naj bodo jasno prikazani, po potrebi v obliki slik in preglednic.
- Razprava, v kateri naj bodo prikazane povezave in posplošitve, uporabljene za pridobitev rezultatov. Prikazana naj bo tudi pomembnost rezultatov in primerjava s poprej objavljenimi deli. (Zaradi narave posameznih raziskav so lahko rezultati in razprava, za jasnost in preprostejše bralčevo razumevanje, združeni v eno poglavje.)
- Sklepi, v katerih naj bo prikazan en ali več sklepov, ki izhajajo iz rezultatov in razprave.
- Literatura, ki mora biti v besedilu oštevilčena zaporedno in označena z oglatimi oklepaji [1] ter na koncu članka zbrana v seznamu literature. Vse opombe naj bodo označene z uporabo dvignjene številke[1].

OBLIKA ČLANKA

Besedilo članka naj bo pripravljeno v urejevalnilku Microsoft Word. Članek nam dostavite v elektronski obliki.

Ne uporabljajte urejevalnika LaTeX, saj program, s katerim pripravljamo Strojniški vestnik, ne uporablja njegovega formata.

Enačbe naj bodo v besedilu postavljene v ločene vrstice in na desnem robu označene s tekočo številko v okroglih oklepajih

Papers submitted for publication should comprise:
- Title, Abstract, Main Body of Text and Figure Captions in Slovene and English,
- Bilingual Tables and Figures (graphs, drawings or photographs),
- List of references and
- Information about the authors.

Since 1992, the Journal of Mechanical Engineering has been published bilingually, in Slovenian and English. The two texts must be compatible both in terms of technical content and language. Papers should be as short as possible and should on average comprise 8 pages. In exceptional cases, at the request of the authors, speciality papers may be written only in Slovene, but must include an English abstract.

For papers from abroad (in case that none of authors is Slovene) authors should provide Slovenian translation. Translation could be organised by editorial, but the authors have to pay for it. If the paper is reviewed as scientific, it can be published only in English language with Slovenian abstract, that is prepared by the editorial board.

THE FORMAT OF THE PAPER

The paper should be written in the following format:
- A Title, which adequately describes the content of the paper.
- An Abstract, which should be viewed as a mini version of the paper and should not exceed 250 words. The Abstract should state the principal objectives and the scope of the investigation, the methodology employed, summarize the results and state the principal conclusions.
- An Introduction, which should provide a review of recent literature and sufficient background information to allow the results of the paper to be understood and evaluated.
- A Theory
- An Experimental section, which should provide details of the experimental set-up and the methods used for obtaining the results.
- A Results section, which should clearly and concisely present the data using figures and tables where appropriate.
- A Discussion section, which should describe the relationships and generalisations shown by the results and discuss the significance of the results making comparisons with previously published work. (Because of the nature of some studies it may be appropriate to combine the Results and Discussion sections into a single section to improve the clarity and make it easier for the reader.)
- Conclusions, which should present one or more conclusions that have been drawn from the results and subsequent discussion.
- References, which must be numbered consecutively in the text using square brackets [1] and collected together in a reference list at the end of the paper. Any footnotes should be indicated by the use of a superscript[1].

THE LAYOUT OF THE TEXT

Texts should be written in Microsoft Word format. Paper must be submitted in electronic version.

Do not use a LaTeX text editor, since this is not compatible with the publishing procedure of the Journal of Mechanical Engineering.

Equations should be on a separate line in the main body of the text and marked on the right-hand side of the page with numbers in round brackets.

Enote in okrajšave

V besedilu, preglednicah in slikah uporabljajte le standardne označbe in okrajšave SI. Simbole fizikalnih veličin v besedilu pišite poševno (kurzivno), (npr. *v, T, n* itn.). Simbole enot, ki sestojijo iz črk, pa pokončno (npr. ms^{-1}, K, min, mm itn.).

Vse okrajšave naj bodo, ko se prvič pojavijo, napisane v celoti v slovenskem jeziku, npr. časovno spremenljiva geometrija (ČSG).

Slike

Slike morajo biti zaporedno oštevilčene in označene, v besedilu in podnaslovu, kot sl. 1, sl. 2 itn. Posnete naj bodo v ločljivosti, primerni za tisk, v kateremkoli od razširjenih formatov, npr. BMP, JPG, GIF. Diagrami in risbe morajo biti pripravljeni v vektorskem formatu, npr. CDR, AI.

Pri označevanju osi v diagramih, kadar je le mogoče, uporabite označbe veličin (npr. *t, v, m* itn.), da ni potrebno dvojezično označevanje. V diagramih z več krivuljami, mora biti vsaka krivulja označena. Pomen oznake mora biti pojasnjen v podnapisu slike.

Vse označbe na slikah morajo biti dvojezične.

Preglednice

Preglednice morajo biti zaporedno oštevilčene in označene, v besedilu in podnaslovu, kot preglednica 1, preglednica 2 itn. V preglednicah ne uporabljajte izpisanih imen veličin, ampak samo ustrezne simbole, da se izognemo dvojezični podvojitvi imen. K fizikalnim veličinam, npr. *t* (pisano poševno), pripišite enote (pisano pokončno) v novo vrsto brez oklepajev.

Vsi podnaslovi preglednic morajo biti dvojezični.

Seznam literature

Vsa literatura mora biti navedena v seznamu na koncu članka v prikazani obliki po vrsti za revije, zbornike in knjige:

[1] A. Wagner, I. Bajsić, M. Fajdiga (2004) Measurement of the surface-temperature field in a fog lamp using resistance-based temperature detectors, *Stroj. vestn.* 2(2004), pp. 72-79.

[2] Vesenjak, M., Ren Z. (2003) Dinamična simulacija deformiranja cestne varnostne ograje pri naletu vozila. *Kuhljevi dnevi '03*, Zreče, 25.-26. september 2003.

[3] Muhs, D. et al. (2003) Roloff/Matek Maschinenelemente – Tabellen, 16. Auflage. *Vieweg Verlag*, Wiesbaden.

SPREJEM ČLANKOV IN AVTORSKE PRAVICE

Uredništvo Strojniškega vestnika si pridržuje pravico do odločanja o sprejemu članka za objavo, strokovno oceno recenzentov in morebitnem predlogu za krajšanje ali izpopolnitev ter terminološke in jezikovne korekture.

Avtor mora predložiti pisno izjavo, da je besedilo njegovo izvirno delo in ni bilo v dani obliki še nikjer objavljeno. Z objavo preidejo avtorske pravice na Strojniški vestnik. Pri morebitnih kasnejših objavah mora biti SV naveden kot vir.

PLAČILO OBJAVE

Avtorji vseh prispevkov morajo za objavo plačati prispevek v višini 20,00 EUR na stiskano stran prispevka. Prispevek se zaračuna po sprejemu članka za objavo na seji Uredniškega odbora.

Units and abbreviations

Only standard SI symbols and abbreviations should be used in the text, tables and figures. Symbols for physical quantities in the text should be written in italics (e.g. *v, T, n,* etc.). Symbols for units that consist of letters should be in plain text (e.g. ms^{-1}, K, min, mm, etc.).

All abbreviations should be spelt out in full on first appearance, e.g., variable time geometry (VTG).

Figures

Figures must be cited in consecutive numerical order in the text and referred to in both the text and the caption as Fig. 1, Fig. 2, etc. Pictures may be saved in resolution good enough for printing in any common format, e.g. BMP, GIF, JPG. However, graphs and line drawings sholud be prepared as vector images, e.g. CDR, AI.

When labelling axes, physical quantities, e.g. *t, v, m,* etc. should be used whenever possible to minimise the need to label the axes in two languages. Multi-curve graphs should have individual curves marked with a symbol, the meaning of the symbol should be explained in the figure caption.

All figure captions must be bilingual.

Tables

Tables must be cited in consecutive numerical order in the text and referred to in both the text and the caption as Table 1, Table 2, etc. The use of names for quantities in tables should be avoided if possible: corresponding symbols are preferred to minimise the need to use both Slovenian and English names. In addition to the physical quantity, e.g. *t* (in italics), units (normal text), should be added in new line without brackets.

All table captions must be bilingual.

The list of references

References should be collected at the end of the paper in the following styles for journals, proceedings and books, respectively:

[1] A. Wagner, I. Bajsić, M. Fajdiga (2004) Measurement of the surface-temperature field in a fog lamp using resistance-based temperature detectors, *Stroj. vestn.* 2(2004), pp. 72-79.

[2] Vesenjak, M., Ren Z. (2003) Dinamična simulacija deformiranja cestne varnostne ograje pri naletu vozila. *Kuhljevi dnevi '03*, Zreče, 25.-26. september 2003.

[3] Muhs, D. et al. (2003) Roloff/Matek Maschinenelemente – Tabellen, 16. Auflage. *Vieweg Verlag*, Wiesbaden.

ACCEPTANCE OF PAPERS AND COPYRIGHT

The Editorial Committee of the Journal of Mechanical Engineering reserves the right to decide whether a paper is acceptable for publication, obtain professional reviews for submitted papers, and if necessary, require changes to the content, length or language.

Authors must also enclose a written statement that the paper is original unpublished work, and not under consideration for publication elsewhere. On publication, copyright for the paper shall pass to the Journal of Mechanical Engineering. The JME must be stated as a source in all later publications.

PUBLICATION FEE

For all papers authors will be asked to pay a publication fee prior to the paper appearing in the journal. However, this fee only needs to be paid after the paper is accepted by the Editorial Board. The fee is €20.00 per printed paper page.